Numerical investigation of the effects of cracking and embedded reinforcement on surface concrete resistivity measurements using Wenner probe

by

Mustafa Salehi

A thesis submitted to the Faculty of Graduate and Postdoctoral Affairs in partial fulfillment of the requirements for the degree of

Master of Applied Science

in

Civil Engineering

Carleton University
Ottawa, Ontario

Ottawa-Carleton Institute of Civil and Environmental Engineering

Abstract

Electrical resistivity of concrete plays a major role in controlling the corrosion rate of embedded reinforcement in concrete. In addition, many recent studies have shown that resistivity and micro-structural changes as well as ion (e.g. chloride) ingress in concrete are highly correlated. Four-probe Wenner probe technique is the most commonly used resistivity measurement method in concrete. In the past, a number of studies have identified the factors affecting the resistivity measurements using four-point Wenner probe and provided guidelines for minimizing their disturbing effects on the readings. However, the effects of existing surface cracks and embedded reinforcement in concrete on the measurements have not been studied systematically. In this numerical study, finite element method has been used to investigate this issue by carrying out a parametric investigation. Some of the analysis parameters of the study involved (1) crack dimensions, (2) crack locations and orientations with respect to the probe position, (3) density and location of embedded reinforcement, (4) orientation of the probe with respect to reinforcement, and (5) moisture content of concrete. It was demonstrated that depending on the location and geometrical properties of the crack as well as its angle with respect to the Wenner probe, concrete resistivity measurements can contain considerable errors. The presence of rebar mesh and its misalignment with respect to the crack and the measurement direction exacerbated the errors – in some cases by over 100%. Suggestions were provided to help minimize the effects of the cracks on electrical resistivity measurements.

Acknowledgements

I would like to express my sincere gratitude to Professor O. Burkan Isgor for his endless support and guidance throughout this study. He has been a great mentor in every step of the way with his extensive knowledge and experience in this field, paying attention to details, demonstrating high level of professionalism and working ethics, and most importantly being friendly and considerate. It has been a great honor for me to work under his supervision.

I would also like to deeply appreciate all the support and guidance provided by my co-supervisor Dr. Pouria Ghods. His creativity and enthusiasm in work and positive energy that is provided to everyone around him is exceptional. It was a great pleasure for me to work under his supervision.

I cannot find words to express my gratitude towards my family, in particular my parents. Their encouragement gave me strength, their happiness cheered me up and thinking about their love was always a source of relief especially during hard times.

Support from the technical team at Giatec Scientific Inc., especially Dr. Aali R. Alizadeh is highly appreciated. I am also thankful to my colleague Mr. H. Burak Gunay for his assistance during initial stages of this research.

Financial support from the National Science and Engineering Council of Canada (NSERC) and the Department of Civil and Environmental Engineering at Carleton University is also greatly acknowledged.

Table of Contents

List of Tables

List of Figures

List of Symbols

Symbols & Acronyms	Explanation
a	Electrode spacing of Wenner probe (mm)
C	Conductive crack
C_d	Crack distance to the probe (mm)
C_h	Crack height (mm)
C_l	Crack length (mm)
C_w	Crack width (mm)
I	Insulated crack; Electrical current (A)
L1, L2, L3	Crack locations intersecting the probe
P	Crack parallel to the probe
S	Rebar spacing (mm)
T	Concrete cover thickness (mm)
Γ_i	Domain boundary *i*
θ	Crack angle (°)
ρ	Electrical resistivity (Ω.m)
ϕ	Rebar diameter (mm)
Ω_i	Subdomain *i*

1. Introduction

1.1 Background

Concrete is the most widely used construction material in the world (PCA, 2011). It is used to build nations' civil infrastructure that includes highways, bridges, dams, sewage and water systems, and numerous other applications. With this widespread range and amount of utilization, it is critical to guarantee that concrete that is used in structures has the highest possible quality and specified properties. Since the deterioration of reinforced concrete infrastructure is a serious issue with significant safety and cost implications, it is also necessary to monitor the performance of concrete during service. Numerous catastrophic events in the past highlight the importance of producing high quality concrete and monitoring its performance.

Testing of concrete for its critical mechanical properties during new construction and in service follows well-established and standardized practices. For example, all concrete produced for structural applications need to be tested for mechanical properties (e.g. compressive strength as per ASTM C39, 2012). Mechanical tests can also be conducted on cores taken from structures in service. These tests are quite easy and fast, and they generally provide adequate information about the mechanical properties of concrete. However, mechanical properties of concrete are not the only indicators about how a structure performs in service. A number of deteriorative processes can take place during the service life, and these processes may affect the long-term performance of the structure as well. Some examples are chloride and carbonation induced corrosion of steel in concrete, alkali-aggregate reaction within concrete, and sulfate attack (Mehta and

Monteiro, 2006). Mechanical testing alone cannot provide the necessary information about these durability-related processes; therefore, additional standardized or non-standard tests are used to evaluate them.

Existing test methods for testing durability-related performance issues in concrete generally require time-consuming and expensive laboratory investigations on cores taken from structures. For example, there are a number of standardized test methods available for measuring chloride ingress in concrete (Lane et al., 2010). ASTM C1556 (2011) is the bulk chloride diffusion test that requires taking cores from structure, grinding the concrete core in layers into powder, and using chemical titration to obtain acid soluble total chloride content along the depth of the core. ASTM C1556 (2011) test is rather time consuming (takes several days to a week) and expensive. ASTM C1202 (2012) is the rapid chloride penetration test (RCPT), which monitors electrical charge movement in a concrete core under an applied electrical potential. The test is typically faster than ASTM C1556 (takes about six hours), but it is still considered to be a time-consuming test to be used as a rapid method. ASTM C1202 (2012) also has a number of technical issues since it does not provide the direct measure of chloride content, but rather, measures total electrical charge passing through the concrete core that is considered to be related to chloride content. Technical deficiencies of these test methods are discussed in detail in other publications (Lane et al., 2010).

Another example can be given from monitoring reinforcement corrosion in concrete structures. The only standardized test method for corrosion monitoring, namely half-cell potential mapping technique as per ASTM C876 (2009), only provides the probability of corrosion but does not measure corrosion rates. Existing non-standard

corrosion rate measurement techniques, on the other hand, do not provide accurate, consistent and reliable data (Gu and Beaudoin, 1998; Andrade and Alonso, 2001; Martinez et al., 2008; Pease, 2010); in addition, these tests are quite time consuming and expensive.

In summary, as far as durability-related performance indicators are concerned, the construction industry is in need for a quick, accurate and reliable performance indicator or index. In recent years, electrical resistivity of concrete has emerged as a performance index with a considerable potential to satisfy this need. Several investigations have shown the existence of reasonable relationships between the electrical resistivity of concrete and other durability-related parameters (Millard, 1991; Gowers and Millard, 1999; Hamilton et al., 2007; Sengul and Gjorv, 2008; Shahroodi, 2010). For example, Figure 1-1 illustrates the relationship between electrical resistivity of concrete with bulk diffusion coefficient obtained using ASTM C1556 (2011). In Figure 1-2, the correlation between electrical resistivity measurements and charge passing in an RCPT test is presented. Figure 1-3 shows the relationship between concrete resistivity and corrosion rate of steel in concrete. Similar comparisons with other non-destructive tests are also available (Gucunski et al., 2013). It should also be noted that concrete resistivity measurements have been getting increased attention in monitoring early-age properties and microstructural changes of concrete (Xiao and Li, 2008; Wei and Li, 2006).

All these recent developments have led to increased efforts to standardize concrete resistivity measurement procedures. Standardization efforts are in progress both in Canada (CSA A23.2) and in other countries (e.g. by organizations like ASTM and AASHTO). Some jurisdictions even started requiring resistivity measurements as part of

ongoing construction and maintenance procedures (Hamilton et al., 2007). The number of companies producing concrete resistivity measurement devices has been increasing.

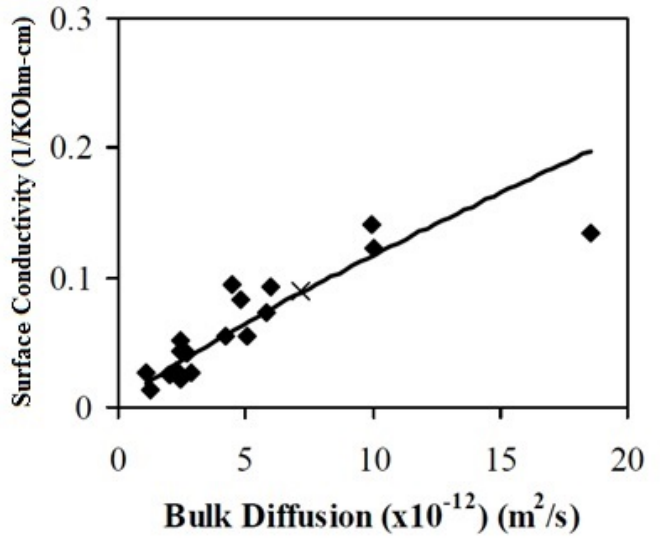

Figure 1-1: Relationship between surface resistivity of concrete with bulk chloride diffusion coefficient measured using ASTM C1556 (taken from Hamilton et al., 2007).

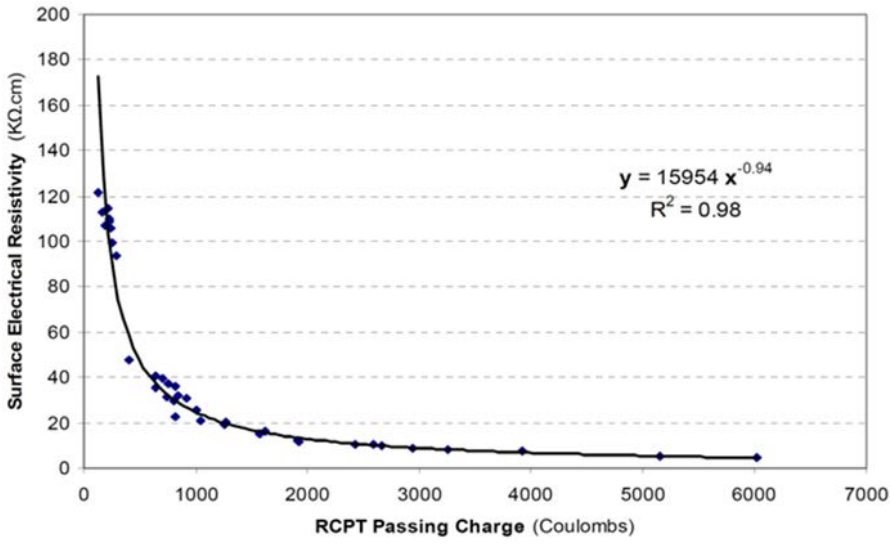

Figure 1-2: Surface resistivity of concrete cylinders versus passing charge by RCPT (taken from Shahroodi, 2010).

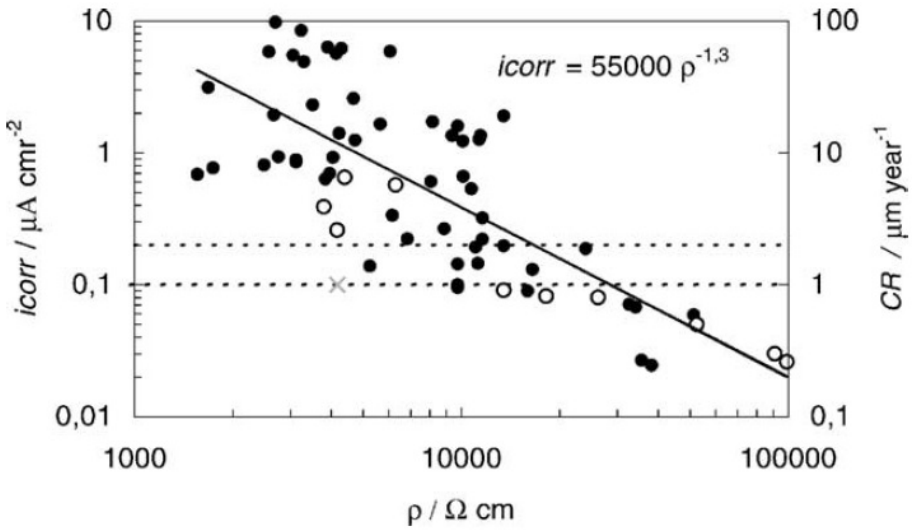

Figure 1-3: Resistivity of concrete cylinders versus corrosion rate (taken from Morris et al., 2004). In this figure, CR: corrosion rate; icorr: corrosion current density.

1.2 Concrete Resistivity Measurement using the Wenner Probe

There are a number of techniques to measure concrete resistivity (Millard, 1991; Polder et al., 2000); however, the four-probe Wenner probe technique is the most commonly used technique because of its speed, simplicity, and practicality. It can be used to measure the resistivity of concrete from the surface in seconds without any intrusive process such as coring. Four-point methods have being widely used in other fields, and their application is not limited to concrete. In all four-point techniques, there are four electrodes in the system: two electrodes are used to impose a certain amount of electrical current into the medium being investigated. The other two electrodes are used for measuring the electrical potential difference at two specific locations. These four electrodes can be arranged in a variety of configurations; the Wenner probe configuration is just one of these arrangements. In this configuration, all four electrodes are aligned on a straight line at equal distance from each other as depicted in Figure 1-4. By the

introduction of recent quality control guidelines the Wenner probe technique is also becoming the industry standard for measuring concrete resistivity (FM 5-578, 2004; AASHTO TP095-11, 2011).

Wenner probe makes certain assumptions to calculate the electrical resistivity of concrete using the applied current and measured potential difference. These assumptions are summarized as follows (Telford et al., 1990):

- the medium is homogeneous and isotropic;
- the medium is semi-infinite without any obstacle or barrier;
- the electrodes have zero contact area; i.e., the contact surfaces are considered to be points;
- the air or any other material (e.g. water) above concrete will not conduct electricity.

With these assumptions, concrete resistivity is calculated via:

$$\rho = 2\pi\, a\, \frac{\Delta V}{I} \qquad 1\text{-}1$$

where ρ (Ω-m) is the electrical resistivity, a (m) is the distance between electrodes, ΔV (V) is the measured potential difference between the two potential measurement electrodes, and I (A) is the imposed electrical current.

However, not all the aforementioned assumptions will be met when measurements are taken over a real concrete structure. For example, taking measurements over a small column or beam is far from having a semi-infinite geometry. Any deviation from the initial assumptions will cause the measured resistivity to be different from the actual resistivity of concrete under test. Limited attempts have been made in the past to identify

influential parameters and characterise performance of the Wenner probe in those situations. The reviews of these studies are provided in chapter 2.

(a)

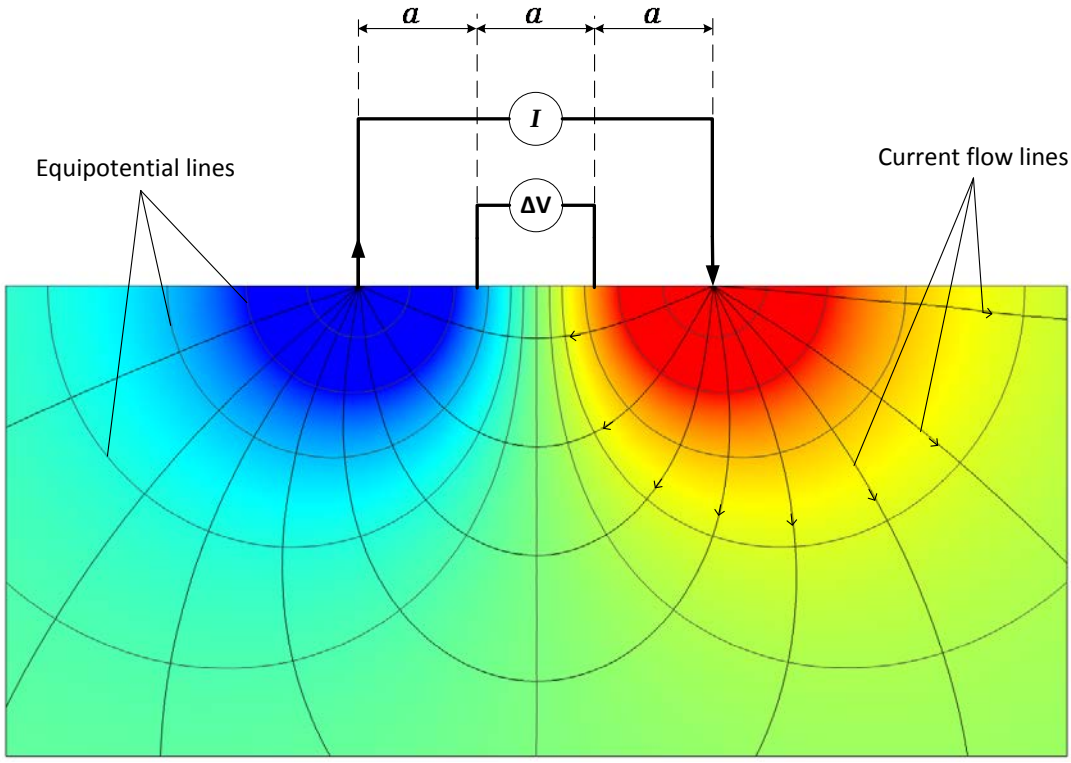

(b)

Figure 1-4: Wenner probe configuration and the resultant equipotential line and current flow distribution inside the media under test: (a) commercial Wenner probe; (b) FEM image. In this figure, a is the distance between the electrodes, I (A) is the imposed electrical current and ΔV (V) is the measured electrical potential difference.

1.3 Problem Definition

Numerous error-inducing factors can affect concrete resistivity measurements made by Wenner probes, and in practice, readings contain a certain level of error. The research on these effects is quite limited; however, in the past two decades a number of researchers have studied some of these parameters. A comprehensive literature review of these studies is provided in Chapter 2. It is clear from this review that the effects of cracks on resistivity measurements have not been studied systematically. In particular, the following gaps in the literature that define the problem addressed in this thesis were identified:

- In general, there is no systematic study showing how Wenner probe would behave in the presence of a crack.
- Although a limited number of studies revealed that the performance of the Wenner probe could be affected when there is a rebar mesh within concrete, these studies were not comprehensive enough to cover a wide variety of possible cases with dense reinforcement detailing, different concrete cover thicknesses, and probe placement configurations on concrete surface.
- There is no study in the literature that shows how resistivity measurements would be affected when both reinforcement mesh and cracks are present in the measured area.

1.4 Objectives and Scope

The overall objective of this study is to investigate the gaps identified in existing research regarding concrete resistivity measurements using the Wenner probe technique.

To carry out this objective, a numerical parametric research approach that is based on finite element modelling was utilized. A commercial finite element analysis software was used to develop the model and simulate each scenario. To study the effect of reinforcement, resistivity measurements taken over an orthogonal rebar mesh were modelled; this study incorporated using the Wenner probe at different locations and orientations with respect to the mesh. Variations in the spacing of rebars, concrete cover thickness as well as the diameter of the bars and electrode spacing of the probe were investigated. The performance of the Wenner probe in the presence of a crack in concrete was studied considering insulated and conductive cracks. The effects of crack location with respect to the probe, depth of the crack as well as its orientation were explored. Lastly, the combined effect of the presence of rebar mesh and crack was investigated.

1.5 Organization of the Thesis

The chapters of this thesis are organized as follows: Chapter 1 provides a background on the research and presents the objectives and the scope of the study. Chapter 2 is dedicated to reviewing previous studies on the performance of four-point resistivity measurements on concrete surface, particularly when Wenner probe was used. Chapter 3 explains the numerical approach used in the study. Chapter 4 presents the research methodology. Chapter 5 presents the results and discussion of the numerical investigation. Chapter 6 summarizes the work, presents the main conclusions, and provides recommendations for future studies.

2. Literature Review

2.1 Introduction

As discussed in Chapter 1, the electrical resistivity is one of the most useful and practical performance indicators of concrete. The Wenner Probe is the most commonly used device for measuring surface resistivity of concrete because of its simplicity. However, number of factors affect concrete resistivity measurements made by the Wenner probe, reducing its performance such that in practice readings contain a certain level of inaccuracy. The research on these confounding effects is quite limited; however, in the past two decades a number of researchers have studied some of these parameters and their influence on surface resistivity measurements of concrete (Ewins, 1990; Millard, 1991; Morris et al., 1996; Moreno et al., 2009; Sengol and Gjorv, 2009). A limited number of researchers provided best practice guidelines (Gowers and Millard, 1999; Poler et al. 2000). In particular, although some attempts have been made to characterize cracks in concrete by means of electrical resistivity measurements, the effect of cracks on resistivity measurements were not studied systematically. This chapter reviews the pertinent literature on the topic.

2.2 Studies on Probe Specification

2.2.1 Studies on electrode spacing

One of the main assumptions behind the Wenner probe measurements is that concrete is considered to be a homogeneous material. Several researchers identified this

assumption as a likely source of error (Millard, 1991; Morris et al., 1996; Gowers and Millard, 1999). In fact, compared to cement paste, aggregates generally have higher resistivity and their location and size vary widely in concrete; therefore, it was suggested that the non-homogeneity of concrete might affect resistivity measurements. To mitigate this issue, it was suggested that probe spacing should be wide enough to minimize the effect of non-homogeneity caused by the presence of aggregates. In addition, it was recommended that several measurements should be taken at different locations, and these readings should be averaged (Millard, 1991; Morris et al., 1996).

Millard (1991) experimented on a sample concrete with maximum aggregate size of 20 mm and studied Wenner probe measurements with electrode spacing of 16 mm, 25 mm and 50 mm. It was observed that as the electrode spacing became closer to the maximum aggregate size, the scattering in the obtained data increased. Hence, larger electrode spacing was identified to be more suitable for practical use in order to eliminate the local effects of aggregates.

Morris et al. (1996) also experimented on three different samples made of different aggregate types and sizes and concluded that increase in aggregate size, while the probe spacing was kept constant, caused higher variance in resistivity measurements. Later, Gowers and Millard (1999) suggested that having electrode spacing 1.5 times larger than the maximum aggregate size would help reduce standard deviation of electrical resistivity measurements to around 5%. As depicted in Figure 2-1, when electrode spacing of Wenner probe became smaller than the maximum aggregate size (i.e., $a/h_{agg} < 1$ in the figure) standard deviation in the measurements increased to around 10%.

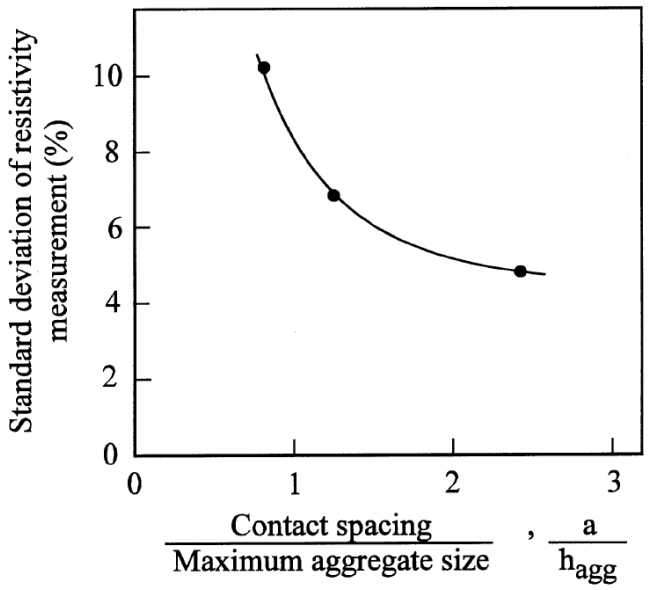

Figure 2-1: Influence of maximum aggregate size with respect to electrode spacing on resistivity measurement using Wenner probe (taken from Gowers and Millard, 1999).

2.2.2 Studies on electrode contact area

Millard (1991) and Gowers and Millard (1999) observed that contact area between the electrodes and concrete surface does not influence the results significantly in Wenner probe resistivity measurements. They conducted experiments in electrolytic tanks (container filled with conductive solution having homogeneous resistivity) and finite element modeling to draw their conclusions. Millard (1991) reported a maximum error of 6% in resistivity once the diameter of electrode contact area varied from 1 mm to 40 mm, while electrode spacing was kept constant at 50 mm. However, it was not clear in their report whether increasing contact area would result in higher or lower readings for the measured resistivity. In addition, the relationship between variations in contact area and electrode spacing was not studied since only one electrode spacing of 50 mm was used.

From a practical perspective, electrode contact area becomes important for both external current imposing and internal potential measurement electrodes. Ewins (1990) demonstrated that for small contact areas, contact resistance between the electrodes and surface of the concrete could increase significantly. The introduction of this new resistance might affect the symmetry of the system and adversely affect the performance of the probe; this effect was also confirmed by Gowers et al. (1991).

2.2.3 Studies on electrical signal shape and frequency

Since the introduction of the Wenner Probe technique it became clear that direct current (DC) signals complicated the electrical resistivity measurements because of the polarizing effect on the electrodes. To overcome this issue, a number of researchers suggested the use of alternating current (AC) signals (Ewins, 1990; Telford et al., 1991; Millard, 1991; Polder et al., 2000). Usually sine-wave or square-wave AC currents are used for taking resistivity measurements.

Ewins (1990) compared the performance of the Wenner probe when sinusoidal and square wave signals were used. It was reported that errors up to 800% might occur if measurements were taken with high frequency (600 Hz) sinusoidal signals while poor contact was made between electrodes and the surface of concrete. Both theoretical and experimental approaches were utilized to determine the source of this error. It was concluded that the presence of unavoidable parasitic capacitors that form between potential measurement electrodes and systems electrical ground, as well as uneven contact resistance between the electrodes and concrete, were the main sources of such large errors. Poor contact between the electrodes and surface of concrete was the main

cause of changing the symmetry of the system. The parasitic capacitors were created due to internal electrical circuitry of the device as well as using a long cable for connecting the measurement head to the instrument base. Combination of both abovementioned conditions affected the accuracy of the measurements; however, impact from parasitic capacitors was larger. As the measurement frequency increased, the adverse effect of parasitic capacitance amplified and increased the errors. It was also noted that as electrical current imposed by the probe decreased, the percentage of errors increased due to existence of unwanted offset potential present in the electronic measurement system. To reduce such effects, using low frequency square wave signal, instead of sine wave, was suggested. More importantly, instead of measuring the effective value of current and potential signals (root-mean-square value), taking readings at the mid span of the square pulse was recommended.

Following Ewins (1990), Millard et al. (1991) compared the performance of a Wenner probe with different signal shapes and frequencies. Sine wave signal with different frequencies was utilized for taking resistivity measurements and results were compared with a square wave Wenner probe working at 30 Hz. In order to investigate the sensitivity of the probe used for the study, external resistors were added to the measurement circuitry to mimic unbalanced contact resistance between electrodes and concrete. Similar to Ewins' results, sine wave Wenner probe working at 300 Hz was adversely affected by the addition of external resistors compared to the case for which square wave Wenner probe was used or frequency of the sine wave signal was reduced. Figure 2-2 shows the performance of Wenner probe when different AC signals with different frequencies were used to measure concrete resistivity while additional contact

resistors were added to the system. In Figure 2-2(a) external resistors were added to one of the two electrodes in both current imposing pair and potential measurement electrodes. The value of the additional resistor to the current imposing electrode was varied to evaluate how it would affect measurement accuracy. Readings as high as twenty times the original resistivity of concrete were reported when sinusoidal AC signal having frequency of 300 Hz was used. At the same time square wave or low frequency sine wave signals provided reasonably accurate results.

On the other hand, in Figure 2-2(b) potential electrodes were balanced with two 1 MΩ resistors while a resistor was added to one of the current electrodes. Although readings twice the original resistivity of concrete was reported for the sinusoidal 300 Hz AC signal, the impact was considerably smaller. It was then concluded that having unbalanced contact resistor in the potential measurement circuit has the most significant impact on the accuracy of the Wenner probe when high frequency sinusoidal AC signal is being used.

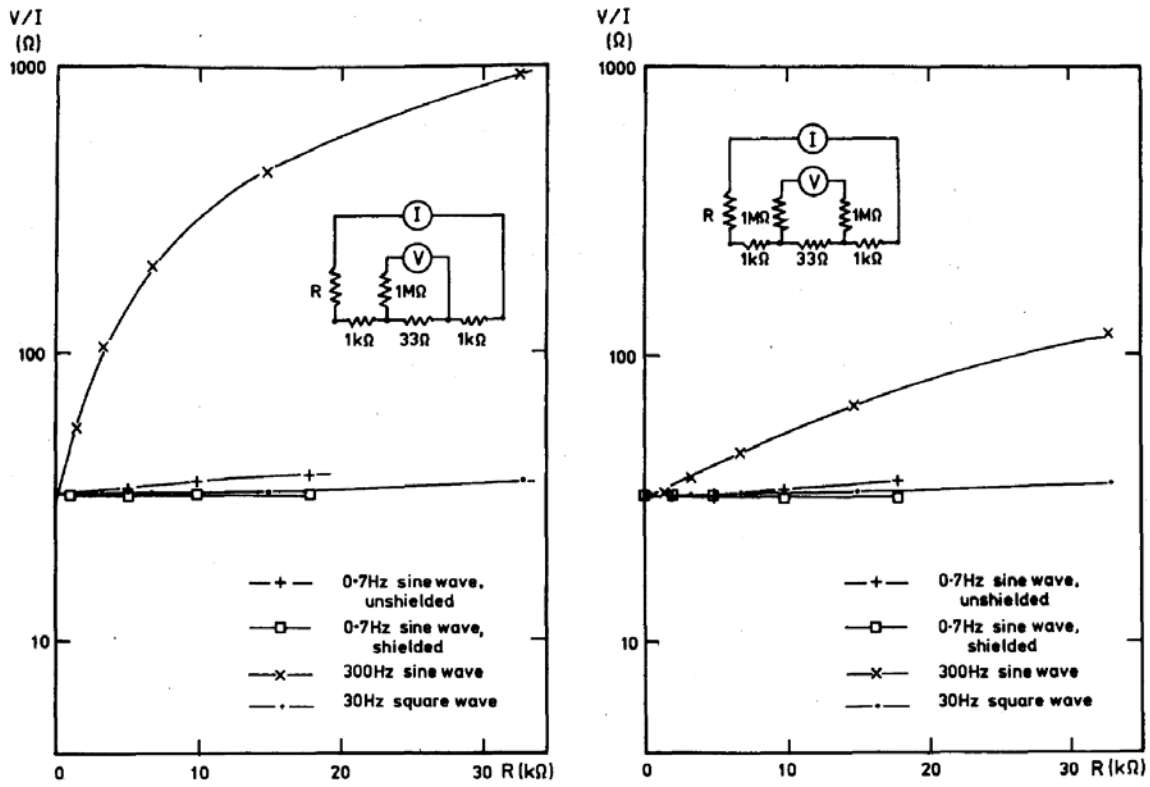

(a) (b)

Figure 2-2: Performance of Wenner probe using different types of AC signals for taking resistivity measurements when unbalanced resistive circuit due to poor contact with concrete is experienced (taken from Millard et al., 1991): (a) results when external resistor R added to one of the current electrodes while a fixed 1 MΩ resistor was added to one of the potential electrodes unbalancing the resistive circuitry for both electrode pairs; (b) results when external resistor R was added to one of the current electrodes while potential electrodes were balanced with two external 1 MΩ resistor creating only unbalanced resistive circuit for current electrodes pair.

2.3 Studies on Geometrical Factors

It was discussed in Section 1.2 that values provided by the Wenner probe for electrical resistivity were based on the assumption that the domain where the measurements are made is a semi-infinite medium. In practice, however, this assumption is not accurate. Deviation from the ideal condition of having infinitely large geometry

occurs in different directions of the probe (i.e., depth or lateral sides). Several researchers have all identified this problem; however, very limited data are provided in these studies regarding this issue (Millard, 1991; Morris et al., 1996; Gowers and Millard, 1999).

Millard (1991) reported that one should expect to see errors less than 10% for cases in which the depth or width of the concrete sample is four times the electrode spacing. Also for measurements taken at the corners, as long as a minimum distance of double the electrode spacing is taken from the edge, errors would also be less than 10%. For resistivity readings that are made close to sample edges (that are perpendicular to the axis of the Wenner probe) it was stated that no significant effect was observed. However, placing one of the current electrodes on the edge would cause errors up to 10%. It should be noted that these observations were derived from experimental measurements for which test conditions were not explained clearly by the researcher.

Morris et al. (1996) also provided correction factors for non-infinite geometry in Wenner probe resistivity measurements. Although this work was mainly on concrete cylinders, the researchers claimed that geometrical limitations could be compensated. Finite element modeling was used to investigate a wide range of geometrical variations in concrete cylinders. Limited experimental measurements verified modeled scenarios. Experimental results were obtained only for a single electrode spacing of 25.4 mm while it is not clear whether finite element modeling incorporated larger electrode spacing. Thus generalized conclusions made in this study would not be applicable for all electrode spacing.

Gowers and Millard (1999) provided charts depicting variations in resistivity measurement observed due to several different geometrical limitations. Electrical currents

were considered to be confined within the available geometry and did not reside in infinitely large dimensions. The main source of data for this study was experiments carried out on samples with different geometries to quantify limitations in depth and width of the samples as well as closeness of the measurement probe to the edges. Figure 2-3 represents some of the charts from this work. It can be seen in the figure that as the domain of the medium becomes smaller than the ideal semi-infinite condition, measured resistivity tends to overestimate the actual resistivity of concrete. This work along the earlier studies made by Millard in 1991 are amongst the most comprehensive studies in the literature that provides insight on the behaviour of the Wenner probe.

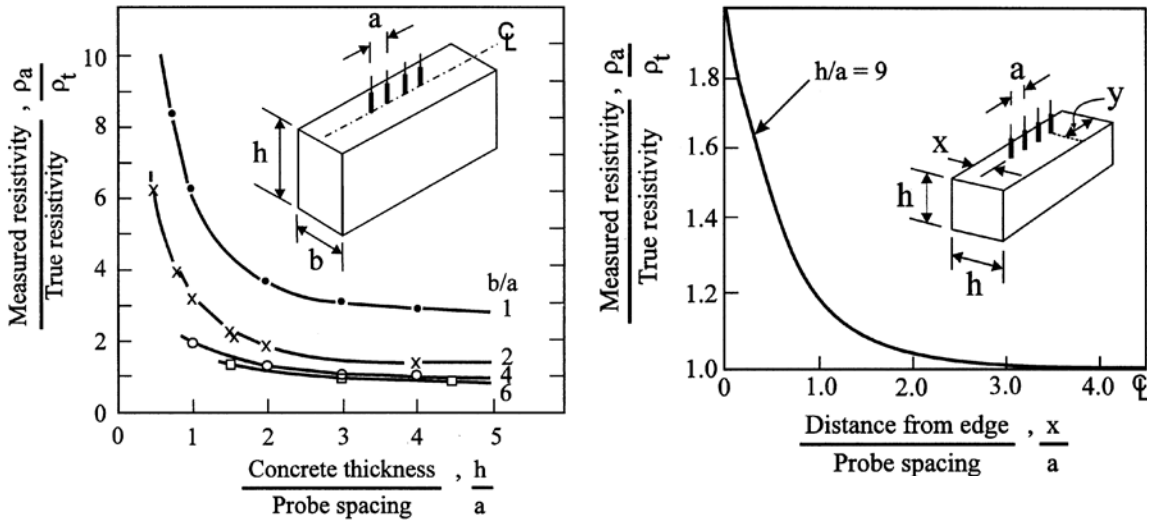

Figure 2-3: Effect of geometrical limitations on Wenner probe resistivity measurement (taken from Gowers and Millard, 1999): (a) effect of variation in the dimension of the concrete section; (b) effect of taking measurements at the proximity of an edge.

2.4 Studies on the Presence of Rebar

A number of researchers studied the effect of embedded rebar presence on Wenner probe resistivity measurements. In theory, electrical current fluxes inside a medium take paths with the least amount of resistivity. The less resistive a path the more current flows through it. When there is embedded rebar in concrete, a different type of non-homogeneity is introduced; ratio of resistivity of concrete to steel rebar is in the order of 10^6. Due to this large difference in resistivity, current fluxes created inside concrete by the Wenner probe would be altered when steel rebar is present. However many factors including orientation of the rebar with respect to the probe, depth at which it is located or size of it could play a role in this alteration (Millard, 1991; Weydert and Gehlen, 1999; Gowers and Millard, 1991).

Millard (1991) characterized the effects of concrete cover thickness, rebar diameter and rebar spacing on the measured concrete resistivity. Both experimental measurements taken on tanks filled with conductive solutions with steel rebar in it and finite element modeling was utilized for this purpose. The research only focused on rebars that were placed parallel to the direction of the Wenner probe. Distance between the probe and embedded rebar was reported to be the main influential parameter while taking measurements on top of the embedded rebar as well as rebar diameter, were not found to be as influential. In addition, by taking measurements between two parallel rebars, it was concluded that reduced rebar spacing increased measurement errors. For cover thickness of 20 mm, electrode spacing of 50 mm and rebar spacing of 50 mm, reported measured resistivity became less than half the value when no rebar was in the tank. Figure 2-4 summarizes the results from Millard's work. Both charts in this figure are normalized

with respect to the Wenner probe electrode spacing “a”. However, it was not clear whether all parameters were just normalized according to electrode spacing of 50 mm mentioned earlier or resistivity measurements using other electrode spacings were also involved in preparing the charts. In addition, no measurements on a real concrete with embedded rebar were made to further validate obtained results from the conductive solution tank.

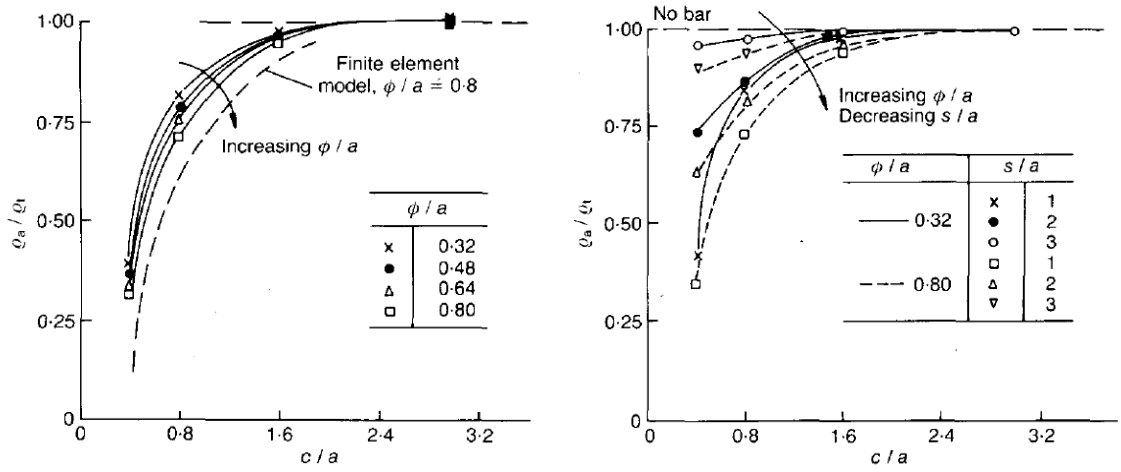

(a) (b)

Figure 2-4: Presence of rebar and its influence on Wenner probe resistivity measurement (taken from Millard, 1991). In this figure, a is the electrode spacing, c is the cover thickness, ρ_a is the apparent mesured resistivity , ρ_t is the true resistivity, Φ is the rebar diameter, S is the rebar spacing: (a) resistivity measurement over a single rebar; (b) resistivity measurement midway between two parallel rebars.

Weydert and Gehlen (1999) also studied resistivity measurements using Wenner probe in the presence of steel reinforcement. Although studying rebar effect was not the main interest in the study, from experimental results taken on a concrete block with embedded rebars it was reported that placing Wenner probe perpendicular to rebars reduced their effect considerably on resistivity measurements. It should be noted,

however, that no lateral rebars were present in the tested concrete block. In practical cases rebars in both directions are present and electrically connected to each other.

Polder et al. (2000) provided practical general guidelines for taking resistivity measurements on concrete by revisiting and summarizing existing literature. Due to lack of research on resistivity measurements over rebar meshes, it was suggested that resistivity measurements taken in diagonal orientations from the mesh. Taking several measurements at this orientation and averaging the results were also recommended. Figure 2-5 depicts the proposed scheme for taking resistivity measurement over a rebar mesh. There are no experimental or theoretical studies supporting the suggested scheme in Polder et al.'s work. Moreover, depending on the spacing between rebars and electrodes of the Wenner probe, it is not possible to have all four electrodes inside the rectangle unit created by the rebars at all times. Thus, in some scenarios it is possible to have one or more of the electrodes located on top of the rebars; and this arrangement might significantly affect resistivity measurements.

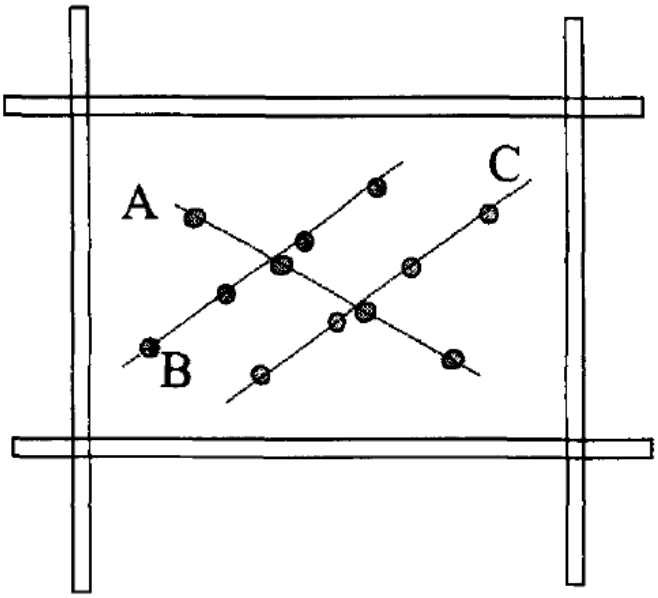

Figure 2-5: Suggested scheme for taking resistivity measurement using Wenner probe over rebar mesh (taken form Polder et al., 2000). In this figure, A, B, and C demonstrate taking measurements at different spots in diagonal orientation inside the mesh which needs to be averaged out eventually.

Sengul and Gjorv's work (2009) is one of the recent attempts to study the effect of rebar on concrete resistivity measurement using Wenner probe. The study focused on the influence of Wenner probe position with respect to the embedded rebar. A range of different electrode spacings was utilized for this purpose. Overall, five different positions for the probe with respect to the location of the embedded steel rebar were considered. Four of these configurations were in parallel to the rebar and the last one was perpendicular, as illustrated in Figure 2-6. Only a single rebar was placed in the slab being investigated while two different cover thicknesses of 50 mm and 70 mm were studied. Similar to the findings of Weydert and Gehlen (1999) and Gowers and Millards (1999), Sengul and Gjorv also concluded that measurements taken perpendicular to the rebar were not significantly influenced by the rebar. In contrast, measurements taken

directly above and parallel to the rebar contained noticeable errors. It was also reported that measurements obtained with electrode spacing of less than 30 mm was not significantly influenced by the rebar even for cover thickness of 50 mm. Furthermore, as the distance between the probe and location of the rebar increased, the influence of rebar on resistivity measurements decreased. Since only one embedded rebar was considered in these studies, these conclusions are difficult to extrapolate to real cases. In addition, the use of small slab size possibly exacerbated the effect of rebar on resistivity measurements as well as making it difficult to interpret the results.

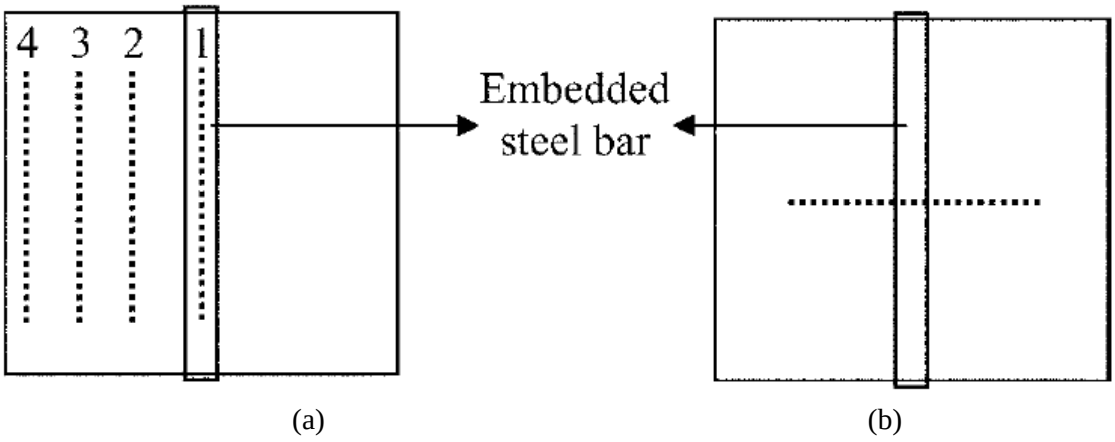

Figure 2-6: Wenner probe measurement positions with respect to the embedded rebar for Sengul and Gjorv (2009) study: (a) measurements taken parallel to the rebar at locations 1, directly above; 2, 35 mm away; 3, 70 mm away; 4, 105 mm away from the rebar; (b) measurement taken perpendicular to the rebar.

The last and the most recent study in this category belongs to Moreno et al. (2009) who studied the location and angle of the Wenner probe with respect to rebar alignment, as well as the effect of the number and configuration of embedded rebars on resistivity measurements. This work is one of the few studies that took into account the effect of rebar mesh as well as orientation of the Wenner probe. Moreno et al. used two electrode spacings of 30 mm and 50 mm and conducted both experimental measurements on real

samples and finite element modeling. Figure 2-7 illustrates typical results from finite element modeling of a 0.3 m x 0.3 m x 0.15 m slab with one rebar (a) and four rebars (b). The resistivity of concrete was assumed to be 1 KΩ-cm. The results showed that when there was only one rebar, for different orientations and locations of the Wenner probe, resistivity measurements were mostly above 1 KΩ-cm. This implies that the simulations were mostly under the influence of geometrical limitations of the slab. When a rebar mesh was used instead, in the same slab with the same geometry, all simulations yielded resistivities below 1 KΩ-cm, indicating the dominant effect of the rebar mesh. This study suggests that prior observations and conclusions that were based on models and tests with only one rebar present cannot truly capture the real behaviour of Wenner probe when there is a rebar mesh embedded in concrete. Taking measurement perpendicular to the rebar is one of those recommendations that need to be reconsidered.

Moreno et al. work's (2009) demonstrated the difference between the data obtained once there is a rebar mesh rather than a single rebar. However, the study does not show how Wenner probe performance might vary depending on variation in rebar spacing, cover thickness or location and orientation of the probe with respect to the rebar mesh.

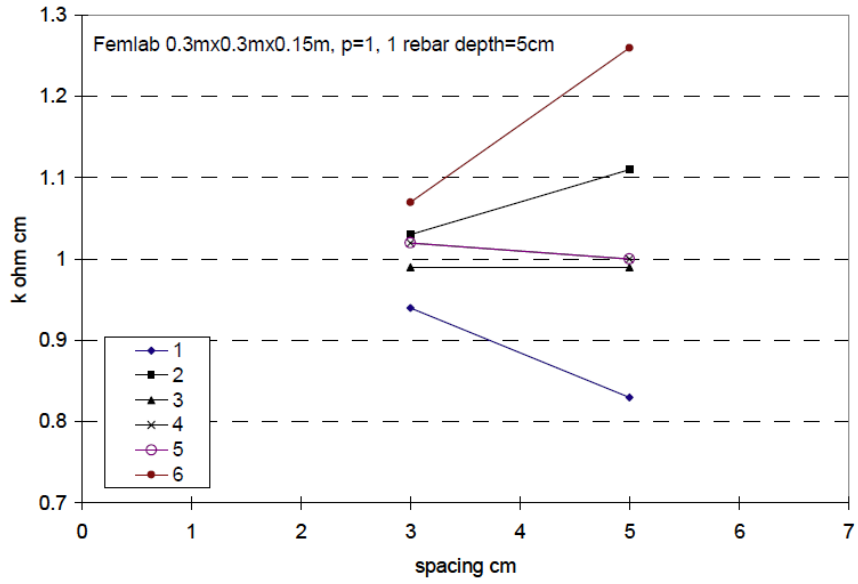

(a)

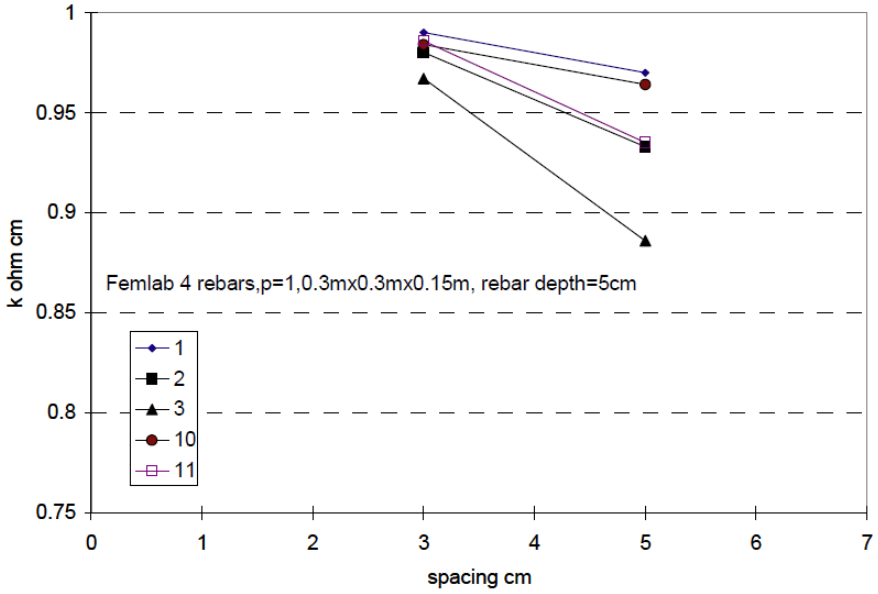

(b)

Figure 2-7: Finite Element modeling results for measurements on a slab with one and four rebars for electrode spacing of 30 mm and 50 mm (taken from Moreno et al., 2009): (a) results from resistivity measurement simulation with one rebar being present taken at six different orientations and locations; (b) results from resistivity measurement simulation with four rebars being present taken at five different orientations and locations.

2.5 Studies on the Presence of Concrete Cracks

The presence of cracks can be interpreted as another deviation from the initial assumption that concrete is homogeneous and isotropic with semi-infinite geometry. It is expected that presence of cracks may alter the electrical resistivity measurements by Wenner probe. Although some attempts have been made to characterize cracks in concrete by means of electrical resistivity measurements, the effect of cracks on resistivity measurements were not studied systematically.

Lataste et al. (2003) used specifically built measurement probe to investigate cracks on concrete. In the utilized instrument, which is illustrated in Figure 2-8, the four electrodes were placed in a square configuration rather than on a straight line as typically used in the Wenner probe. The purpose was to facilitate taking measurements in two orthogonal directions without the need for rotating the probe. This was done using an electrical switch that changed the function of electrodes from current imposing to potential measurement accordingly.

After taking resistivity measurements on a concrete slab with a crack it was reported that electrical resistivity measurements could be used to detect and characterize cracks. Numerical modeling was used to investigate the influence of different crack parameters on resistivity measurements using the developed square probe. A 35 cm x 35 cm x 15 cm (W x L x H) block with constant resistivity of 800 Ω-m was implemented as their concrete and a rectangle with constant width of 0.2 mm along the length of the domain was considered as representative of the crack. Obtained results are summarised in Figure 2-9.

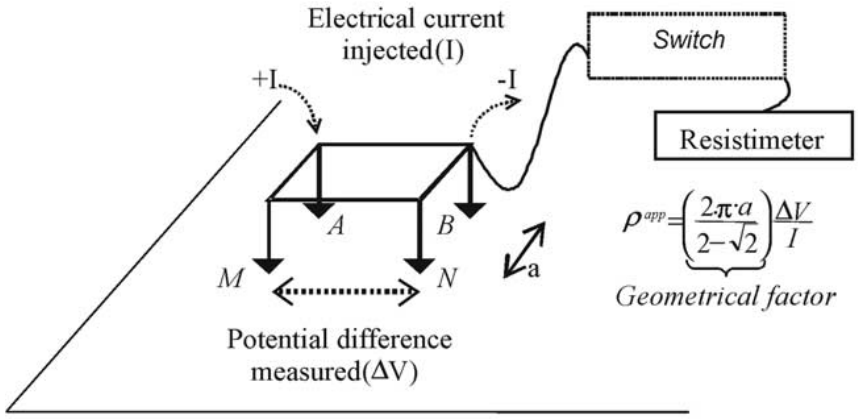

(a)

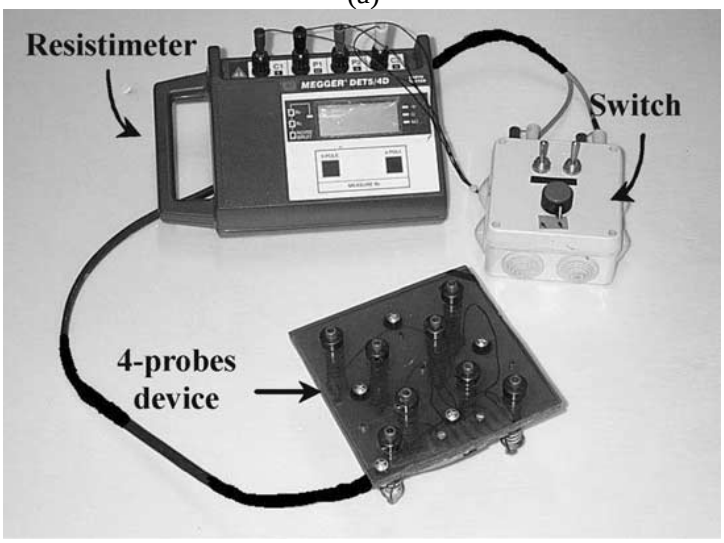

(b)

Figure 2-8: Square probe utilized for measuring electrical resistivity of concrete (taken from Lataste et al., 2003): (a) schematic view of the utilized system for resistivity measurement; (b) picture of the complete measurement instrument.

Lataste et al. (2003) reported that when an insulated crack was present, as shown in Figure 2-9(a), readings could underestimate or overestimate the actual resistivity depending on the orientation of the imposed current. When current was imposed parallel to the crack, resistivity measured dropped below the initial value for the concrete without crack. In contrast, measured resistivity increased when current was imposed

perpendicular to the orientation of crack. Considering Figure 2-9(b), in the presence of a conductive crack though, when electrical current was imposed perpendicular to the crack no impact was observed whereas the crack in parallel to the direction of the imposed current reduced electrical resistivity measurement. Overall, as shown in Figure 2-9, as the crack depth increased so did its adverse effect on the results. It was reported that in order to detect the presence of an insulated crack via electrical resistivity measurement using a square probe, the crack should be at least hundred times more resistive than the concrete. If the crack was conductive it should be at least three hundred times less resistive than the concrete to be detectable by the probe.

The study conducted by Lataste et al. (2003) is unique in a way that it considers the influence of several different characteristics of a crack on electrical resistivity measurements; however, there are some assumptions and conclusions that might not be compatible with reality. First, the influence of rebar was assumed to be independent of the crack regardless of type or depth of the crack. Although this assumption might be true for a single rebar there is no guarantee that the same conditions apply with a rebar mesh. This becomes more critical when a conductive crack exists at the vicinity of the mesh and is deep enough to intersect it. Second, simulations were carried out in a block with limited size hence there is a possibility that influence of the crack was intensified. Finally, Lataste et al. (2003) investigated performance of a probe that had four electrodes arranged in a square configuration which in presence of a crack, the location and distance of each one of those electrodes are different from the case for which Wenner probe is typically used. Thus it is likely to see different behaviour from the two probes.

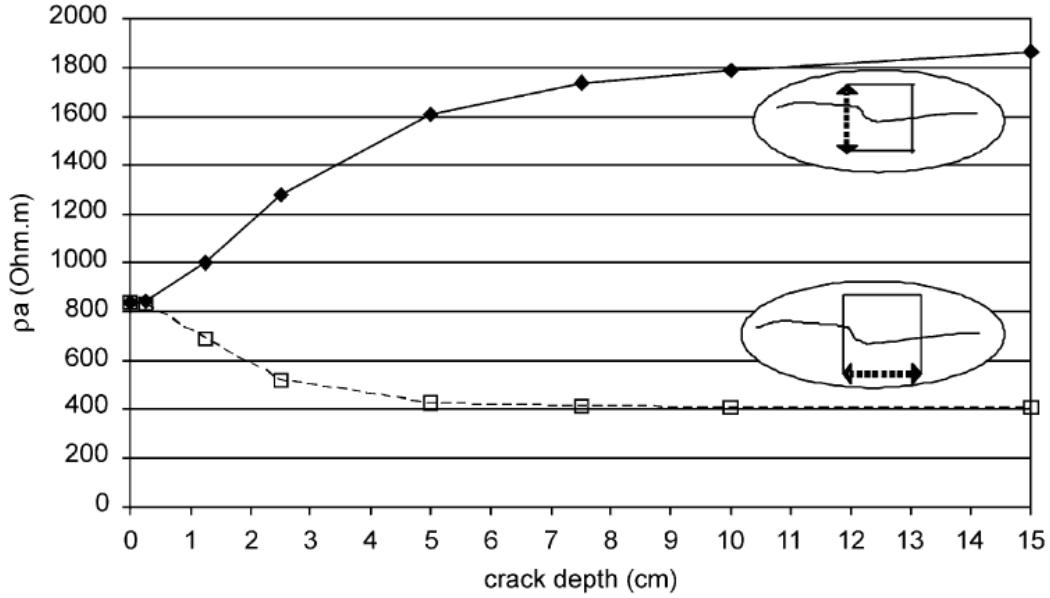

(a)

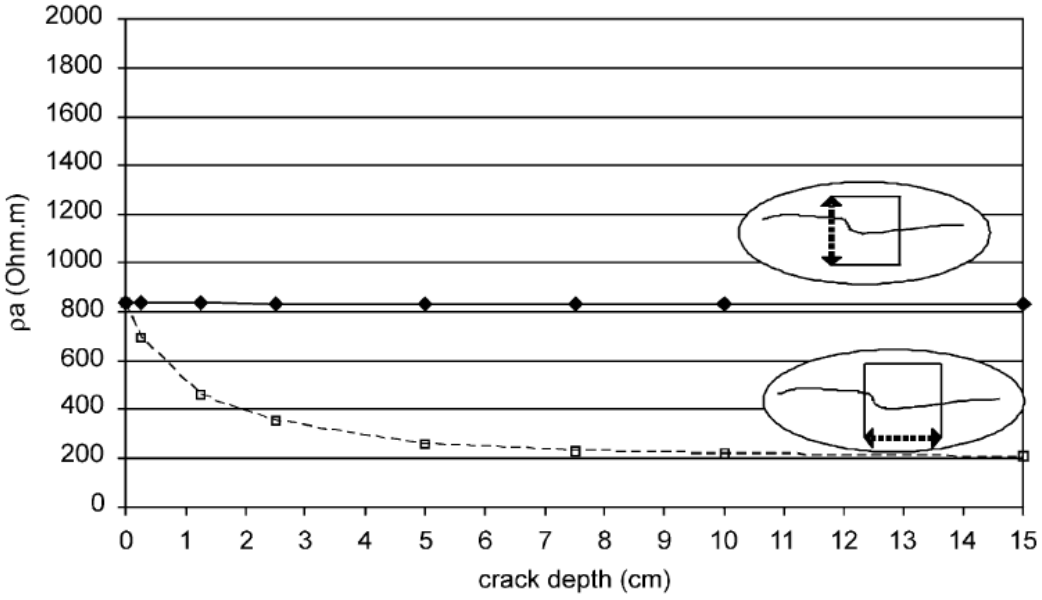

(b)

Figure 2-9: Resistivity measurement simulation in the presence of a crack using a square probe with electrode spacing of 50 mm (taken from Lataste et al., 2003). In this figure, the double headed arrow indicates two current imposing electrodes of the probe: (a) results from simulating resistivity measurement with insulated crack present; (b) results from simulating resistivity measurement with conductive crack present.

Goueygou et al. (2008) compared electrical resistivity measurements with transmission of ultrasonic waves for detecting surface cracks. Measurements were taken

on a sample concrete slab that was cracked via three-point loading. For electrical resistivity measurement, the same instrument as the one used by Lataste et al. (2003) was used, and both directions (parallel and perpendicular) were investigated. Goueygou et al. concluded that detecting mechanical damage in concrete is possible by means of electrical resistivity measurement for a single simple crack. However, as the number of cracks increased the interpretation of patterns became complex, and in most cases, impossible.

Wiwattanachang and Giao (2011) also experimentally investigated the possibility of monitoring crack development in concrete using electrical resistivity measurements. A Wenner probe configuration with varied electrode spacing was used to obtain electrical resistivity at different depths of beams. The obtained data were combined to draw a simulated image of electrical resistivity inside the beam. A sample concrete beam with inserted plastic sheets as artificial cracks and a beam with cracks being developed in it using four-point loading were used in the experiment. After correcting resistivity measurements for limitation in the geometry of the beam, results were presented; Figure 2-10 depicts some of the results obtained. In Figure 2-10(a) in which plastic sheets were implemented inside the beam to represent the crack, high electrical resistivity regions were observed at the proximity of the sheets indicating a major change in the measured electrical resistivity. Similarly in Figure 2-10(b) in which cracks resulted from four-point loading of the beam, distortion in the electrical resistivity image indicated changes in the electrical resistivity measurement at the proximity of the crack.

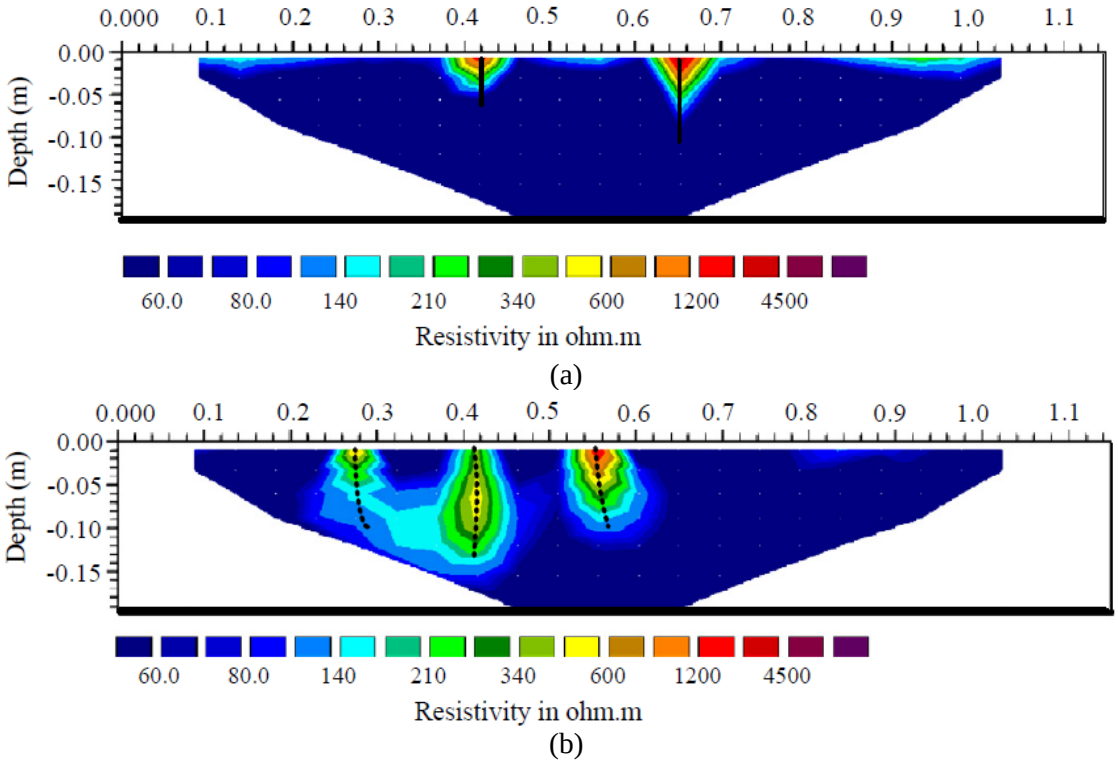

Figure 2-10: Electrical resistivity image of a concrete beam with cracks (Wiwattanachang and Giao, 2011): (a) concrete beam with artificial plastic sheets as crack; (b) concrete with cracks being developed from a four-point loading.

Despite of showing the possibility of using electrical resistivity measurement for detecting crack in concrete, Wiwattanachang and Giao didn't consider different types of cracks (i.e. conductive or insulated). Only insulated cracks were studied. Additionally, orientation of the crack toward the probe and its effect on resistivity measurements were ignored.

2.6 Multi-layered Structure

Most influential factors covered so far could be categorized as physical factors. There are other additional factors affecting electrical resistivity measurements in concrete. Factors such as carbonation, salt ingress or even moisture content could be

listed in this category, and this section reviews the literature on these factors (Millard, 1991; Morris et al., 1996; Saleem et al., 1996; Weydert and Gehlen, 1999; Sengul and Gjorv, 2008; Moreno et al., 2009).

Any variation on the surface of concrete could have an impact on the electrical resistivity measurements by the Wenner probe. One mechanism that has been addressed in the literature is the ingress of external ions through concrete cover. The section from the surface to the depth at which those ions have penetrated can be presumed to be a layer with different properties from the concrete below. Such processes create multilayered structures, and for these cases the assumption of homogeneity cannot be made. It should be noted that existence of such multilayered structures is not limited to ion ingress. Having uneven moisture content at the surface of concrete compared to its deeper sections, or partial carbonation of concrete cover, could also cause multiple layers in concrete. In addition, poor curing conditions might cause surface defects imitating such structure (Millard, 1991; Morris et al., 1996).

Saleem et al. (1996) showed that salt contamination would reduce the electrical resistivity of concrete. The amount of reduction was dependent on type of the ions, with chloride showing more adverse effects than sulphates. For concrete with 2% moisture content and additional 4.8 kg/m^3 of chloride concentration, the measured electrical resistivity was 140 Ω.m, whereas with 7.2 kg/m^3 of additional sulphate, electrical resistivity was in excess of 250 Ω.m. Increase in the moisture content was also found to decrease electrical resistivity of concrete (McCarter and Garvin, 1989; Saleem et al., 1996; Ostvik et al., 2006; Sengul and Gjorv, 2008). On the contrary, carbonation increases the electrical resistivity of concrete (Millard, 1991; Chi et al., 2002; Moreno et

al., 2009). Few researchers have tried to identify and quantify the influence of such multilayered structures on electrical resistivity measurements using Wenner probe.

Millard (1991) utilized finite element modeling and ran experiments on tank filled with conductive solutions to investigate the effect of multiple layers in concrete. Specifically, the presence of only one surface layer with the depth variable relative to electrode spacing was investigated. It was reported that depending on the resistivity of the surface layer one should expect different behaviour. For layers with resistivity higher than bulk concrete, if layer thickness was relatively small compared to electrode spacing, no significant effect was observed. Once the thickness of high resistivity layer increased to values close to electrode spacing, measurements mostly represented the resistivity of the surface layer rather than the bulk concrete. On the contrary, for a layer with smaller resistivity than the bulk concrete, even small layer thickness had significant influence on the results. It was also noted that the difference between the resistivity of the surface layer and the bulk concrete was an important factor.

Weydert and Gehlen (1999) also acknowledged the effect of multilayered structure and its influence on resistivity measurements. Experiments were carried out on concrete block specimens while taking resistivity measurement using a Wenner probe and a multi-ring electrode embedded in the block capable of measuring resistivity at certain depths. In this work, a multilayered concrete cover was created by partially carbonating the specimens and exposing the surface to water. The measurements were taken both in wet and dry conditions. Figure 2-11 illustrates the measured resistivity values in this study. First, considering the results for the driest condition (i.e., at 300 h), it can be seen that carbonated surface layer showed higher resistivity than the bulk concrete. More

importantly, while the resistivities at depths of 31 mm and 41 mm are the same, they are different at depths of 11 mm and 6 mm. This difference can be explained by considering the fact that moisture content and the degree of carbonation were different at different depths of concrete cover. Looking at the first half of this figure starting from time 0 to hour 150 h, designated as wetted concrete surface, it can be seen that as water penetrated into the block the resistivity of concrete decreased. Besides, the depth at which it was affecting varied with time. Measurements taken by the Wenner probe provided values which were neither the bulk resistivity nor the carbonation layers during the time which water was penetrating into the block. Weydert and Gehlen concluded that once concrete is wetted, Wenner probe resistivity measurements should be taken at least 50 hours afterwards to obtain stable results.

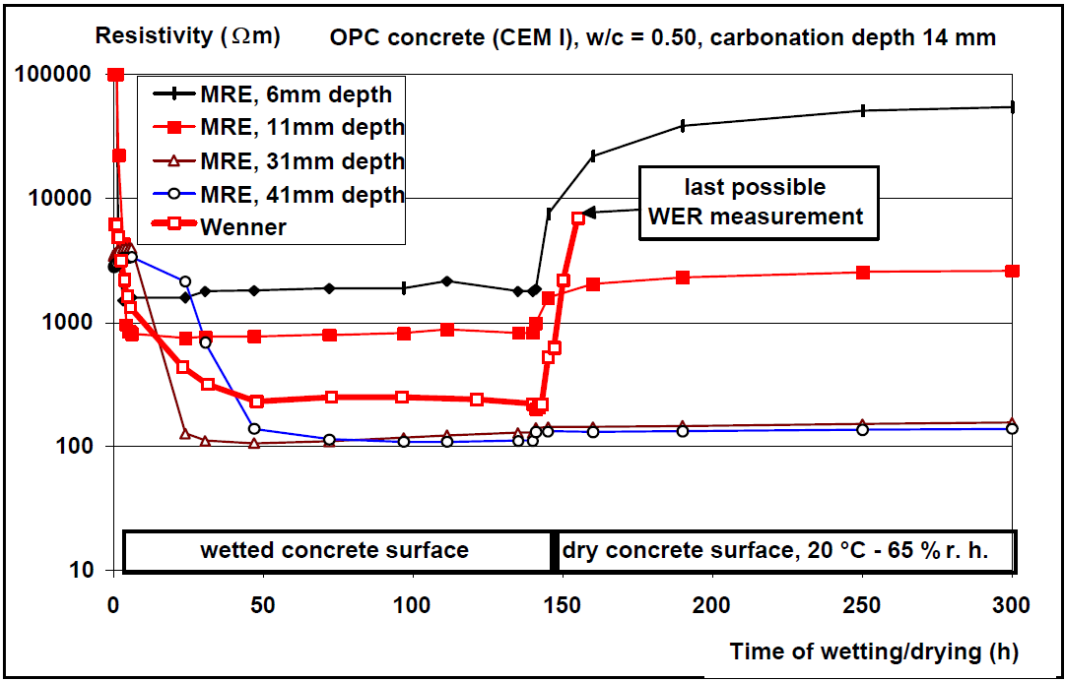

Figure 2-11: Resistivity measured variation on a wetted concrete slab with respect to time (taken from Weydert and Gehlen, 1999). In this figure, MRE represents Multilayer electrode ring that is capable of providing electrical resistivity at different depth.

Gowers and Millard (1999) provided more comprehensive data on the behaviour of Wenner probe in the presence of a multi-layered structure concrete. Both analytical solution for a multi-layered resistivity measurement and real measurements taken on a mortar or concrete were used in the study. Figure 2-12 depicts data provided for two different conditions. It was concluded that both thickness and resistivity of the surface layer plays a role on measurements taken. Similar to Millard (1991), having a surface layer with smaller resistivity was found to have more impact. More importantly, it was shown that once a carbonated concrete is wetted, a three layer structure would be created, and the influence of this configuration cannot be easily predicted.

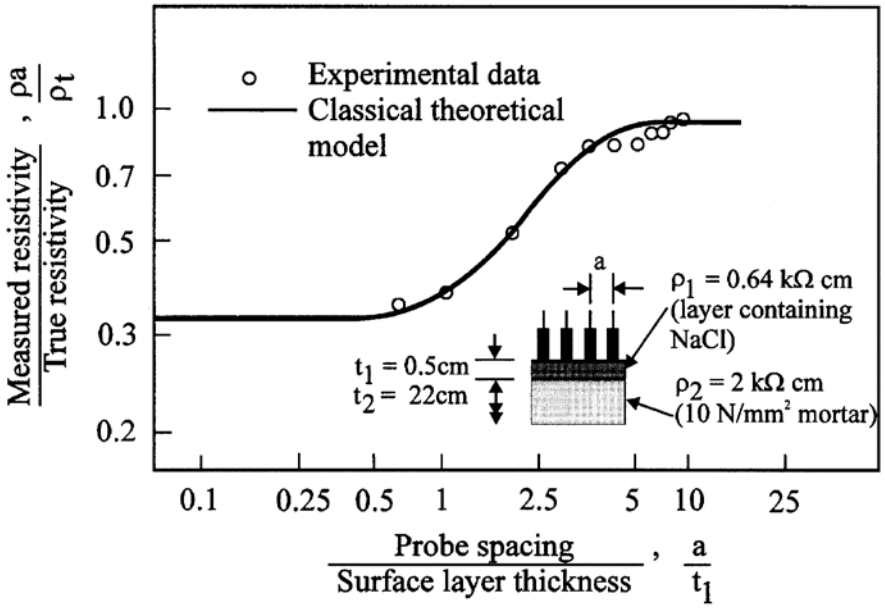

(a)

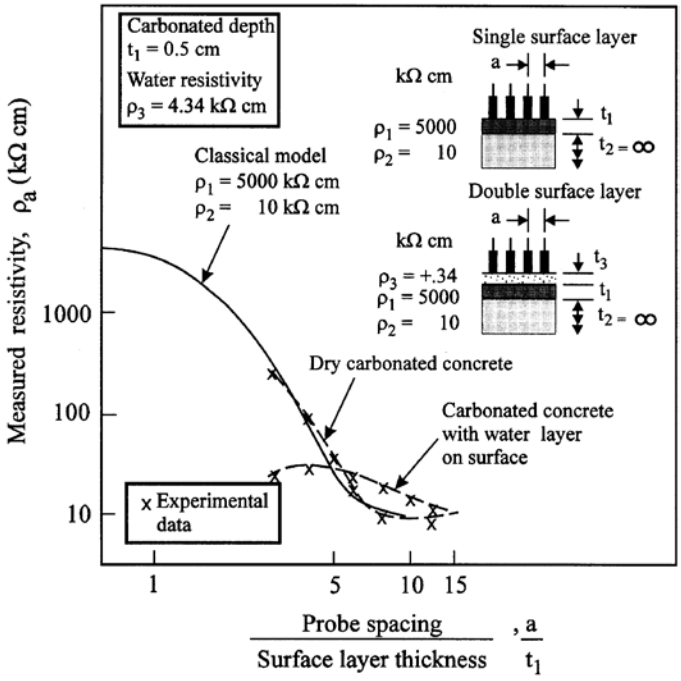

(b)

Figure 2-12: Impact from existence of multi-layered concrete cover on Wenner probe resistivity measurements (take from Gowers and Millard, 1999): (a) two layers one having resistivity less than the resistivity of concrete; (b) three layers one with a single additional layer with resistivity higher than concrete and two additional layers with lower and higher resistivity layers present.

Moreno et al. (2009) also studied the effect of multi-layered concrete structure on electrical resistivity measurements using Wenner probe using finite element modelling. Analytical solution for two layer structure was used to verify their FEM model for the multi-layered structure and all data presented and analyzed were obtained only from the FEM modeling approach. Only two-layer configuration for the effect of multi-layered concrete structure was considered; other investigated parameters were the depth of the surface layer and its resistivity, electrode spacing, presence of a single rebar, and the location of measurement with respect to the rebar. Results showed similar behaviour to previous works in the literature (Gowers and Millard, 1999). The main difference between this study and works done by others was addition of a rebar to the model and considering measurements taken at different locations with respect to the rebar. It was reported that the presence of rebar caused reduction in the electrical resistivity measurements regardless of the surface layer resistivity. Although new factors such as existence of rebar and location of the probe with respect to it was incorporated in the study of multilayered structure, simplification of reinforcement in concrete is one of the drawbacks. Impacts from possible crack on measurements were also ignored. Finally, neither a guideline was provided nor a specific conclusion was made for taking measurements using Wenner probe for actual practice of electrical resistivity measurement in the field when a rebar mesh was present.

2.7 Environmental Factors

The last category of influential parameters on the electrical resistivity of concrete is the environmental conditions in which measurements are taken. Some conditions such as rainfall on concrete or its exposure to chemicals although can be accounted as

environmental factors were discussed in Section 2.6 due to their special effect on creating a multi-layered structure. Temperature and humidity, on the other hand, is considered as parameters directly related to the ambient conditions in which measurements are taken.

Unlike conductive solid media such as metals in which electrons carry charges by creating a current flux, in concrete, ions are responsible for charge transfer. Both cases are directly under the influence of temperature; however, via different mechanisms. For electrolytes in which ions transfer electrical charges, as in the case of concrete, increase in temperature would cause the electrical resistivity to decrease since internal ionic frictions decrease (Polder et al., 2000; Chrisp et al., 2001; Brameshuber and Raupach, 2003). Relative humidity is also known to affect electrical resistivity of concrete. There is a relationship between relative humidity and moisture content in concrete, which can be presented by adsorption/desorption isotherm curves under equilibrium conditions (Enevoldsen et al., 1994).. Since moisture content in concrete affects its electrical resistivity and relative humidity has an influence on the moisture content, the electrical resistivity of concrete is affected by the variation of relative humidity (Polder et al., 2000). Moreover, Andrade et al. (1999) and Poyet (2009) have shown that temperature has an impact on concrete isotherm curves in such a way that at a constant relative humidity, increase in temperature tends to cause decrease in moisture content of concrete. It appears that variation in temperature has influence on concrete electrical resistivity both directly affecting ion movements and indirectly affecting the amount of water content inside concrete. Therefore, considering the impact of temperature and humidity on electrical resistivity is a complex task but essential (Polder et al., 2000). Unlike most factors covered in this chapter, influence of temperature and humidity on the electrical

resistivity measurement of concrete is independent of the technique. Hence, only a few studies will be reviewed in this section.

Millard (1991) used prism samples to investigate the effect of changes in temperature and humidity on electrical resistivity of concrete. It was concluded that in British environment, variations in relative humidity did not cause significant changes in concrete resistivity. This was related to the slow process of adsorption/desorption of water in ambient temperatures. Temperature variations, however, showed immediate and more noticeable effect. It was found that as temperature increased, the resistivity decreased. The results reported by Millard (1991) were obtained through measuring concrete resistivity using an inserted probe inside the concrete samples. Results represented the behaviour of concrete resistivity to change in temperature even though it was not obtained using Wenner probe.

Gowers and Millard (1999) have re-evaluated the earlier work done by Millard in 1991 to study the influence of environmental conditions on resistivity measurements. Unlike the earlier work, this time resistivity measurements were taken on prism concrete samples using a Wenner probe. In addition, temperature was measured inside the concrete, on its surface and in the air as well as recording relative humidity of the air. Similar to what Millard (1991) reported, it was also concluded that decrease in ambient temperature led to increase in resistivity readings. A correction factor of 0.33 KΩ-cm/°C was suggested to compensate for the variation in temperature as shown in Figure 2-13. On the other hand, it was reported that no clear correlation was found between changes in relative humidity of air and electrical resistivity. In spite of their effort to quantify the influence of temperature change on electrical resistivity measurement, the range of

temperatures used to make their conclusion (> 8°C and < 20°V) was limited and mostly applicable to British environment.

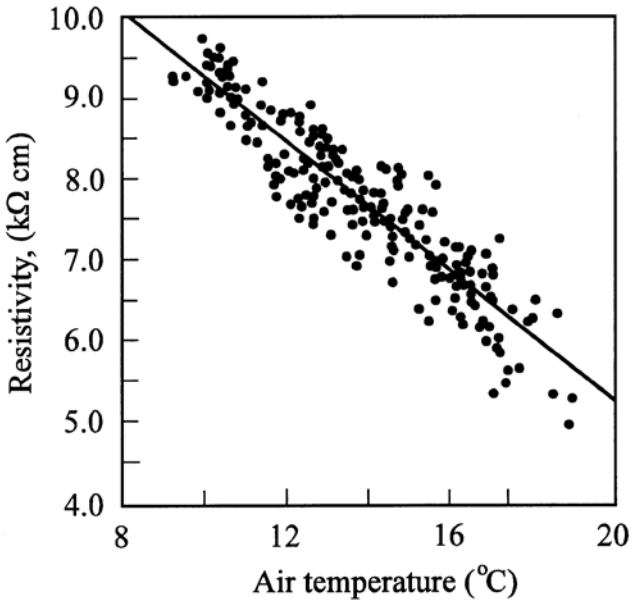

Figure 2-13: Relationship between ambient temperature and electrical resistivity of concrete (taken from Gowers and Millard, 1999).

Polder et al. (2000) suggested resistivity measurements on concrete not to be taken when ambient temperature is very cold or hot. Concluding prior studies on temperature dependence nature of electrical resistivity of concrete, a general correction figure of 3 ~ 5% per degree change in temperature was suggested to compensate this effect. It was also suggested by Polder (2000) that the temperature and humidity data during the measurements are recorded and reported along with resistivity data.

2.8 Summary and Gaps in Literature

A review of previous studies on parameters that might affect surface electrical resistivity measurement of concrete using Wenner probe was presented in this chapter. These factors were related to the specifications of the probe, the condition of the concrete

under investigation and its geometry, and environmental conditions. The effects of the presence of reinforcement and cracks in concrete were also reviewed.

As a result of this comprehensive literature review, the following areas were found not to be adequately investigated, and these areas establish the basis of the present research:

- In general, there is no systematic study showing how Wenner probe would behave in the presence of a crack. Lataste et al. (2003) showed that electrical resistivity measurements could be affected when there is a crack present in the vicinity of the probe. The orientation of the crack and its electrical characteristics would dictate how measurements would be altered. However, the probe used in the aforementioned study had different electrode configurations than the Wenner probe. Since location of the electrodes and direction of the imposed current with respect to the crack both impact measurements, it is expected to see different behaviour when Wenner probe is used.
- Study by Moreno et al. (2009) revealed that the performance of the Wenner probe could be affected when there is a rebar mesh within concrete. However, only a mesh with rebars spaced 200 mm apart and embedded 50 mm from the concrete surface were investigated. For more dense reinforcement detailing or different concrete cover thicknesses, it is not evident how measurements would be affected. The issue becomes more complex when probe electrode contact areas are directly above underlying rebars.

- There is no study in the literature showing how resistivity measurements would be affected when both reinforcement mesh and cracks are present in the measured area.

3. Numerical Modelling Approach

3.1 Introduction

The focus of this chapter is to provide an overview of the numerical solution algorithm used in the present study. It includes the details of the numerical model, mesh and domain analyses, and the experimental verification and benchmarking processes before it is used as a numerical tool to investigate different configurations and parameters that may affect Wenner probe based resistivity measurements.

3.2 Numerical Model

3.2.1 Governing differential equation

As explained in detail in Chapter 1, Wenner probes use four electrodes to make resistivity measurements on a concrete surface. Two outer electrodes are used to pass a stable AC current through concrete and the inner two electrodes are used to measure potential difference that form during this excitation at two specific points on concrete surface. The governing differential equation to model this process will need to simulate the electrical current flow and electrical potential distribution within the domain. The purpose of using AC signal in real life practice is to avoid polarization of electrodes in contact with concrete surface that occurs when a DC signal is being used. The presence of ions as the main source of carrying electrical charges in concrete is the cause of this polarization phenomenon. In typical finite element modelling of electrical current flow and potential distribution, differential equations that govern the behaviour of electrical

charge transfer are modelled independent of any specific type of electrical charge carrier, i.e., ions or electrons. Disturbing polarization effects can be eliminated in modelling studies by assuming perfect contact between electrodes and concrete surface. Thus, both AC and DC signals would produce similar results when electrical resistivity is modelled using the finite element method.

Assuming that a linear relationship exists between electrical potential distribution and current (Zimney et al., 2007), electrical current density vector, ***J***, passing thorough an enclosed surface within a control domain is directly related to the electrical field vector, ***E***, by a ratio defined as conductivity of the material via Ohm's Law (Telford et al., 1990):

$$\boldsymbol{J} = \frac{1}{\rho}\boldsymbol{E} \qquad \textit{3-1}$$

where ***J*** (A/m^2) is the current density vector, ***E*** (V/m) is electrical field vector, and ρ (Ω-m) is the electrical resistivity of the material, which is the inverse of electrical conductivity, σ.

Electrical field vector, ***E***, is the gradient of the electrical potential, *V* (V), such that:

$$\boldsymbol{E} = -\nabla \mathrm{V} \qquad \textit{3-2}$$

$$\boldsymbol{J} = -\rho^{-1}\,\nabla \mathrm{V} \qquad \textit{3-3}$$

Accumulation of electrical charge, does not happen when there is electrical conductivity and the total amount of electrical charge is conserved; i.e., the amount of current flux entering an enclosed surface of a conductive material will be equal to the amount of current flux exiting the surface; hence (Telford et al., 1990):

$$\nabla \cdot \boldsymbol{J} = -\frac{\partial Q}{\partial t} = 0 \qquad 3\text{-}4$$

where Q (C) is the electrical charge and t (s) is time.

Combining Equations 3-3 and 3-4 will yield:

$$\nabla \cdot (-\rho^{-1}\, \nabla V) = 0$$
$$\nabla \rho^{-1} \cdot \nabla V + \rho^{-1} \nabla^2 V = 0 \qquad 3\text{-}5$$

The first term in Equation 3-5, which contains the gradient of resistivity, can be eliminated if the medium is assumed homogeneous and isotropic. The remaining equation takes the form of the Laplace's equation, which governs the process electrical charge transfer in a material that typical Wenner probes use to make resistivity measurements:

$$\rho^{-1}\, \nabla^2 V = 0 \qquad 3\text{-}6$$

3.2.2 Domain and boundary conditions

Figure 3-1 illustrates the domain and different types of boundaries used solve the governing equation given in Equation 3-5 within a given domain. For the clarity of presentation, the subdomains and boundary are shown on a two-dimensional cross section taken from the actual three-dimensional domain. Two types of boundary conditions were used in this study: those governing internal boundaries between subdomains (Ω_1 to Ω_8), and those imposed on external boundaries. Internal boundaries (shown as Γ_{11} to Γ_{19} in Figure 3-1(b)) define current fluxes normal to the surface of the boundary on either sides that are equal and opposite to each other such that:

$$\boldsymbol{n} \cdot \boldsymbol{J_1} - \boldsymbol{n} \cdot \boldsymbol{J_2} = 0 \quad \therefore \quad \boldsymbol{n} \cdot \left(\frac{\boldsymbol{E}}{\rho_1}\right) = \boldsymbol{n} \cdot \left(\frac{\boldsymbol{E}}{\rho_2}\right) \qquad 3\text{-}7$$

where indices 1 and 2 represent two adjacent domains sharing the same internal boundary. These boundary conditions do not need to be defined in the finite element method as they are implicitly imposed within the algorithms such that electrical potential V (V) has the same value at the shared nodes between the two adjacent subdomains:

$$V_1 = V_2 \qquad 3\text{-}8$$

For the external boundaries (shown as Γ_1 to Γ_{10} in Figure 3-1(b)), Neumann boundary conditions were imposed. Neumann boundary condition dictates the amount of current flux passing through a surface in the direction normal to the surface. For insulated boundaries the flux was assumed zero such that:

$$\boldsymbol{n} \cdot \nabla V = 0 \quad \therefore \quad \boldsymbol{n} \cdot -\boldsymbol{E} = 0 \quad \therefore \quad \boldsymbol{n} \cdot \boldsymbol{J} = 0 \qquad 3\text{-}9$$

Electrical current imposed by the Wenner probe is the external source of current that will create internal current fluxes. Two point current sources, P_1 and P_2, as depicted in Figure 3-1(b) were used for simulating injection of an external electrical current. The two current sources should have equal and opposite values considering Equation 3-4. Calculation of electrical resistivity using Wenner probe is independent from the value of this electrical current, thus for ease of calculations, a value of 1 A was used in this study such that:

$$\text{P1: } \nabla \cdot \boldsymbol{J} = \frac{\partial Q}{\partial t} = \frac{-1\text{C}}{\text{s}} = -1\ \text{A}$$

$$\text{P2: } \nabla \cdot \boldsymbol{J} = \frac{\partial Q}{\partial t} = \frac{1\text{C}}{\text{s}} = 1\ \text{A}$$

In Figure 3-1(c), typical subdomains are shown: Ω_1 to Ω_6 represent concrete while Ω_7 and Ω_8 represent embedded rebars. Ω_1 is the main subdomain where electrical potential and current flux distributions are investigated. The external subdomains labeled Ω_2 to Ω_6 are discretized such that they represent infinite element subdomains to eliminate the size effect of the domain on the numerical solution.

For cases in which a crack was present, as illustrated in Figure 3-2, crack boundaries Γ_{20}, Γ_{21} and Γ_{22} were modelled as Neumann boundary conditions. For insulated cracks, the current flux was assumed equal to zero. For conductive cracks these boundaries acted as internal boundaries between the concrete and the conductive crack.

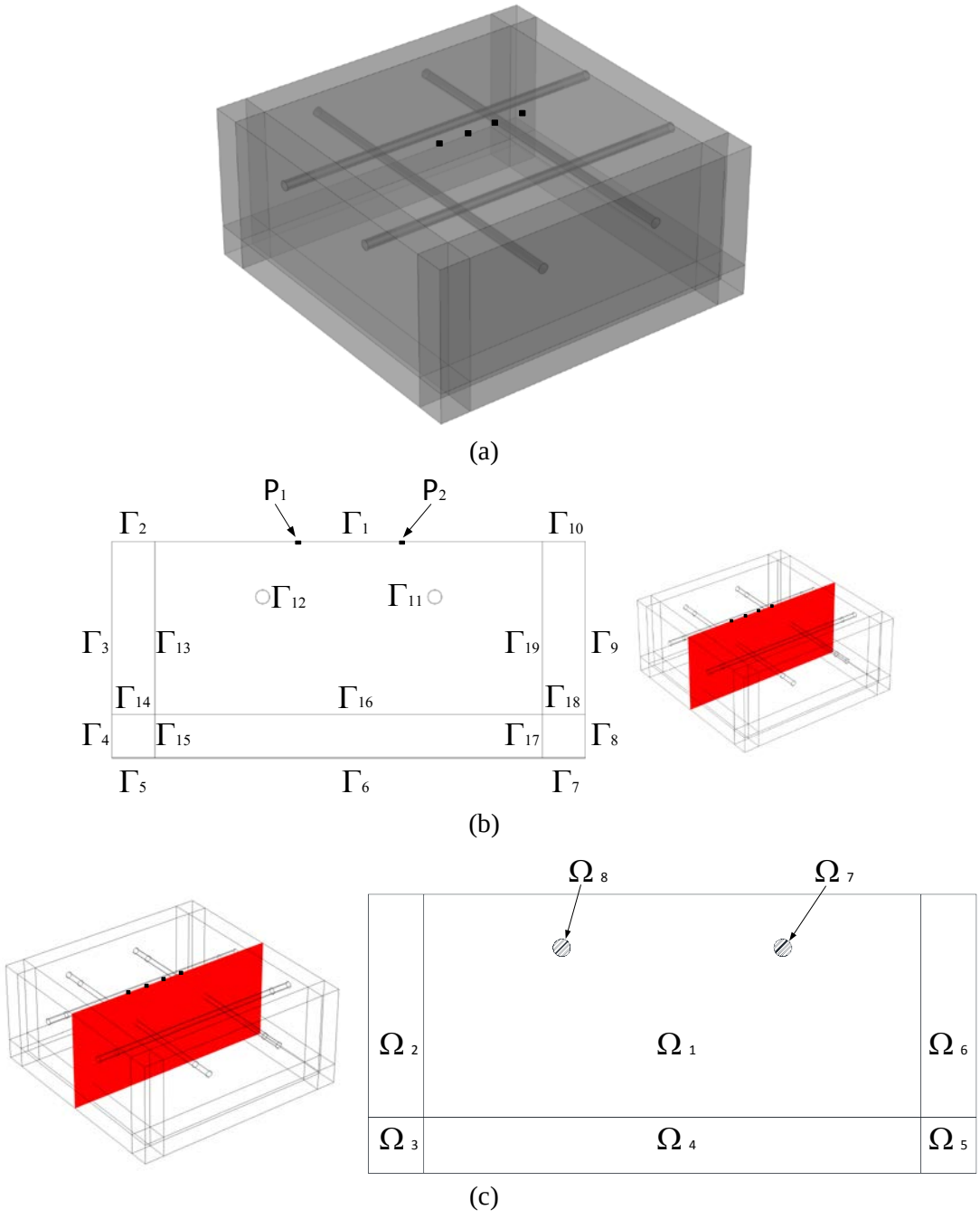

Figure 3-1: Domain and boundaries of a typical case with reinforcement solved for predicting electrical resistivity measurement using the Wenner probe: (a) the domain with embedded rebars; (b) internal and external boundaries shown on a cross section passing through the domain; (c) subdomains labeled on a cross section of the domain.

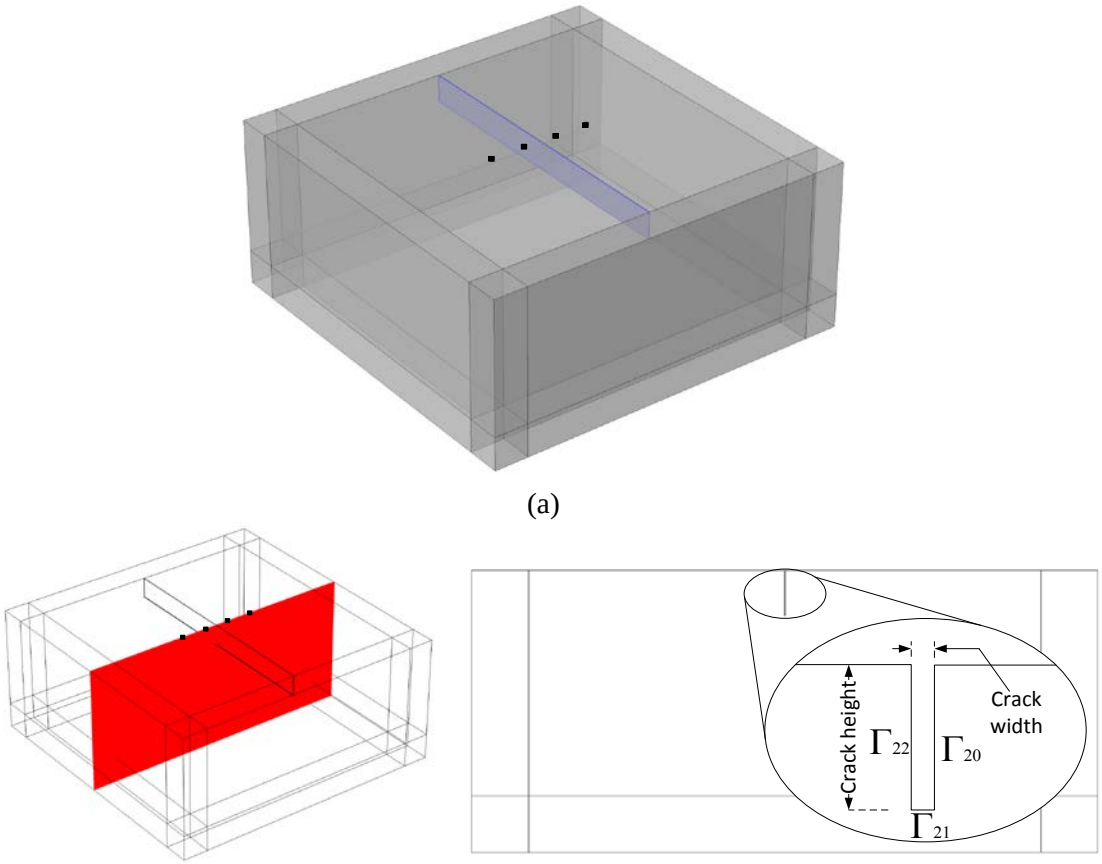

Figure 3-2: Domain and boundaries of a typical case including a crack solved for predicting electrical resistivity measurement using the Wenner probe: (a) the domain with crack as its feature; (b) a cross section of the domain and detailed view of boundaries related to the crack on the cross section.

3.2.3 Solution process

The numerical problem described in Sections 3.2.1 and 3.2.2 was solved using a commercial finite element analysis software package called COMSOL Multiphysics V4.3a. As an example, Figure 3-3 illustrates one of the implemented cases used for predicting electrical resistivity measurement using the Wenner probe.

The subdomain Ω_1 was a block with dimensions of L = 450 mm, W = 450 mm, and H = 200 mm. Subdomains Ω_2-Ω_6 were created around Ω_1 by extending domain by a thickness of 50 mm in all directions except at the top, as illustrated in Figure 3-3 (c). To keep the main subdomain size small for computational efficiency and accuracy, these surrounding subdomains were discretized using infinite elements (COMSOL, 2012).

An electrical resistivity of 40 Ω-m was assigned to the finite elements in all subdomains representing concrete. Finite elements representing rebars were assigned an electrical resistivity of 25×10^{-6} Ω-m. Other properties of the model are shown in Table 3-1.

Table 3-1: Parameters and their values for a sample case simulated to predict performance of Wenner probe.

Parameter Name	**Parameter Description**	**Assigned value**
$\rho_{concrete}$	Resistivity of domain representing concrete	40 Ω-m
ρ_{rebar}	Resistivity of domain representing rebars	25×10^{-6} Ω-m
ϕ	Diameter of rebars	16 mm
S	Rebar spacing	200 mm
a	Electrode spacing of the Wenner probe	50 mm
I	Electrical current imposed into the domain	1 A

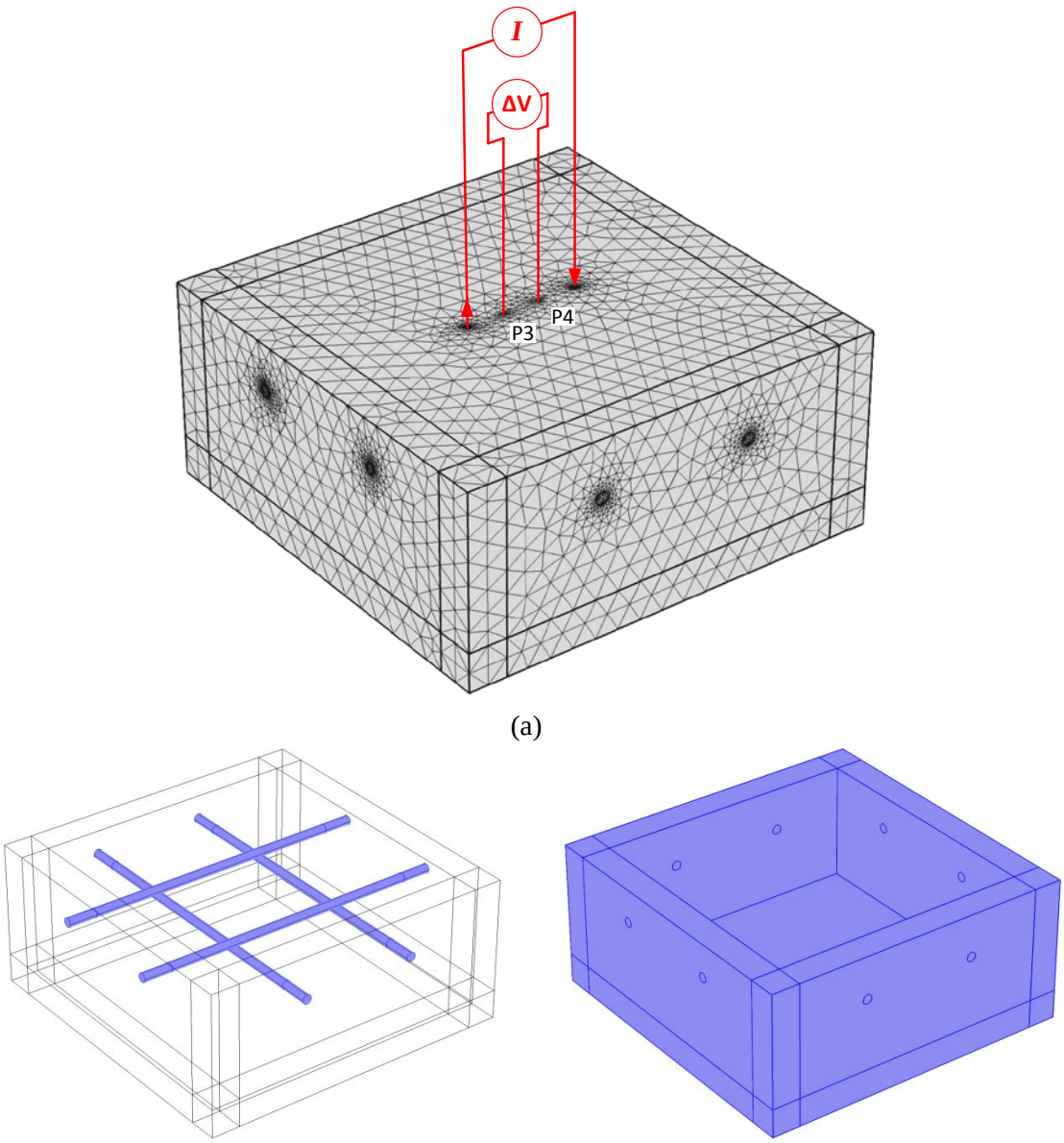

Figure 3-3: The domain for the sample analysis: (a) the discretized domain; (b) embedded rebars implemented as subdomains with an electrical resistivity of 25×10^{-6} Ω-m; (c) infinite element subdomains.

The control parameters for the discretization of the domain are explained in detail in Section 3.3. The default conjugate gradients solver was used to solve the matrix equations to obtain the electrical potential, *V*, for every node in the domain; after post-processing of the finite element results current fluxes in each element were also obtained.

Figure 3-4 illustrates the distribution of current flux and equipotential lines inside the domain across a cut section in the middle that passes through four points representing Wenner probe electrodes. Comparing this figure with the one shown in Figure 1-4(b), one can easily recognize major differences in the current flux and equipotential lines from the ideal distributions without the presence of rebar mesh.

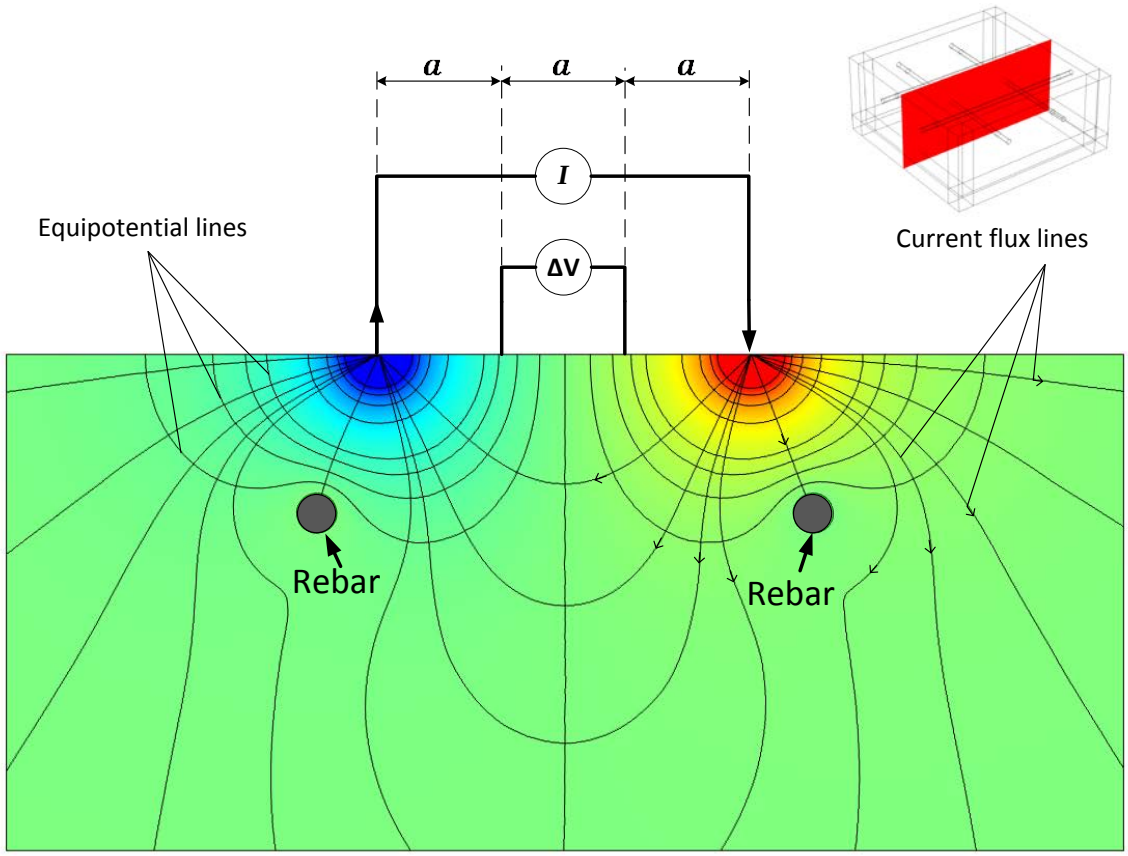

Figure 3-4: Electrical potential distribution and current flow lines for simulated Wenner probe resistivity measurement in the presence of a rebar mesh. Note: Infinite element subdomains are not shown in this figure.

In Wenner probes, the amount of electrical current imposed is usually predefined or measured internally; in either case it is a known parameter for the device. The distances between the electrodes are also known to the instrument. The only parameter being measured that is related to the resistivity of concrete is the electrical potential difference

between the two inner electrodes. Once all the known and measured data are used in Equation 1-1, the electrical resistivity of the concrete is calculated. For consistency, a similar approach should be followed numerically to predict Wenner probes performance. Hence, the following approach is used to extract concrete resistivity information from the finite element simulation data: a fixed 1 A electrical current was imposed into the domain. Once the solution for electrical potential distribution was obtained, the electrical potential difference between the two inner points, P3 and P4 in Figure 3-3(a), was calculated. For the example case presented in this section, the electrical potential of each point was, P3 = -55.2 V, P4 = 55.2 V. Electrical potential difference was ΔV = 110.4 V. Using Equation 1-1 predicted electrical resistivity was:

$$\rho = 2\pi a \frac{\Delta V}{I} = 2\pi \times 0.05\ (m) \frac{110.4\ (V)}{1\ (A)} = 34.7\ (\Omega\text{m})$$

It should be noted that the electrical resistivity of concrete in the model was defined to be 40 Ω-m. This indicates using electrical potential difference between the two inner electrodes of the Wenner probe and Equation 1-1 which was derived based on homogeneity and isotropic performance of a material under test would provide a resistivity value that is an underestimate of the actual electrical resistivity of concrete in the presence of the rebar mesh. By dividing this calculated electrical resistivity to the actual predefined value for the domain, a ratio could be obtained indicating scale of deviations that can be experience when real Wenner probe is used in the same conditions.

3.3 Mesh Analysis and Domain Optimization

An extensive study was carried out to investigate the effect of different mesh configurations on the performance of the model. For this purpose, the mesh size and type

as well as the size of the domain were examined in six stages. Mesh analysis was conducted using COMSOL's default mesh analysis settings, which allow the user to control the predefined finite element size parameter (e.g. "*Normal*", "*Fine*", "*Finer*", "*Extra Fine*", and "*Extremely Fine*"). The domain was discretized using linear tetrahedral elements as shown in Figure 3-5. Details regarding to properties of predefined mesh sizes are shown in Table 3-2. In this table, maximum and minimum element size, refer to the length of longest edge of a tetrahedral element.

Table 3-2: Parameters for the predefined element sizes in COMSOL.

	Predefined element size type				
Parameters	**Normal**	**Fine**	**Finer**	**Extra Fine**	**Extremely Fine**
Max. element size (m)	0.055	0.044	0.0303	0.0193	0.011
Min. element size (m)	0.0099	0.0055	0.0022	8.25×10^{-4}	1.1×10^{-4}
Max. element growth rate	1.5	1.45	1.4	1.35	1.3
Resolution of curvature	0.6	0.5	0.4	0.3	0.2
Resolution of narrow regions	0.5	0.6	0.7	0.85	1

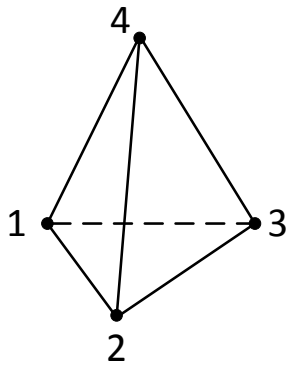

Figure 3-5: Linear tetrahedral mesh element with four nodes.

The initial geometry of the domain was selected with respect to prior recommendations made by Gowers and Millard (1999) to minimize the effect of

geometry on Wenner probe measurements. The configuration is depicted in Figure 3-6. The electrode spacing of 50 mm was used for mesh analysis and domain optimization similar to Gowers and Millard (1999). Based on their recommendation, Wenner probe resistivity measurements should be taken on a surface with a clear distance of twice the electrode spacing with the sides and four times of the electrode spacing to the bottom of the material. To satisfy this condition, the following dimensions were used for the domain Ω_1: L = 350 mm, W = 200 mm and H = 200 mm.

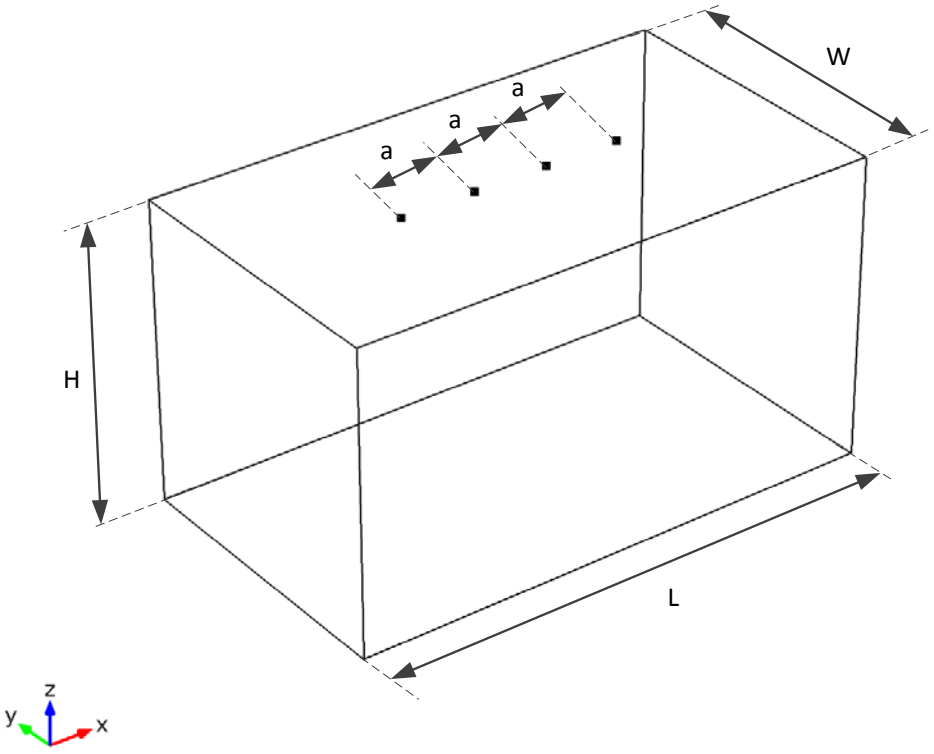

Figure 3-6: Initial domain geometry considered for mesh analysis i.e., Ω_1.

In order to obtain a quantitative measure for the quality of the simulation results, a coefficient of determination (R^2) was calculated via (Berthouex and Brown, 2002; Dean and Illowsky, 2013):

$$R^2 = 1 - \frac{SS_{err}}{SS_{tot}}$$

$$SS_{err} = \sum (y_i - f_i)^2 \qquad \textit{3-10}$$

$$SS_{tot} = \sum (y_i - \overline{y})^2$$

where SS_{err} is the residual sum of squares, SS_{tot} is the total sum of squares, y_i is actual value for a given node *i*, f_i is the predicted value for point *i* and $\bar{y}$ is the mean of the actual values at all nodes. When R^2 becomes closer to one, predicted parameter using a certain model would be better for a set of data.

For comparison with analytical results, a misfit function can be defined such that:

$$misfit = 1 - R^2 = \frac{SS_{err}}{SS_{tot}} = \frac{\int (V_a - V_n)^2 \, dV}{\int (V_a - \bar{V}_a)^2 \, dV} \qquad \textit{3-11}$$

where V_a is the electrical potential calculated for a given node in the domain from analytical solution, and V_n is the electrical potential obtained from numerical solution for the same node.

Misfit value provides a measure of how close numerical values are to the analytical solution. It should be noted that this approach must be used with caution since it will consider the misfit between the model predictions and the analytical values for the entire domain (for all nodes); the error in localized zones (e.g. near current probes on the concrete surface) within the domain can still be large. These cases will be studied separately in Section 3.3.8. As the misfit function gets closer to zero the model results

would be more accurate with respect to the analytical solution in general (Butler and Sinha 2012). In COMSOL, both residual sum of squares and total sum of squares in Equation 3-11 were calculated by taking the integral over the volume of the central subdomain surrounded by infinite subdomains. Due to the symmetry of the model caused by the two equal and opposite current sources, the mean value ($\overline{V_a}$) in Equation 3-11 is equal to zero.

3.3.1 Analytical solution

In order to conduct mesh and domain analysis studies as well as to verify the finite element model developed for this research, the analytical solution of a simple case was used for comparison purposes. Figure 3-7 shows a simple idealistic scenario for which one current imposing electrode is located on the surface of semi-infinite homogeneous isotropic material while the other electrode for returning current is located at infinity (not shown).

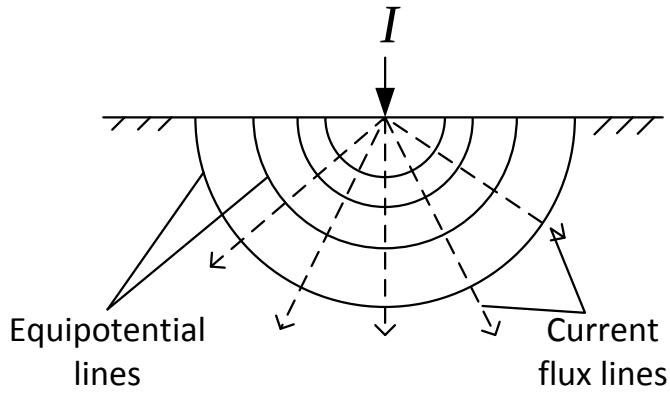

Figure 3-7: Equipotential and current flux lines created inside a semi-infinite domain where one electrode is on the surface and the other one is at infinity.

The electrical potential of any point inside this material can be calculated via (Telford et al., 1990):

$$V = \left(\frac{I\rho}{2\pi}\right)\frac{1}{r} \qquad 3\text{-}12$$

where r (m) is the radial distance from the current source, I (A) is the amount of current injected into the material.

Considering two independent current electrodes are placed on the surface of a material as illustrated in Figure 3-8 (one injects current in the opposite direction of the other electrode), electrical potential at any point can be calculated using superposition.

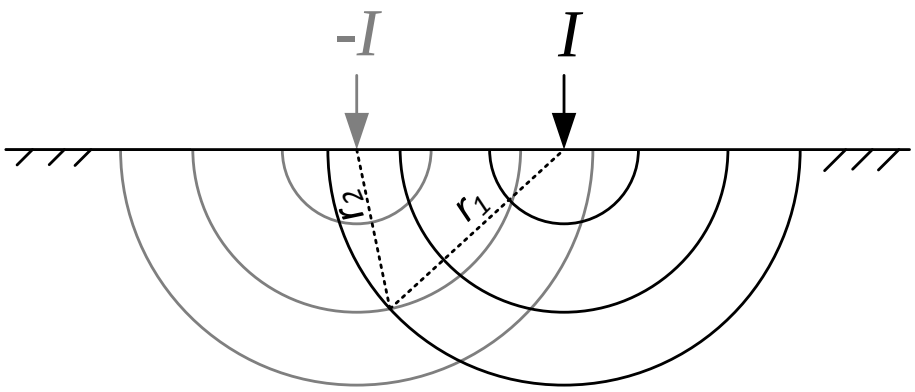

Figure 3-8: Equipotential lines and current flux distribution inside a material when two independent current electrodes are placed on the surface concrete.

Electrical potential of any points is the summation of electrical potential created by each one of the current sources that can be obtained via:

$$V = \left(\frac{I\rho}{2\pi}\right)\frac{1}{r_1} - \left(\frac{I\rho}{2\pi}\right)\frac{1}{r_2} \qquad 3\text{-}13$$

where r_1 (m) is the radial distance from the first current source point and r_2 (m) is the distance to the second current source.

Extending this scenario to the case for which Wenner probe is used, as illustrated in Figure 3-9, the potential difference between the two inner electrodes can be calculated using Equation 3-13 such that:

$$\Delta V = \left(\frac{I\rho}{2\pi}\right)\left\{\left(\frac{1}{a}-\frac{1}{2a}\right)-\left(\frac{1}{2a}-\frac{1}{a}\right)\right\} = \left(\frac{I\rho}{2\pi}\right)\frac{1}{a} \qquad 3\text{-}14$$

With a known value of current (I) and measured potential (ΔV), Wenner probe can be used to obtain resistivity (ρ) of the medium using Equation 3-14.

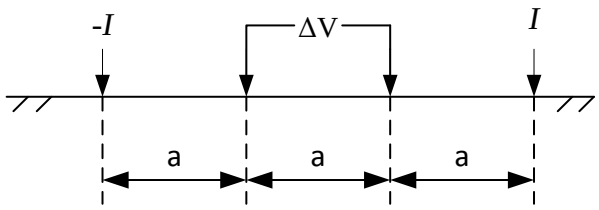

Figure 3-9: The schematic for the Wenner probe electrical potential calculation scheme.

3.3.2 Mesh analysis stage 1 - effect of mesh size

The effect of different mesh sizes on the quality of the results was evaluated in the first stage. Results showed that by decreasing mesh size in general more accurate predictions were obtained; however, the number of elements created in the domain increased as well. This led to longer simulation times and larger files to store the data. As seen in Table 3-3, value for the misfit function, which is always a number between 0 and 1 with 0 being the best and 1 the worst, is considerably high being close to 0.7 for all cases at this stage. This means that even considering the guidelines provided by Gowers and Millard (1999) to obtain the initial domain size, Figure 3-6, is not suitable for modeling purposes as the electrical potential distribution inside the central subdomain is

very different from the analytical solution. This happened since current fluxes were confined from the sides and depth of the domain that in theory assumed to be infinite. The *"Finer"* meshing style that provided reasonably good results with the minimum amount of the processing time, was selected as a base for the next stage.

3.3.3 Mesh analysis stage 2 - effect of mesh size around current electrodes

In theory, the electrical potentials at the current insertion points should reach infinity (either positive or negative depending on the direction of the current introduced). The implication of this is that electrical potentials should have an asymptotic shape in the proximity of current probes. Sharp changes in the electrical potential close to current injection points would disturb both the solution and misfit value at the proximity of these locations, and this effect would depend on local mesh discretization. Therefore, to have a consistent way of measuring the misfit value it is essential to control the size of the mesh around current electrodes (Butler and Sinha, 2012). This effect was studied in this stage so that the optimum mesh size around current electrode probes is determined. The values for the maximum mesh size as well as the obtained results are available in Table 3-3. As the mesh size reduced, the solutions quality and the consistency of the results were slightly improved. Therefore, for next stages, maximum mesh size possible was selected using the element size of 10^{-4} m at the vicinity of current insertion points.

3.3.4 Mesh analysis stage 3 - effect of domain depth on the solution

Infinite element subdomain was introduced in this stage to numerically mimic the increase in the model size in the z-direction (domain height). The addition of the infinite

element domain to the model in the z-direction is illustrated in Figure 3-10. The advantage of infinite elements is its capability to simulate infinite sizes with limited additional number of elements. The size of the infinite subdomain was varied in order to see its effect on the results. No significant changes were observed as the size of the subdomain increased; however, 70% decrease in the value of the misfit was observed as infinite element was introduced. Deviation of the predicted electrical resistivity from its assigned value was also reduced to around 10% which complies with expected value reported by Gowers and Millard (1999).

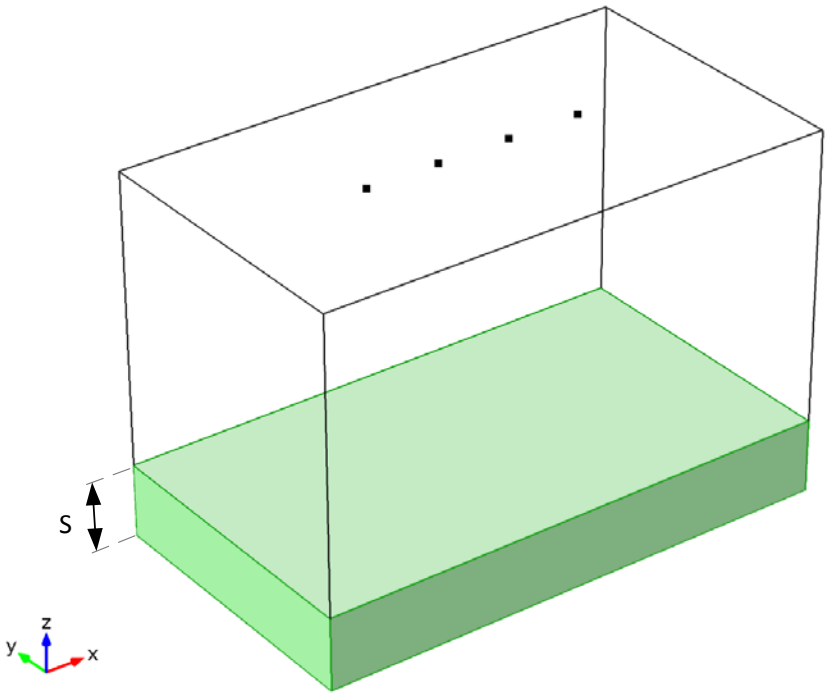

Figure 3-10: Infinite element subdomain added for stage 3 of mesh analysis.

3.3.5 Mesh analysis stage 4 - effect of model geometry

Following the addition of the infinite element subdomain in the z-direction, it was then added to the other two directions (X and Y) as illustrated in Figure 3-11. Similar to

the previous stage, the thickness of the infinite elements was varied and the results were recorded. As shown in Table 3-3, the misfit value dropped significantly by more than three orders of magnitude once the infinite elements were introduced. Butler and Sinha (2012) reported that size of these subdomains had significant effect on the quality of the model and the corresponding results. It was also suggested that the size of the infinite elements should be kept larger than 20% of the dimension intended to be expanded. On the contrary, outcomes of this analysis showed that even infinite elements with the size as small as 10% did not influence the results noticeably. This might be due to the fact that the initial geometry used in this study was larger; thus, the size of infinite element subdomains were not as critical. The results confirmed the accuracy of the numerical solution with respect to the analytical one. To account for unknown conditions and also keep the total number of elements as low as possible, the size of infinite element subdomains in all three directions were chosen equal to quarter of the domain height; i.e., $H/4 = 50$ mm.

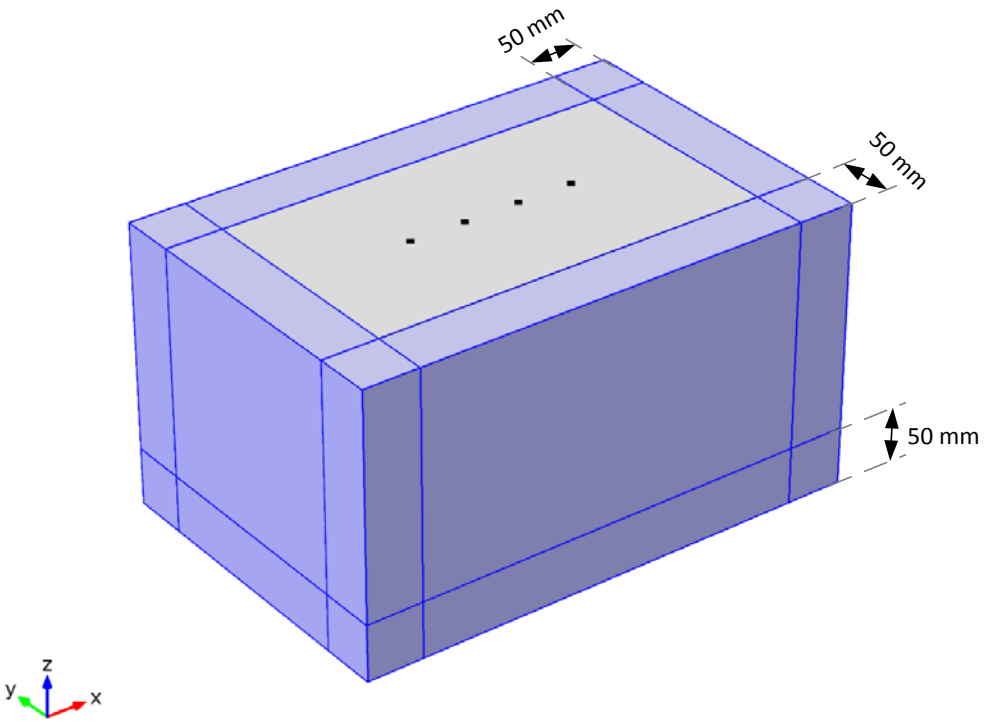

Figure 3-11: Three dimensional infinite element subdomains surrounding the central subdomain used for calculating misfit and predicting electrical resistivity.

3.3.6 Mesh analysis stage 5 - effect of mesh size around potential electrodes

In this stage, further attention was paid to the influence of mesh resolution at the vicinity of the potential reading points. The maximum element size was changed by three orders of magnitude from 10^{-2} m to 10^{-4} m. Simulation results showed that this variation slightly increased the misfit value while at the same time improved electrical resistivity predictions, as shown in Table 3-3. The decrease observed in the quality of the model predictions due to the increased misfit value was not as significant as the improvement achieved through measuring resistivity. Hence, the maximum mesh size of 10^{-3} m was

picked at the proximity of the potential reading electrodes to both increase the resolution and keep the number of total number of elements low.

3.3.7 Mesh analysis stage 6 - mesh size effect re-evaluation

After evaluating and analyzing several aspects of the model in previous stages, a final mesh analysis was performed. This was to reconfirm the model's performance and compare its results with conditions for which smaller mesh sizes had been used in stage 1. Hence, global mesh size was reduced from *"Finer"* to *"Extra fine"* and *"Extremely fine"*. All three mesh sizes produced results that were accurate enough for the purpose of this study, as shown in Table 3-3. The error in the resistivity predictions was lower than 0.15% while the misfit value was in the order of 10^{-5}. The best result was obtained from mesh size of *"extremely fine"* with considerable number of elements, but this case required a large amount of processing time and large hard disk space for storing the data. Both *"Extra fine"* and *"Finer"* general mesh sizes could have been used depending on the condition since they were accurate enough for this study. Eventually, almost all cases were discretized using *"Finer"* mesh size in models used for this study. Figure 3-12 depicts electrical potential distribution at the depth of 50 mm from the surface of the model. The green region on the edges clearly indicates that the infinite element subdomains were extended to infinity where electrical potential reached to a value of zero.

Table 3-3: Summary of the mesh and domain analysis.

	Model type and parameters					Modeling Data			Solution Data	
Stage	**Meshing style**	**Max. element size (m)**		**Infinite elements**		**Misfit (1-R^2)**	**# of elements**	**Min. element quality***	**Predicted to actual resistivity ratio**	**% error in predicted electrical resistivity**
		Current points	**Potential points**	**Direction**	**Size**					
1	normal	-	-	-	-	0.712	5,173	0.46	1.184	18.4
	fine	-	-	-	-	0.705	10,142	0.38	1.183	18.3
	finer	-	-	-	-	0.706	31,984	0.45	1.175	17.5
	extra fine	-	-	-	-	0.700	127,431	0.37	1.179	17.9
2	finer	10^{-2}	-	-	-	0.699	32,011	0.48	1.179	17.9
	finer	10^{-3}	-	-	-	0.697	33,873	0.46	1.178	17.8
	finer	10^{-4}	-	-	-	0.696	38,462	0.38	1.177	17.7
3	finer	10^{-4}	-	Z	H/10	0.213	40,990	0.39	1.118	11.8
	finer	10^{-4}	-	Z	H/4	0.213	44,858	0.41	1.118	11.8
	finer	10^{-4}	-	Z	H/2	0.213	53,185	0.41	1.118	11.8
	finer	10^{-4}	-	Z	H	0.213	48,638	0.40	1.118	11.8
4	finer	10^{-4}	-	X,Y,Z	H/10	6.97×10^{-4}	38,135	0.35	0.993	0.663
	finer	10^{-4}	-	X,Y,Z	H/4	8.83×10^{-5}	41,130	0.35	0.997	0.305
	finer	10^{-4}	-	X,Y,Z	H/2	4.15×10^{-5}	44,349	0.40	1.002	0.205
	finer	10^{-4}	-	X,Y,Z	H	3.20×10^{-5}	47,989	0.40	0.998	0.209
5	finer	10^{-4}	10^{-2}	X,Y,Z	H/4	1.04×10^{-4}	41,539	0.35	0.998	0.180
	finer	10^{-4}	10^{-3}	X,Y,Z	H/4	9.47×10^{-5}	43,682	0.35	0.999	0.142
	finer	10^{-4}	10^{-4}	X,Y,Z	H/4	1.26×10^{-4}	46,989	0.35	0.999	0.146
6	finer	10^{-4}	10^{-3}	X,Y,Z	H/4	9.47×10^{-5}	43,682	0.35	0.999	0.142
	extra fine	10^{-4}	10^{-3}	X,Y,Z	H/4	5.20×10^{-5}	145,369	0.36	0.999	0.082
	extremely fine	10^{-4}	10^{-3}	X,Y,Z	H/4	3.13×10^{-5}	776,150	0.28	1.000	0.037

(*): Minimum element quality is the internal calculated value by the COMSOL software for quality of elements generated during discretization of the model. Valuse > 0.2 are considered not affecting the solution.

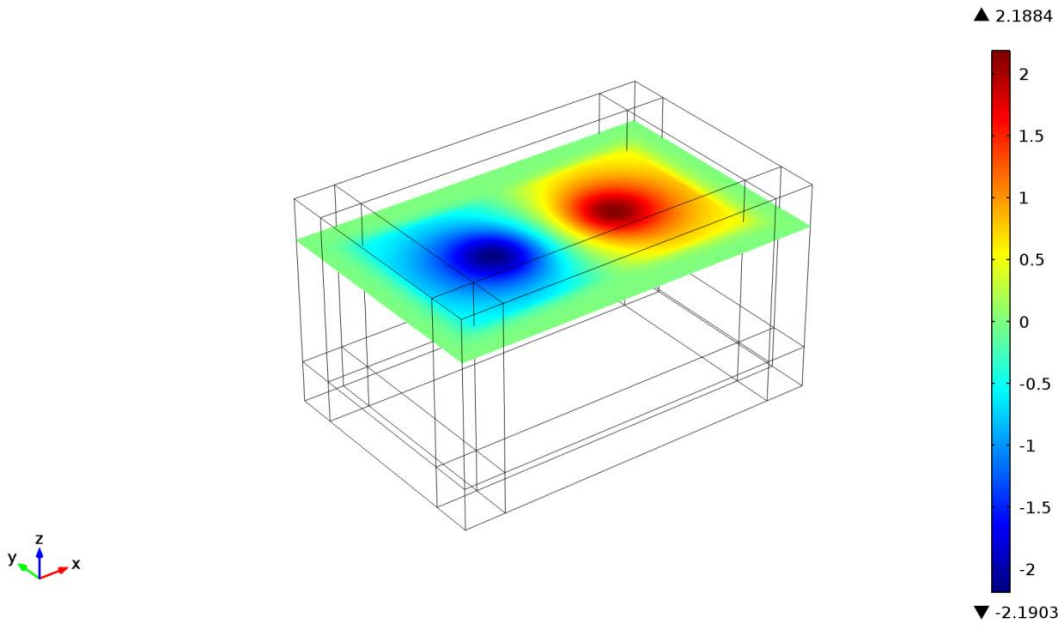

Figure 3-12: Electrical potential distributaion at the depth of 50 mm.

3.3.8 Accuracy of the predictions on the concrete surface

In previous mesh analysis stages, the misfit value was calculated for the entire volume of the central subdomain; however, Wenner probe measurements in practice are made on the surface of concrete. Therefore, it is important to analyze the quality of the model predictions on the surface as well. Electrical potential distribution was studied along a line crossing over the four points representing Wenner probe electrodes on the surface of the domain in the longitudinal direction to investigate possible errors on the surface. Using results from the *"Extra fine"* mesh discretization; both numerical and analytical solutions were plotted in Figure 3-13(a). Although theoretically the electrical potential of a point current source should reach infinity, as expected, this did not happen in the numerical solution. It became significantly higher compared to the rest of the

domain reaching values in the order of 10^4 compared to most areas in the domain. Figure 3-13 also provides a zoomed view of the plots.

The Wenner probe was placed symmetrically around point X= 0 mm. Hence, for a probe spacing of 50 mm, the current electrodes placed at X= ±75 mm and the potential electrodes at X= ±25 mm. Subsequently, the border of the infinite element domains were located at X= ±175 mm. As illustrated in Figure 3-13(b), except in the infinite element domains, the numerical solution is compatible with the analytical solution. Moreover the numerical value for the electrical potential at the current electrodes was also different from infinity. For infinite element subdomains, the numerical results show a clear reduction of electrical potential until it reaches to zero as was expected. On the contrary, the method used for calculating the analytical solution solely uses the actual X coordinate data which are not virtually extended to infinity. This reemphasized the importance of infinite element domains in this modelling study and was the main reason for which the infinite elements were not included in the calculation of the misfit value (Equation 3-11).

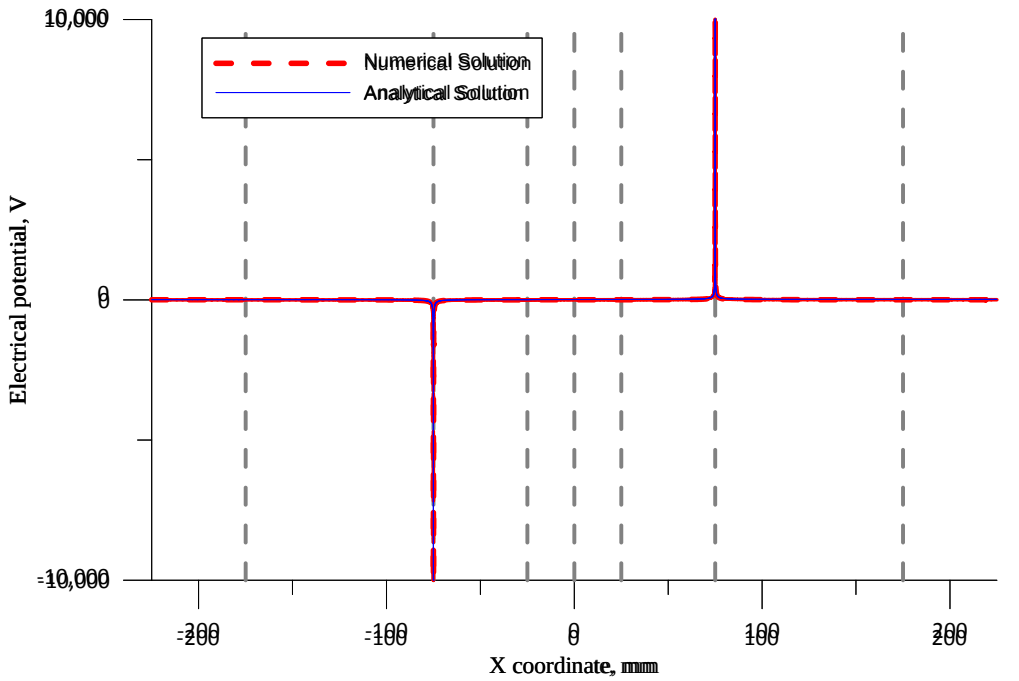

(a)

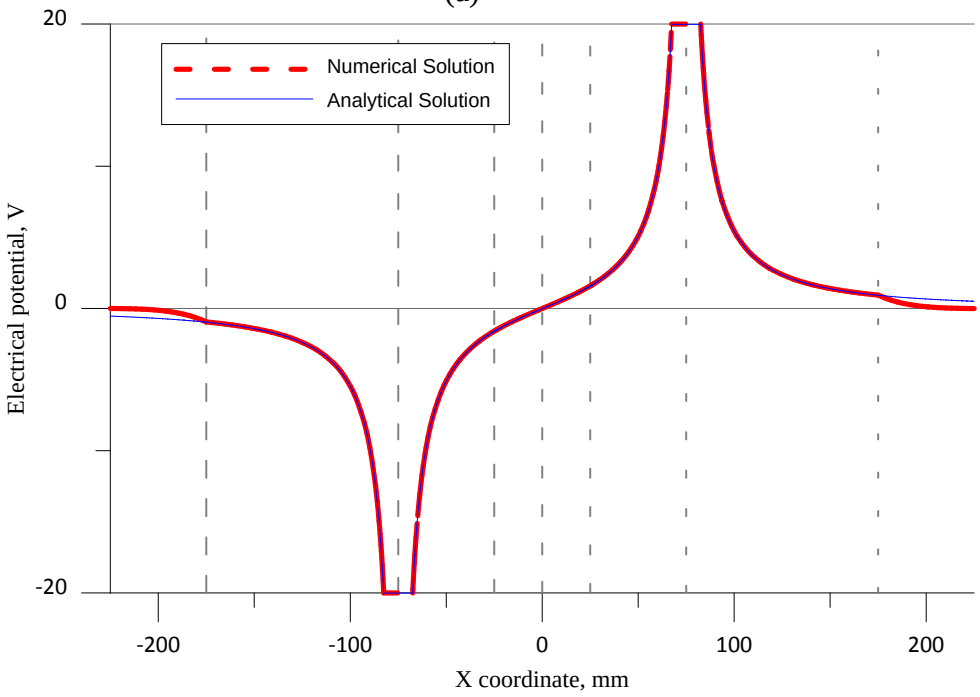

(b)

Figure 3-13: Comparison between electrical potential derived from the numerical and analytical solution along the crossing line on the surface of the domain for electrode spacing of 50 mm: (a) full scale view, (b) vertical axis limited to ±20V for a close up view.

An additional mesh analysis study was conducted to investigate the effect of mesh size on the predictions of the model on the concrete surface. Three different cases were considered. The first one was the investigation of the entire concrete surface that incorporated the current injection points. The second case included the top surface with a small area cut out around the current injection points to exclude them from calculations. Last case included a surface that contained only the area between the two current electrodes. These three conditions are shown in Figure 3-14. Table 3-4 provides the surface misfit values obtained for each of these three scenarios.

Mesh sizes at the proximity of the current and potential electrodes were varied to study their influence on the surface misfit. Based on the data obtained, the worst results were obtained from the surface that included current electrodes (i.e., the first scenario). The surface misfit values were in the order of 10^{-2} while the volumetric misfit was in the order of 10^{-5}.This indicates that major portion of the misfit value came from the hemisphere at the proximity of the current probes. Excluding areas close to the current electrodes as shown in Figure 3-14(b) and (c) (i.e., the second and third scenarios) led to a remarkable reduction in the misfit value, which confirms the effect of current probe proximity on the misfit value. While increasing mesh resolution at the vicinity of the current electrodes improved the quality of the model, reducing mesh size around potential electrodes did not cause significant changes. This indicates that the accuracy of the proposed model for the predication of the concrete electrical resistivity is acceptable.

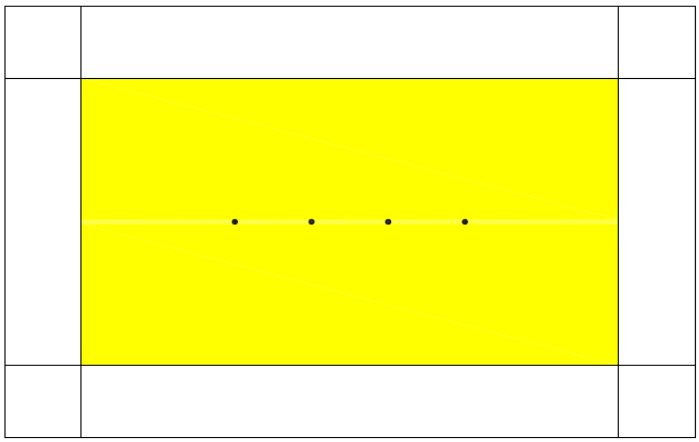

(a)

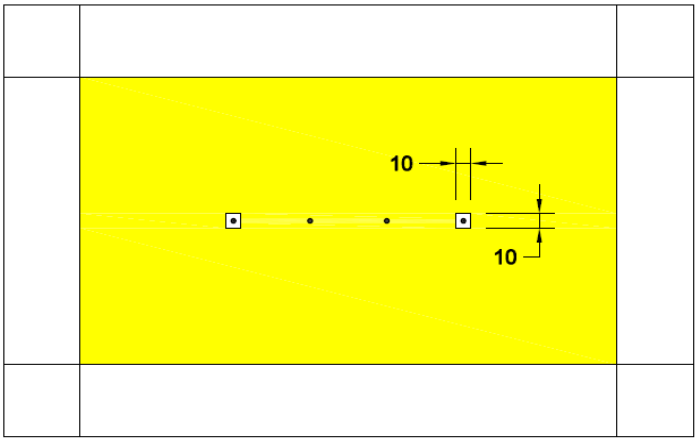

(b)

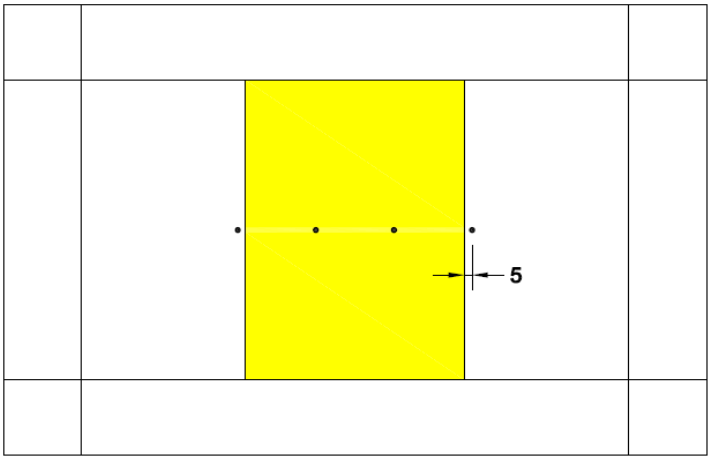

(c)

Figure 3-14: Different schemes used for surface analysis of the models performance: (a) complete top surface; (b) top surface with a square cut out in the location of current electrodes; (c) surface area between the two current electrodes.(units in mm)

Table 3-4: Summary of surface analysis results

Surface Type	Model Type: Meshing style	Model Type: Max. mesh size (m) Current points	Model Type: Max. mesh size (m) Current points	Modeling Data: Surface misfit ($1-R^2$)	Modeling Data: # of elements	Modeling Data: Min. element quality*	Solution Data: Predicted to actual resistivity ratio	Solution Data: % error in predicted electrical resistivity
a	extra fine	10^{-4}	-	2.10×10^{-2}	142,055	0.36	0.999	0.080
	extra fine	10^{-5}	-	7.56×10^{-3}	149,399	0.36	0.999	0.056
	extra fine	10^{-4}	10^{-3}	2.73×10^{-2}	145,369	0.36	0.999	0.082
b	extra fine	10^{-4}	-	4.70×10^{-6}	143,382	0.36	0.999	0.080
	extra fine	10^{-5}	-	4.66×10^{-6}	151,077	0.36	0.999	0.099
	extra fine	10^{-4}	10^{-3}	4.63×10^{-6}	146,712	0.36	0.999	0.080
c	extra fine	10^{-4}	-	1.13×10^{-6}	147,226	0.30	0.999	0.074
	extra fine	10^{-5}	-	1.08×10^{-6}	155,020	0.41	0.999	0.081
	extra fine	10^{-4}	10^{-3}	1.11×10^{-6}	150,134	0.43	0.999	0.081

(*): Minimum element quality is the internal calculated value by the COMSOL software for quality of mesh generated during discretization of the model. Values > 0.2 are considered not affecting the solution.

3.4 Other Modelling Considerations

3.4.1 The effect of electrode contact area

In an actual surface resistivity measurement probe, both current and potential electrodes would have contact areas instead of just being simple nodes acting as a contact points. This non-ideal modelling assumption would introduce some simulation errors. For instance, the electrical potential at the location of the current electrode is inversely affected by the contact area; the larger the contact area, the smaller the potential. Figure 3-15 shows the results from a scenario in which Wenner probe having electrodes with 1 cm^2 contact area is modeled. First point to notice is the drop in the electrical potential at the location of the current electrodes that changed from almost $\pm 10^4$ V to ±42 V for 1 A current injected and electrical resistivity of 1 Ω-m was assigned to the material property of the domain. Another distinction is how the electrical potential remains constant under all four electrodes. This effect is caused by the high conductivity of the electrodes which are typically metals compared to the material of the current investigation i.e. concrete. Table 3-5 provides detailed information about the model performance in two different scenarios: one with Wenner probe having ideal point contacts and other having electrodes with contact area of 1 cm^2. From the misfit value, it can be seen that the quality of the model reduced as electrode contact area increased. Majority of this reduction in quality resulted from the current electrodes rather than the potential electrodes. It is worth mentioning that the analytical solution used as a reference is derived assuming current is inserted through points not a certain contact area. Despite significant increase in misfit value, still acceptable results were obtained for practical applications. Electrical potential

at each of the two inner electrodes were similar to their point counterparts. This can be seen in the zoomed section of Figure 3-15.

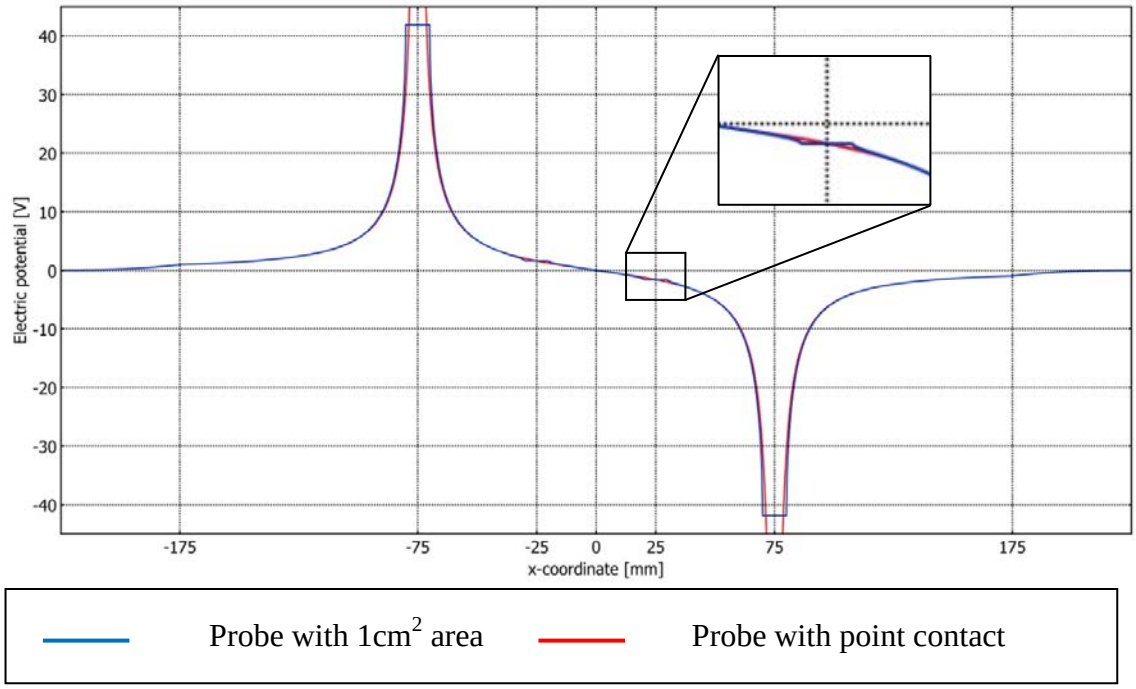

Figure 3-15: Influence of electrode contact area on electrical potential distribution.

Table 3-5: Model performance of a Wenner probe with 1cm^2 electrode contact area

	Model Types		Modeling Data				Solution Data
Case	**Meshing style**	**Electrode type**	**Domain misfit**	**# of elements**	**Min. element quality***	**Resistivity reading scale**	**% error in resistivity reading**
A	extra fine	point	5.20E-05	145,369	0.36	0.999	0.082
B	extra fine	1 cm^2	2.88E-02	189,839	0.35	1.006	0.574

(*): Minimum element quality is the internal calculated value by the COMSOL software for quality of mesh generated during discretization of the model. Values > 0.2 are considered not affecting the solution.

3.4.2 The effect of concrete-to-rebar resistivity ratio

Concrete is a material that has a wide range of resistivity (from 10^6 Ω-m in dry conditions to values ~50 Ω-m in rather moist conditions). In contrast, steel conductivity

has limited variability. Values ranging from 1.6×10^{-7} to 7.2×10^{-7} Ω-m have been reported for electrical resistivity of steel depending on its type (Eddy Current Technology, 2002). A typical value of 2.48×10^{-7} Ω-m was used for the resistivity of steel in this investigation.

Although it is highly unlikely to have concrete with resistivity comparable to steel, some areas such as cracks might have significantly lower resistivity compared to bulk concrete. Cracks filled with moisture and ions could have very low resistivity reaching to values in the order of 10^{-3} Ω-m (Ghods, 2010). Thus, an attempt was made to investigate how variations in the resistivity of concrete with respect to the rebar might influence measurements using the Wenner probe. A scenario in which a single rebar placed directly beneath the Wenner probe was used for this study as shown in Figure 3-16. The ratio of the concrete resistivity to the rebar resistivity was varied from 1 to 10^{7}.

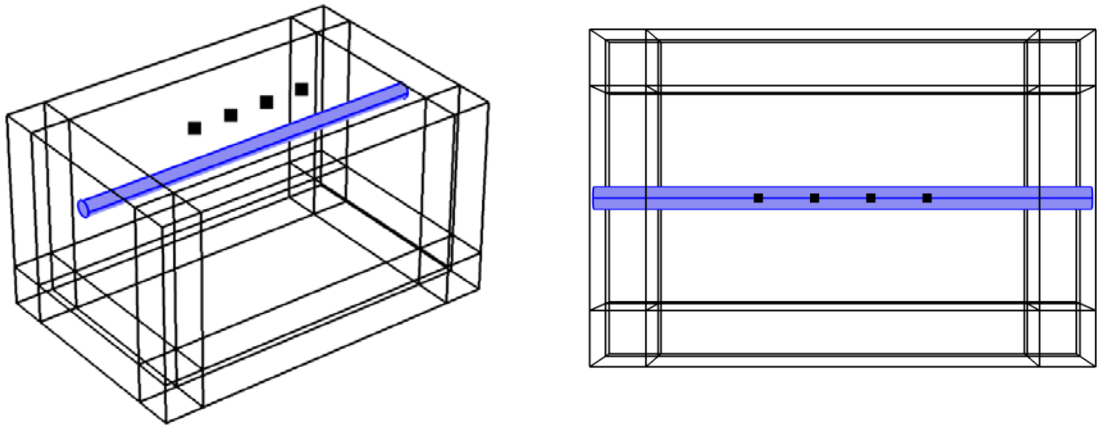

(a) (b)

Figure 3-16: Rebar inside the concrete directly under the Wenner probe: (a) 3-D view; (b) Plan view.

The following parameters were investigated by changing the concrete resistivity within the range defined earlier:

- Concrete cover thicknesses of 25 mm, 40 mm, and 60 mm.
- Electrode spacing of 38 mm and 50 mm.

Predictions were normalized with respect to the electrical resistivity assigned to the concrete material in the first place for which the resistivity would ideally be obtained using a practice similar to using a Wenner probe. Obtained values for the two electrode spacings are provided in Figure 3-17 and Figure 3-18.

Based on the results, both the cover thickness and concrete to rebar resistivity ratio have influence on the measured resistivity. However, variations in measurement due to changes in concrete to rebar resistivity ratio becomes negligible when this ratio exceeds 10^4. This is easily seen as the lines connecting measurement points reach a plateau. Moreover, sensitivity to this variation is higher for electrode spacing of 50 mm compared to 38 mm. Higher sensitivity to the presence of rebar for large electrode spacings in general was mentioned in chapter 2 and similar trend is observed here as well.

On the other hand, assuming there is a rebar inside concrete with a resistivity of at least seven orders of magnitude less than concrete, measurement deviation for lesser ratios is calculated. Calculated values are provided in percent deviation for both electrode spacings in Figure 3-19 and Figure 3-20 .

Considering results depicted in Figure 3-17 to Figure 3-20 and having resistivity of rebar in the order of 10^{-7} Ω-m, it can be concluded that the model is insensitive to variations in concrete resistivity in a typical range of 1 to 10^6 Ω-m. However, for a

scenario that there is a region with different resistivity such as a conductive crack, measurements could be altered.

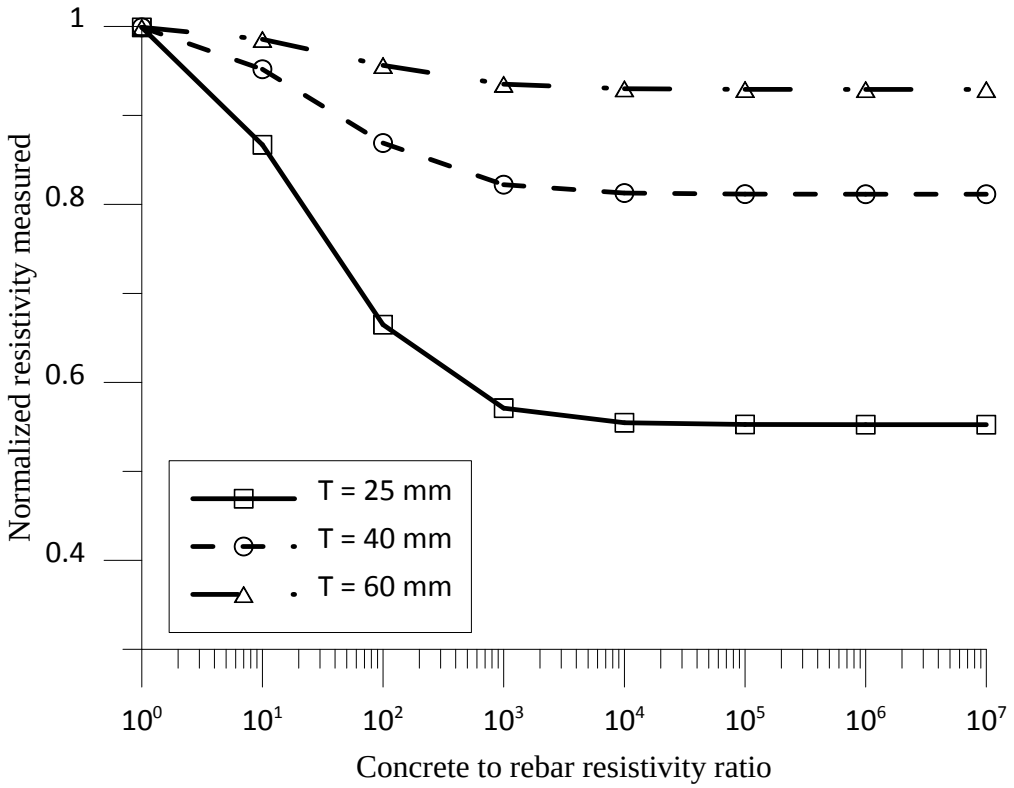

Figure 3-17: Influence of concrete to rebar resistivity ratio variation for different cover thicknesses (electrode spacing 38mm).

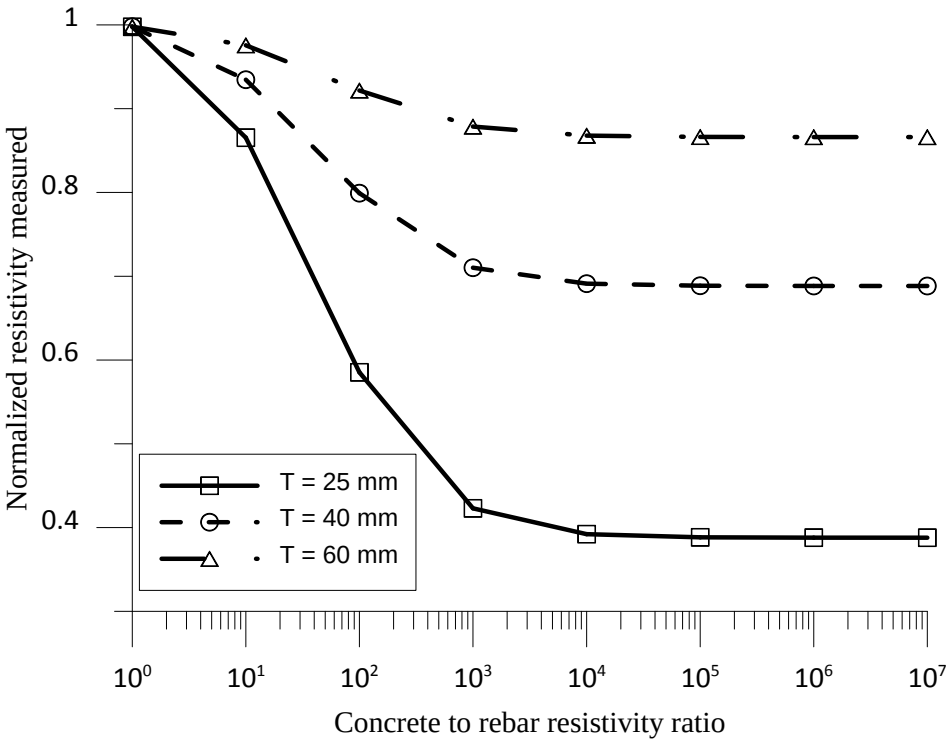

Figure 3-18: Influence of concrete to rebar resistivity ratio variation for different cover thicknesses (electrode spacing 50mm).

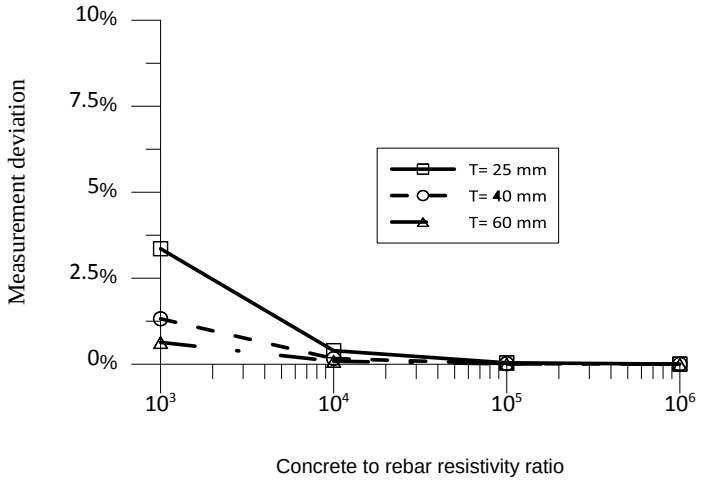

Figure 3-19: Measurement deviation for different ratios of concrete to rebar resistivity for various cover thicknesses (electrode spacing of 38mm).

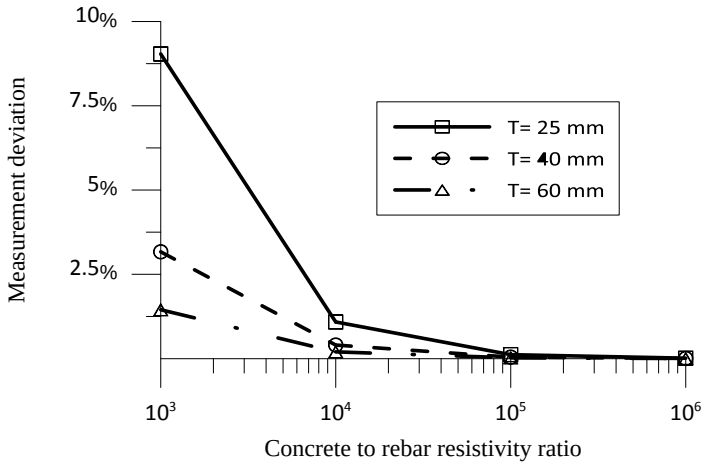

Figure 3-20: Normalized measurement error for different resistivity ratios of concrete and rebar for different cover thicknesses (electrode spacing of 50mm).

3.5 Proposed Analysis Domain for the Numerical Investigation

The initial dimensions selected for the central subdomain, Figure 3-6, were found to be inadequate for implementing all rebar mesh scenarios. Thus, changing the overall size of it was inevitable. The central subdomain was enlarged to L = 450 mm, W = 450 mm and H = 200 mm; however, size of the infinite element subdomains were kept at H/4 i.e., 50 mm as per Mesh analysis stage 4 of this chapter.

An investigation was carried out to reassure that quality of the model was not dramatically affected by this change. Similar to Stage 6 in Table 3-3, data obtained from evaluating the quality of these new dimensions is presented in Table 3-6. Results indicate that misfit value has not changed significantly meaning the performance of the model was not affected by this alteration. Figure 3-21 and Figure 3-22 also show outcomes of the model similar to the conditions explained for Figure 3-12 and Figure 3-13(b) in Sections 3.3.7 and 3.3.8, respectively.

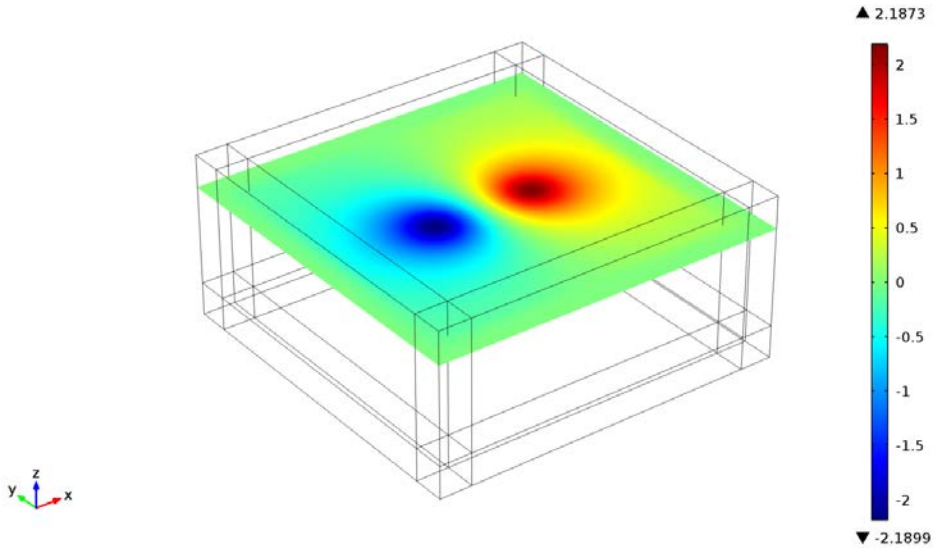

Figure 3-21: Electrical potential distribution at the depth of 50 mm with the new domain geometry.

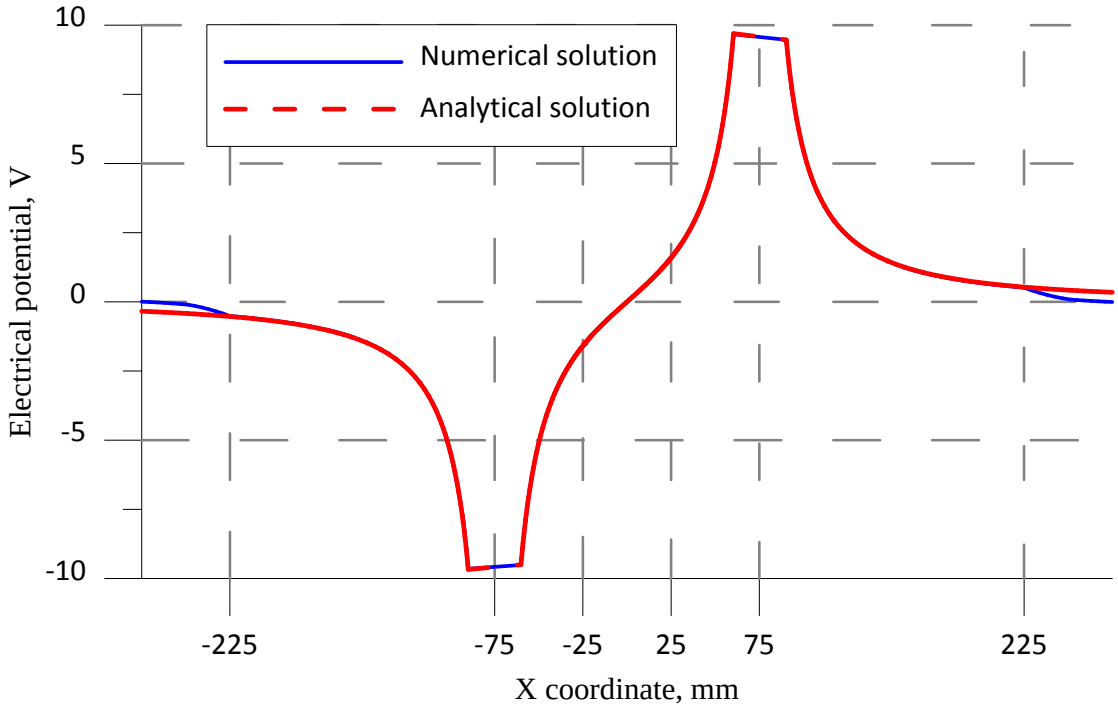

Figure 3-22: Numerical and analytical solution along a crossing line on the surface of the domain.

Table 3-6: Summary of the mesh analysis for the new geometry

Model type and parameters					Modeling Data			Solution Data		
Meshing style	Max. mesh size (m)		Infinite elements		Misfit ($1-R^2$)	# of elements	Min. element quality*	Predicted to actual resistivity ratio	Time to solve (s)	% error in predicted electrical resistivity
	Current points	Current points	Direction	Size						
finer	10^{-4}	10^{-3}	X,Y,Z	H/4	1.19×10^{-4}	46,117	0.13	0.999	19	0.08
extra fine	10^{-4}	10^{-3}	X,Y,Z	H/4	5.46×10^{-5}	175,791	0.16	0.999	80	0.05
extremely fine	10^{-4}	10^{-3}	X,Y,Z	H/4	1.75×10^{-5}	899,867	0.04	1	373	0.02

(*): Minimum mesh quality is the internal calculated value by the COMSOL software for quality of mesh generated during discretization of the model. Values > 0.2 are considered not affecting the solution.

3.6 Experimental Verification and Benchmarking

In the last step, performance of the developed model was evaluated using data from experiments and finite element modeling results provided by other researchers. This would help increase the reliability of the results provided by the developed model. Figure 3-23 demonstrates the correlation between data obtained using the developed model and those extracted from other studies. In order to provide comparable data, similar conditions to those reported in other studies were implemented in the model. Then the outputs were plotted as seen in Figure 3-23. The same approach was followed when comparing data from other models with the current one. Details regarding different conditions implemented are shown in Table 3-7. The comparison showed that the devised model is capable of providing reasonably accurate results with respect to experimental measurements reported by other researchers. Simulated results are more compatible with finite element data provided in the literature. Experimental data are prone to noise and other influential factors such as aggregates, geometrical factors etc. whereas numerical results are not. This is one reason that simulated outputs using the devised model is in good agreement with other finite element modeling data.

Table 3-7: Details of different conditions being reported by previous studies which were simulated to obtain comparable data.

Reference	Data type	Electrode spacing	Concrete cover	Rebar diameter	Rebar orientation
(Millard, 1991)	Experimental	50 mm	40 mm	16 mm	Parallel
(Millard, 1991)	Experimental	50 mm	40 mm	25 mm	Parallel
(Millard, 1991)	Experimental	50 mm	40 mm	16 mm	Parallel
(Millard, 1991)	Experimental	50 mm	40 mm	25 mm	Parallel
(Millard, 1991)	Experimental	50 mm	40 mm	40 mm	Parallel
(Sengul and Gjorv, 2009)	Experimental	20 mm	50 mm	10 mm	Parallel
(Sengul and Gjorv, 2009)	Experimental	50 mm	50 mm	10 mm	Parallel
(Sengul and Gjorv, 2009)	Experimental	50 mm	50 mm	10 mm	Perpendicular
(Millard, 1991)	FE Modeling	50 mm	40 mm	40 mm	Parallel
(Moreno et al., 2009)	FE Modeling	50 mm	25 mm	16 mm	Parallel
(Moreno et al., 2009)	FE Modeling	50 mm	50 mm	16 mm	Parallel

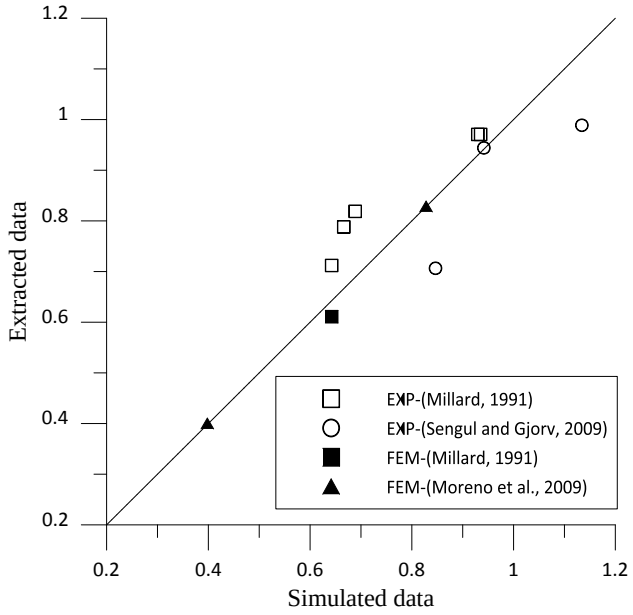

Figure 3-23: Correlation between experimental (EXP) or finite element modeling (FEM) results from other studies and simulated results for the same scenario using the developed model in the current study; solid symbols represent data compared to other models, symbols without filling are data compared to other experimental results.

4. Numerical Investigation

4.1 Introduction

As reviewed in Chapter 2, the use of Wenner probe to measure surface concrete resistivity has been studied to some extent both experimentally and numerically; however, as also became clear in the literature review, the effects of the following three areas of importance on resistivity measurements have not been covered systematically by these studies: (1) the role of realistic reinforcement detailing; (2) the role of cracks; (3) the combined effect of embedded reinforcement and cracking. This chapter provides a background on the numerical investigation that was conducted to fill this gap in the literature.

4.2 Investigation of the Role of Embedded Reinforcement

In this investigation, the role of embedded steel reinforcement on the concrete resistivity measurements using a Wenner probe was studied numerically by considering various rebar configurations and cover thicknesses. Table 4-1 and Figure 4-1 provide the main studied parameters and their variations.

The values for cover concrete thickness were based on the minimum allowable limits defined for different exposure conditions in CAN/CSA A23.2 (2009). Rebar spacing values were selected on multiples of 50 mm; the minimum spacing was in compliance with CAN/CSA A23.3 (2004); the code requires an absolute minimum spacing of 46 mm for a 16 mm diameter rebar. The majority of simulations were carried out using nominal rebar diameter of 16 mm. A limited number of cases were repeated

using other diameters (25 mm and 36 mm) to investigate the effect of rebar diameter on the resistivity measurements. These nominal diameters were selected since they were common in Canadian (CAN/CSA A23.3), American (ACI 318), and European (EN10080:2005) standards as shown in Table 4-2.

Table 4-1: Parameters investigated for the role of embedded reinforcement on resistivity measurements.

Parameter Name	Variable	Studied Range
Concrete cover thickness	T	25 mm, 40 mm, 60 mm
Rebar Spacing*	S	50 mm, 100 mm, 150 mm, 200 mm
Rebar Diameter	ϕ	16 mm, 25 mm, 36 mm

(*): Centre-to-centre spacing

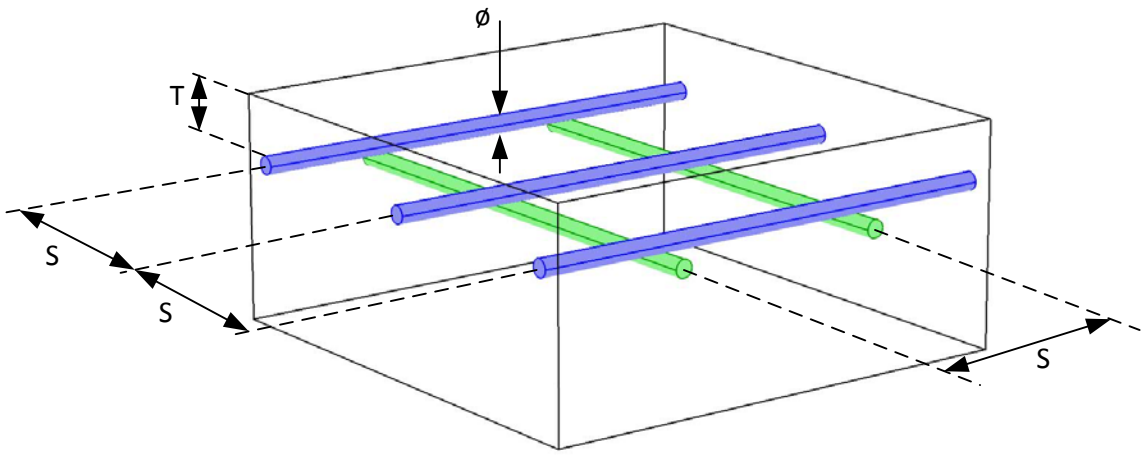

Figure 4-1: Parameters investigated for the role of embedded reinforcement on resistivity measurements

Table 4-2: Rebar sizes in different standards

	CAN/CSA A23.3		ACI 318		EN10080	
Diameter in the model (mm)	**Bar size**	**Nominal Diameter (mm)**	**Bar size**	**Nominal Diameter (mm)**	**Bar size**	**Nominal Diameter (mm)**
16	15M	16.0	#5	15.9	16	16.0
25	25M	25.2	#8	25.4	25	25.0
36	35M	35.7	#11	35.8	32 or 40	32.0-40.0

The electrode spacing of the Wenner probe was also studied along with the parameters discussed above. Two spacing values were used: 50 mm and 38 mm. Most commercial Wenner probes use 50 mm spacing as suggested by Millard (1991) to reduce variances observed in measurements caused by the presence of aggregates. The 38 mm spacing was also investigated since it has been recently introduced for the quality control of concrete samples as per the AASHTO TP095-11-UL (2011) standard.

Since the orientation of the Wenner probe and its location with respect to a single rebar was found to be influential on resistivity measurements (Millard, 1991; Sengul and Gjorv, 2009; Moreno et al., 2009), this effect was systematically studied in the present study using multiple embedded rebars in three dimensional domains. For this purpose, nine configurations covering three groups of probe orientation, as illustrated in Figure 4-2, were investigated. The first two groups of configurations were based on the suggestion by some researchers that rebars perpendicular to the Wenner probe would have no effect on the measurements, while taking measurements midway between parallel rebars would provide the best results (Millard, 1991; Weydert and Gehlen, 1999). Group three however, was based on the suggested theme by Polder et al. (2000). It was proposed that taking measurements diagonally over the regions without rebar, as

illustrated in Figure 2-5, would help improve the accuracy of the resistivity measurements.

In the first group (configurations #1, #2, #3), Wenner probe was oriented perpendicular to the top rebars while it was placed midway between the two lower parallel rebars. Each of the three configurations shows a scenario for which the probe is moved slightly while its orientation is kept constant. In configuration #1, the centre of the probe was placed over the top middle rebar. In configuration #2, one of the current electrodes was placed over one of the top rebars, and in configuration #3, the centre of the probe was located exactly midway between the top two adjacent rebars.

In the second group (configurations #4, #5, #6), the Wenner probe was oriented perpendicular to the lower level rebars and parallel to the upper rebars. These configurations were obtained by rotating the probe by 90 degrees from orientation described for the first group. Once again each of the three configurations was designed to represent a scenario for which the probe is slightly moved as described for the configurations in the first group.

The last group (configurations #7, #8, #9) consisted of configurations for which Wenner probe was oriented diagonal to rebar mesh. In configuration #7, the centre of the probe was placed at the intersection of the two perpendicular rebars. In configuration #8, one of the current electrodes was placed at the intersection, and finally in configuration #9, the centre of the probe as placed exactly at the center of the diagonal line connecting two rebar intersection points.

Lastly, in order to understand if the depth of concrete below the reinforcement has any effect on the resistivity measurements, two concrete depths were investigated. In the

first case 120 mm was used as the depth of the concrete from surface to surface; this selection is in line with the minimum allowable slab thickness as per CAN/CSA A23.3 (2004). The other case simulated a very thick concrete member using infinite elements.

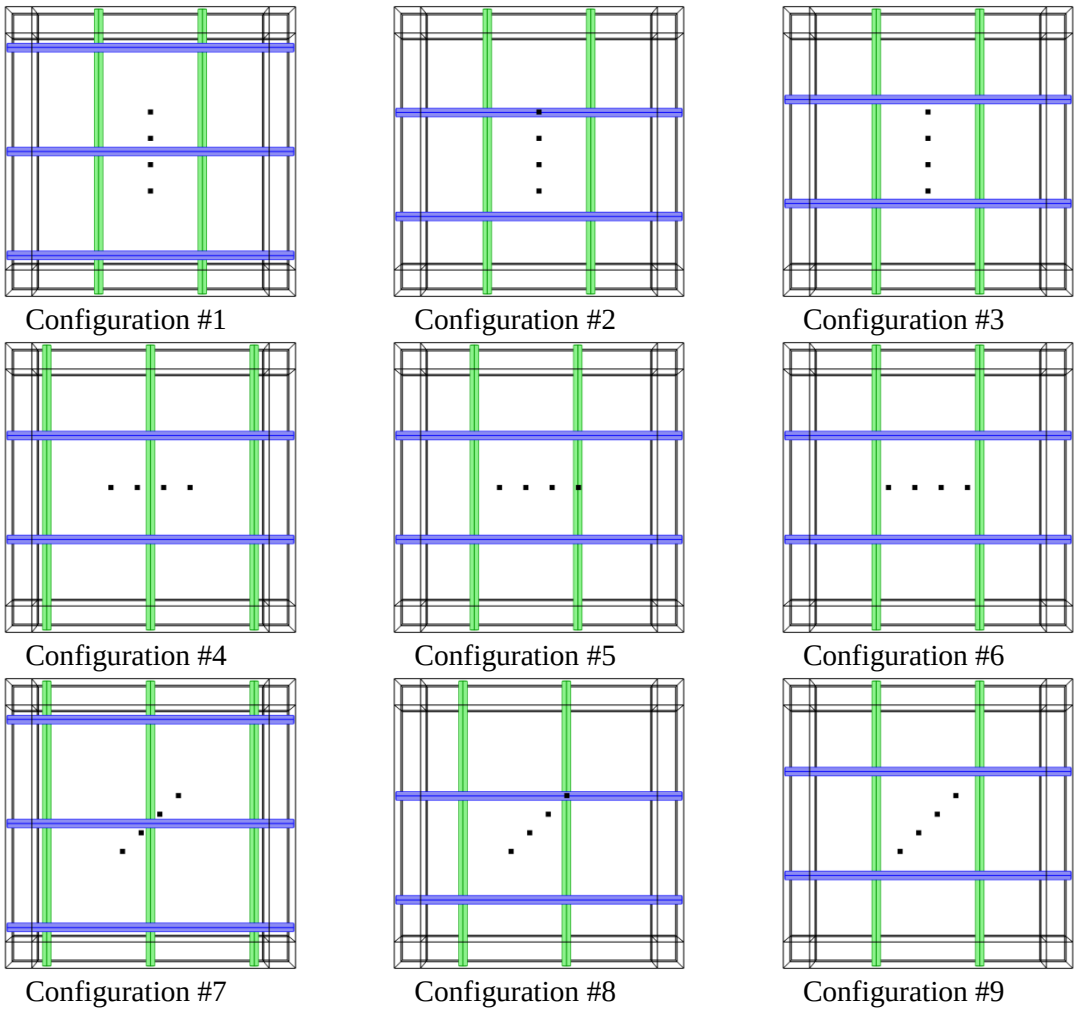

Figure 4-2: Placement of Wenner probe with respect to rebar mesh configurations

4.3 Investigation of the Role of Cracks in the Presence of Embedded Rebar Mesh

Numerical simulations were carried out to investigate the role of cracks on the concrete resistivity measurements using a Wenner probe. Due to the presence of a large number of influential parameters, the investigation was carried out in two stages. Figure

4-3 illustrates 1596 simulation cases studied in the first stage. In this figure each column represents the parameter studied while each box in that specific column shows different configurations or range of values analysed. The goal of this stage was to obtain enough data to identify the most influential parameters affecting Wenner probe measurements. The second stage involved more detailed numerical investigations to study the most important parameters in a more focused way.

The description of parameters considered and range of values selected for each simulation case could help better understand the process; therefore, a background is given here. Earlier research done by Lataste et al. (2003) revealed that resistivity measurements on concrete vary at the vicinity of a crack. It was also showed that the depth of the crack plays a major role in the variation observed around the crack. The possibility of having two types of crack existing in a structure, insulated or conductive, was also considered. The same approach was used in this study by investigating the effects of crack type and depth on resistivity measurements. An insulated crack was considered to occur when two edges of the crack are separated from each other and the crack void is filled with air. A conductive crack was assumed to be a crack filled with water either with or without external ions such as chlorides. This condition leads to an electrolyte that has the capability of carrying electrical current within and across the crack. Experiments by Ghods (2010) showed that conductivity of such electrolyte could cover a wide range from 0.04 Ω-m to 2 Ω-m depending on the type and concentration of ions present.

In this investigation, the combined influence of presence of cracks in a concrete member with embedded rebar mesh on resistivity measurements was also studied. For the combined effect, two mesh configurations from Section 4.2 were considered: #9 and #4.

The first configuration (#9) was the configuration suggested by Polder et al. (2000), and the second configuration (#4) was the one that gave the most accurate resistivity predictions in the preliminary numerical study in this research. Rebar spacing and cover thickness were varied for all cases developed to study the combined effect of cracking and embedded rebar mesh.

The location of the crack with respect to the Wenner probe was another parameter investigated in this research. Wenner probe consists of four electrodes so four possible conditions could occur with one crack. First condition involved cases in which the crack was in the middle section of the probe between the two inner potential measurement electrodes. The second condition involved cases in which a crack located between the current imposing and potential measurement electrodes. The third condition covered cases having a crack placed behind the probe. In the last condition, crack was parallel to the Wenner probe at some distance from it.

Furthermore, the orientation of the crack (regardless of its location with respect to the probe) was suspected to be influential and was investigated in this research. For the Wenner probe itself, only electrode spacing was varied with values and justifications provided in Section 4.2. Table 4-3 presents the list of parameters used and their assumed values for this study.

Table 4-3: Parameters and their values used for studying influence of concrete crack

Parameter Name	Representing Variable	Values implemented
Crack height	C_h	20 mm,40 mm,80 mm
Crack width	C_w	2 mm, 1 mm, 0.3 mm
Crack type	-	Conductive, Insulated
$\frac{\rho_{concrete}}{\rho_{crack}}$	-	10^4, 10^3, 10^2
Domain type	-	With Rebar, W/O Rebar
Rebar mesh configuration	-	#4, #9
Rebar Spacing	S	100 mm, 150 mm, 200 mm
Cover thickness	T	25 mm, 40 mm, 60 mm
Rebar Diameter	ϕ	16 mm
Electrode spacing	a	38 mm, 50 mm
Crack location	-	L1, L2, L3, P
Crack angle	θ	90°, 45°
Crack distance (parallel cracks)	C_d	a

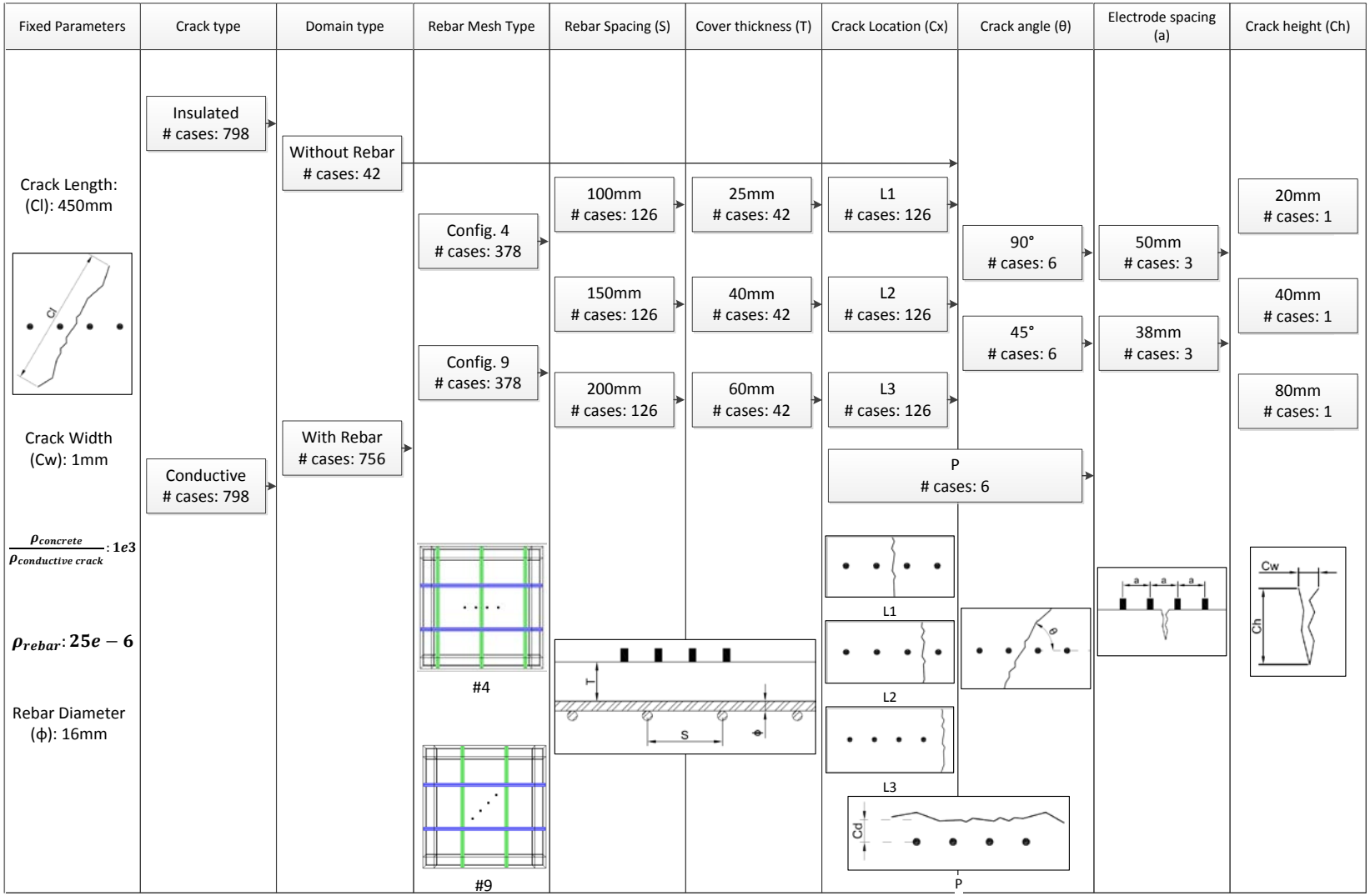

Figure 4-3: Stage one of Wenner probe resistivity measurement on cracked concrete.

5. Results and Discussion

5.1 Introduction

Results and findings of this study are presented in this chapter. There are three main sections. The first section is the study of rebar mesh effect on resistivity measurements. In the second section, the impact of cracks in concrete is studied, and in the last section the combined effect of the two factors is presented. In order to show how resistivity measurements are impacted by any of the aforementioned parameters, the term *"Measured / actual resistivity"* is used in the figures of this chapter. Values obtained from the model on a concrete without any rebar, crack or defects are considered as the *"actual resistivity"* while values obtained from the proposed model on concrete in the presence of the influential parameters such as rebar and cracks are called *"measured resistivity"*. Ratio between these two values is used as an indicator presenting deviations.

5.2 Concrete with Embedded Rebar Mesh

In chapter 4, intentions behind investigating the influence of rebar mesh on Wenner probe was identified. In this section, data obtained from the study of the rebar mesh configuration effect are presented and discussed. Figure 5-1 summarizes the results of 216 different cases; all these predictions relate to resistivity measurements over different rebar mesh configurations. The charts are organized such that each column provides values obtained for specific electrode spacing and each row is dedicated to a certain rebar spacing. The following sections discuss in detail the observations summarized in these plots.

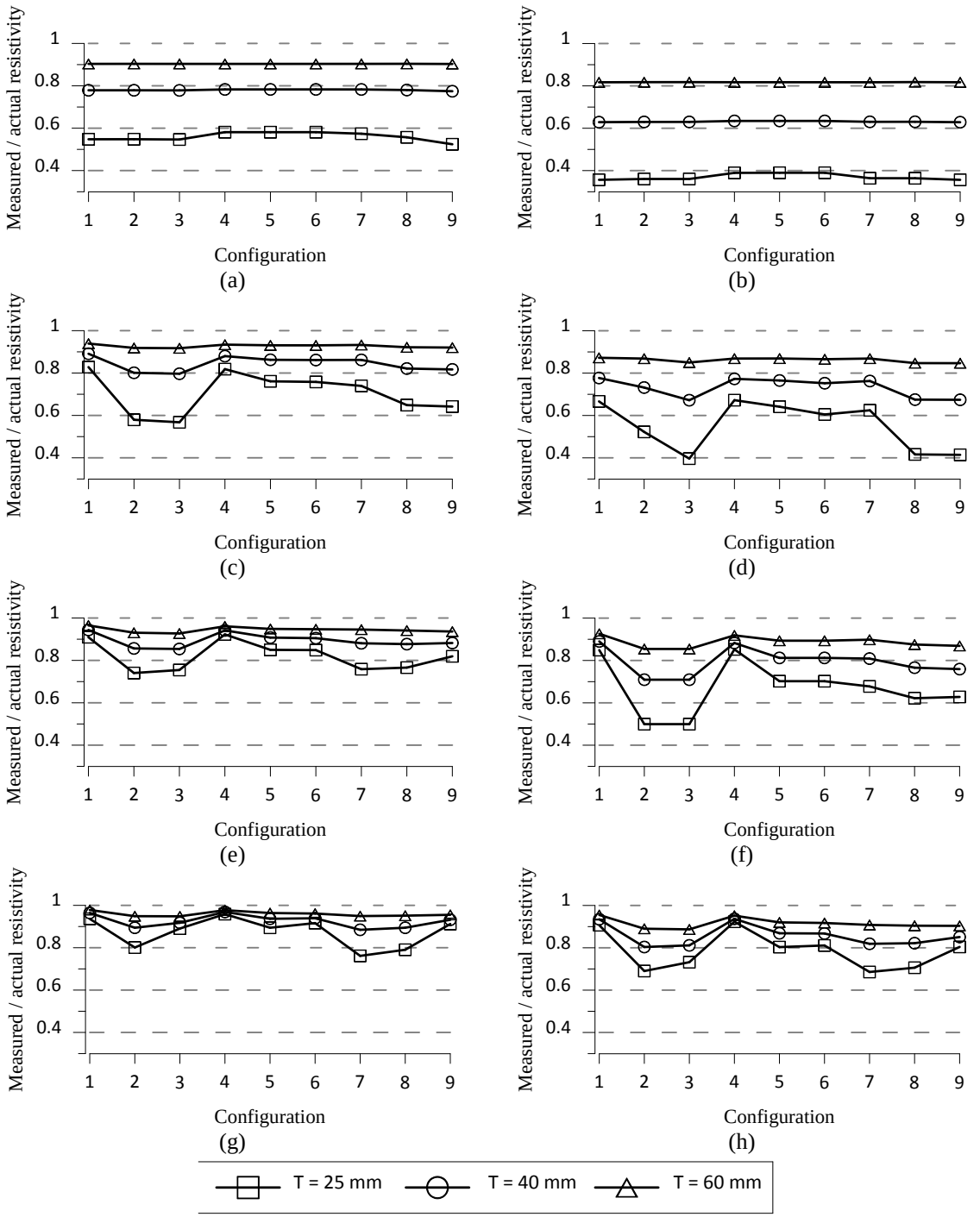

Figure 5-1: Influence of rebar mesh of different spacings on Wenner probe resistivity measurement for different mesh configurations defined in Figure 4-2: (a) a = 38 mm, S = 50 mm; (b) a = 50 mm, S = 50 mm; (c) a = 38 mm, S = 100mm; (d) a = 50 mm, S= 100 mm; (e) a = 38 mm, S = 150 mm; (f) a = 50 mm, S = 150 mm; (g) a = 38 mm, S = 200 mm; (h) a = 50 mm, S = 200 mm.

5.2.1 Effect of probe orientation

In-depth investigation of the results shown in Figure 5-1 reveal that configuration #4 provides the closest value to the actual resistivity of concrete compared to all other eight configurations regardless of the concrete cover thickness or rebar spacing. Configurations #5 and #6 which represent a condition in which Wenner probe is shifted from configuration #4 also provide ratios closer to one than those of the remaining configurations in most scenarios. In some cases, changing measurement configuration results in deviation around 20% in the measured electrical resistivity of concrete. For example, for the measurement of configuration #4 and #9 for rebar spacing of 100 mm and cover thickness of 25 mm (Figure 5-1(d)), difference between the measured data is more than 20%. At higher rebar spacing, i.e., 150 mm and 200 mm, this difference is more than 10% (Figure 5-1(f) and (h)) in most cases. When rebar spacing increased to 200 mm, measurement in configuration #9 provides similar results comparable to #4. Polder et al. (2000) suggested configuration #9 as a suitable way of measurements for Wenner probe technique (i.e., taking measurement in diagonal orientation towards the rebar mesh); however, current study shows that, for rebar spacing $S \leq 200$ mm, this arrangement does not provide the most accurate results. Data from Moreno et al. (2009) depicted in Figure 2-9(b) also shows similar behaviour despite the fact that no details regarding rebar spacing or orientation of the top rebar was provided in their study. Measurement at a mid-span position (similar to either configuration #3 or #6 of this study) provides closer results to the actual concrete resistivity than diagonal measurements. Results from their study showed similar trend to the data provided here although only a few measurements were reported in that study.

In the past, it was assumed that perpendicular rebar has negligible effect on electrical resistivity measurement (Millard, 1991; Gowers and Millard, 1999; Weydert and Gehlen, 1999; Sengul and Gjorv, 2009). The results associated with configurations #1, #2 and #3 in Figure 5-1 show that location of the perpendicular rebars with respect to the Wenner probe also has some influence on the resistivity measurement in the presence of rebar mesh. Measurement deviation as high as 26% can be observed when location of the Wenner probe is changed with respect to the perpendicular rebar (Figure 5-1(d), T = 25 mm). On the other hand, rebars parallel to the probe have more significant negative impact on the accuracy of the Wenner probe measurement because in this case parallel rebars are in the same direction as the current flux inside concrete; therefore, they provide much less resistive paths for the current.

Proximity of rebars to the current electrodes was found to be more influential than the volume of steel in the hemisphere beneath the probe. It is assumed that the resistivity measured using the Wenner probe is representative of a volume of a hemisphere with radius of one electrode spacing beneath the probe (Telford et al., 1990). Considering Figure 5-1(f), it is evident that measurements in configuration #7 are less impacted by rebars than configuration #9. In configuration #7, a rebar intersection is located under the probe whereas in configuration #9, two rebar intersections are close to current electrodes while no rebar is present underneath the probe.

5.2.2 Effect of electrode spacing

Results of this study show that increase in electrode spacing while measuring over rebar mesh leads to less accuracy. This is evident by comparing charts from the two

columns of Figure 5-1 (Figure 5-1(c) and (b) for instance), that represent data from electrode spacing of 38 mm and 50 mm. This happens regardless of the thickness of cover on rebar or space between the rebars in each of the configurations. As electrode spacing increases larger volumes and deeper regions of concrete would become involved in the electrical resistivity measurements (Polder et al., 2000). Rebars not only introduce non-homogeneity to the domain, but also create non-isotropic behaviour. As a result, the larger the electrode spacing becomes the more deviation in resistivity measurement from the actual resistivity of concrete is experienced. Figure 5-2 shows values obtained from Wenner probe with varied electrode spacing for various rebar spacings and cover thicknesses with two selected configurations (#4 and #9). Higher deviation from the actual resistivity of concrete is attained when electrode spacing is 50 mm. This effect is more significant for smaller cover thickness when rebars are very close to the surface of concrete.

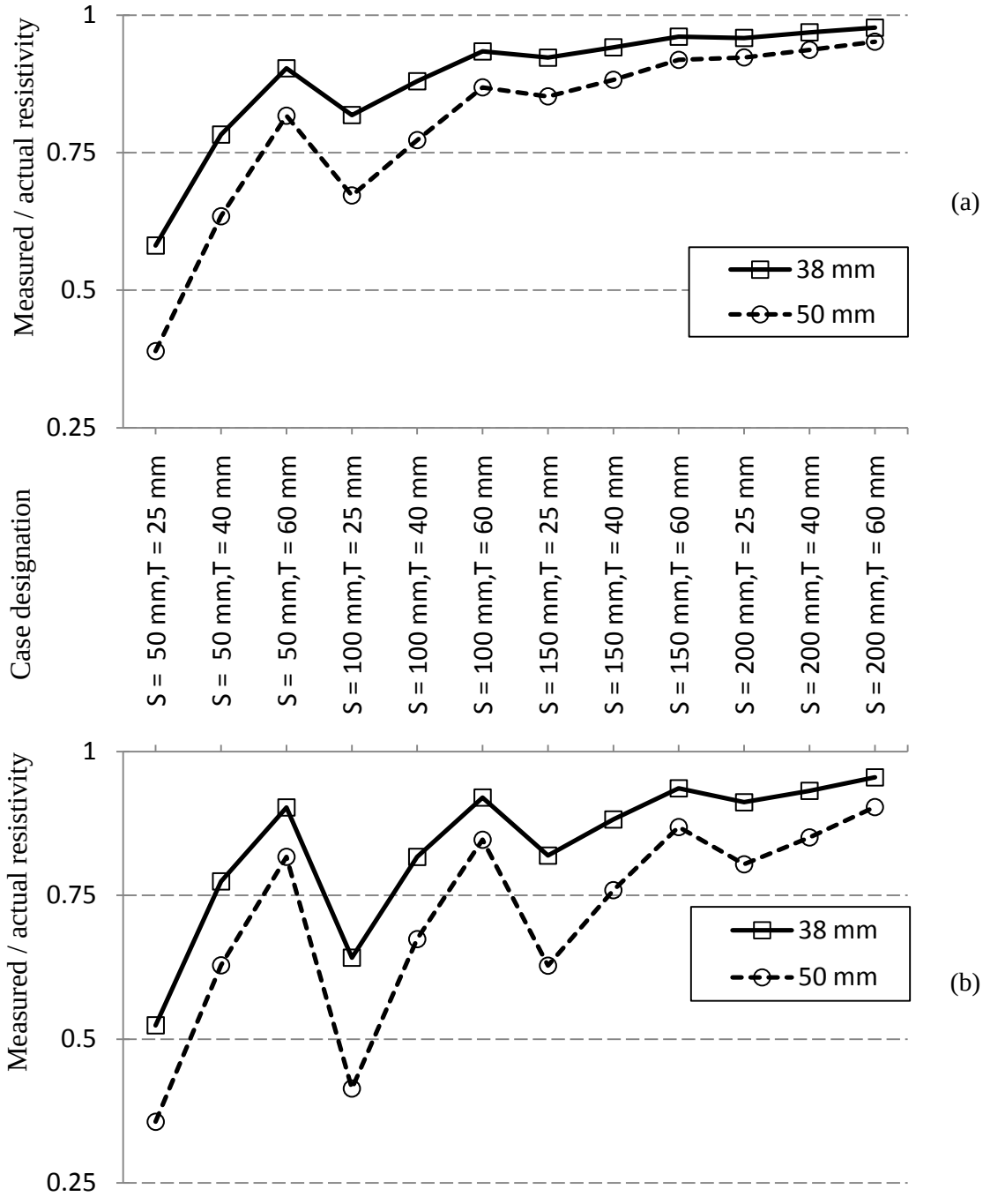

Figure 5-2: Resistivity measurement using the electrode spacing of 38 mm and 50 mm on concrete with different rebar spacing and cover thickness: (a) configuration #4; (b) configuration #9.

5.2.3 Effect of cover thickness

In Figure 5-1, each plot has three distinct data lines each representing measured data for a certain cover thickness. Overall, as the cover thickness increases, errors in the measurements decrease. The reason again is the location of rebars with respect to the electrode spacing where deeper rebars tend to have less influence on the Wenner probe. The top line of each plot in Figure 5-1, with the higher measured resistivity to actual resistivity ratio, belongs to cover thickness of T = 60 mm. In this figure, for cover thickness greater or equal to 60 mm and electrode spacing of 38 mm, regardless of the orientation or location of the Wenner probe and rebar spacing, measurement deviation from actual value of the resistivity of concrete is found to be less than 10%. With the same electrode spacing, for the concrete cover of 40 mm, again regardless of configuration, deviation increases to roughly 20%. In configuration #4, for cover thickness of 40 mm and 60 mm, only measurements with rebar spacing of $S \geq 100$ mm provided results with less than 10% deviation. In other words, measurement deviation of less than 10% regardless of cover thickness can only be achieved once it is taken on concrete with rebar spacing greater or equal to 150 mm with electrode spacing of 38 mm.

A more detailed view of the results related to the influence of cover thickness and rebar spacing is presented in Figure 5-3. In this figure only values taken by electrode spacing of 50 mm in configuration #4 and #9 are illustrated. Configuration #4 was used because of its relatively accurate performance compared to other configurations. Configuration #9 was selected because it was suggested by Polder et al. (2000). It can be seen that both cover thickness and rebar spacing have influence on the results; increase in either one reduces the measurement deviation (Figure 5-3). Moreover, reducing the cover

thickness amplifies the adverse effect of decreasing rebar mesh spacing. When rebar spacing is 50 mm, with concrete cover of 60 mm deviation from the actual resistivity is only 18%, which will increase to 61% when cover thickness is reduced to 25 mm. For rebar spacing of 150 mm on the other hand, measurement deviation for concrete cover of 60 mm is only 8%, which degrades to 15% when cover thickness is decreased to 25 mm. By comparing the accuracy of measurements for both rebar spacings mentioned above, it is clear that decrease in accuracy for electrode spacing of 50 mm is much higher than that for electrode spacing of 150 mm for which cover thickness is reduced from 60 mm to 25 mm.

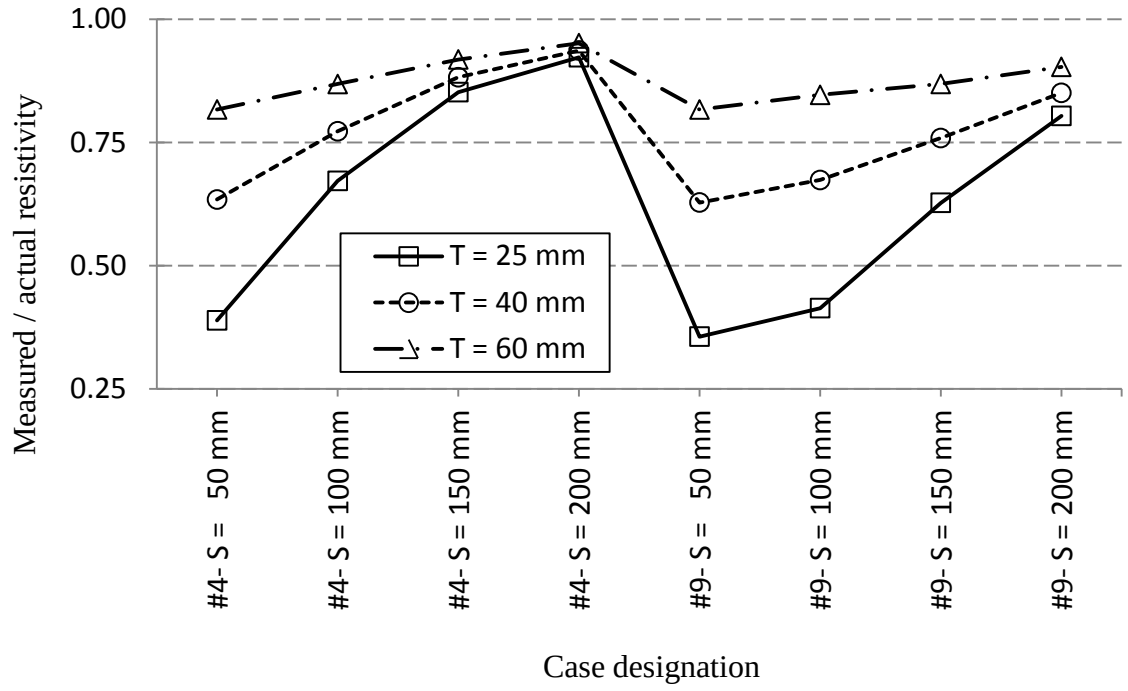

Figure 5-3: Influence of cover thickness and rebar spacing on resistivity measurement for configuration #4 and #9 with electrode spacing of 50 mm.

5.2.4 Effect of rebar spacing

It is seen in Figure 5-1(a) and (b) that at rebar spacing of 50 mm, there is no significant difference between the results of any of the nine configurations. In other words, measurements are highly under the influence of density of the steel reinforcement than the location of the Wenner probe and its orientation. On the contrary, as rebar spacing increases measurements become more dependent on the location or the orientation of the probe. This behaviour becomes more evident as rebar spacing increases. It can be seen in Figure 5-3 that measurement error reduces when rebars are placed more apart. As rebar spacing further increases, i.e., S > 200 mm, the influence of probe orientation or location diminishes. Improvement in measurement accuracy is more visible when cover thickness is 25 mm. For instance, measurement deviation from the actual resistivity of concrete for rebar spacing of 50 mm and cover thickness of 25 mm in configuration #4 is over 60% (i.e., measured over actual resistivity is less than 0.4). This deviation would reduce to less than 10% when electrode spacing increases to 200 mm. The reason behind such behaviour is that as rebar spacing increases, their presence and influence on the volume of concrete reduces leading to a lesser impact on the measurements. Thus, maximum effect of rebar mesh appears when rebar spacing is 50 mm regardless of the Wenner probe location or orientation. Consequently, the Wenner probe technique is not accurate when very dense rebar spacing is present. Other methods such as the one using rebars as one electrode and a disk on top of the concrete as the second electrode (i.e., disk method) might be a better in these cases (Feliu et al., 1996).

5.2.5 Effect of rebar diameter

Variation in rebar diameter and its influence on the measured resistivity was investigated only for configuration #4. Prior results showed that this configuration provides more reasonable outputs, and thus it was selected for this part of the study. Rebar diameters of 16 mm, 25 mm and 36 mm were used along with varying electrode spacing and rebar spacing to investigate how measurements are altered by the change in rebar diameter. As shown in Figure 5-4, increase in rebar diameter causes small changes in the measurements. This change becomes larger as the cover thickness decreases. As shown in Figure 5-4, lines representing values of different rebar diameters are very close to each other. Maximum deviation of around 5% is observed when rebar spacing is 50 mm and cover thickness is 25 mm. Therefore, it is inferred that the influence of changes in rebar diameter is not significant, especially for field application. Similar conclusion and comparable results were reported by Millard (1991) for a single bar; measurements changed by 5% when rebar diameter was varied from 16 mm to 32 mm with concrete cover of 40 mm. In addition, comparing Figure 5-4(a) and (b) it is evident that measurements taken using both electrode spacings (i.e., 38 mm and 50 mm) provide reasonably similar results.

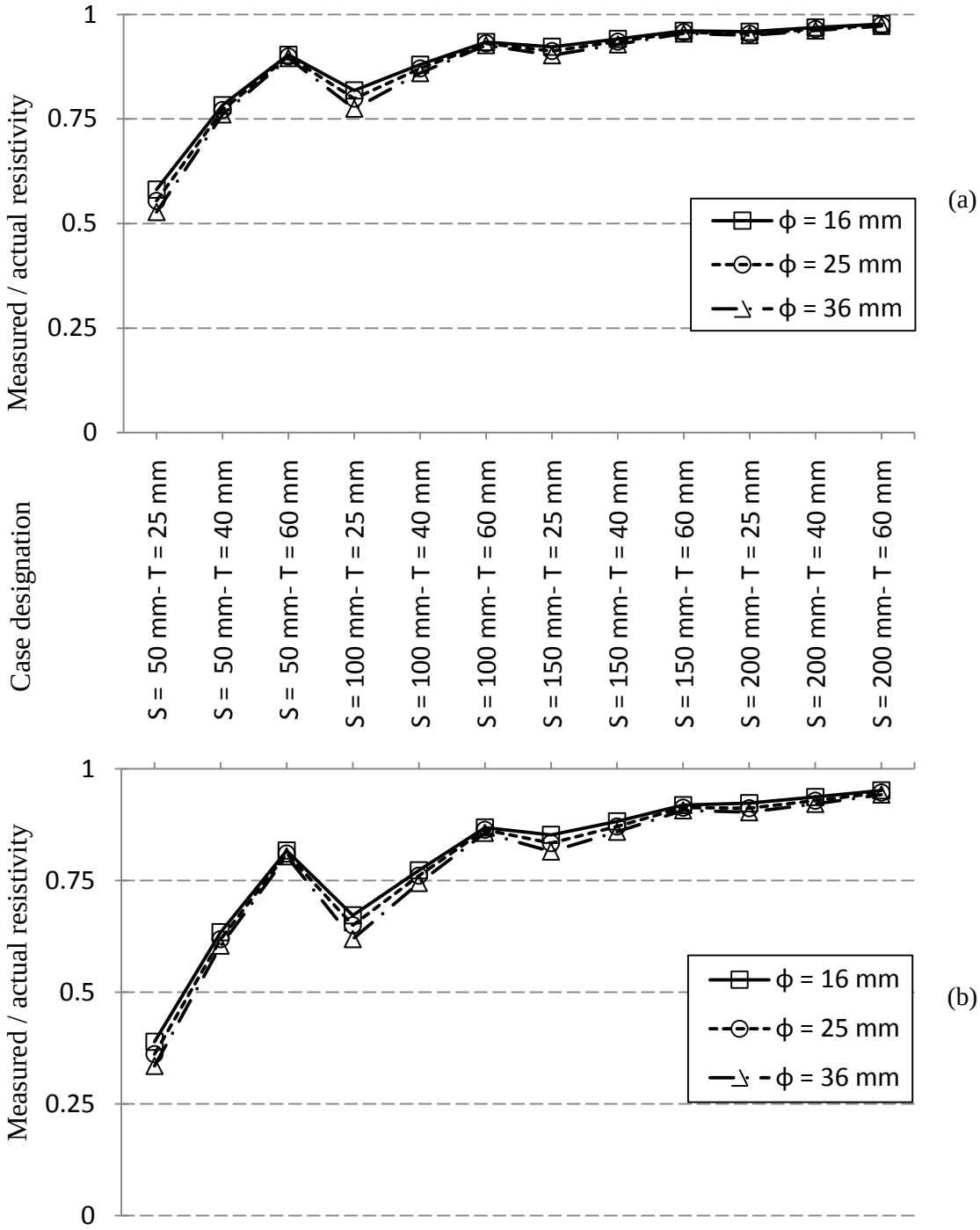

Figure 5-4: Variation in measured resistivity due to change in rebar diameter for configuration #4: (a) electrode spacing of 38 mm; (b) electrode spacing of 50 mm.

5.2.6 Effect of concrete depth

Concrete with two different depths were used to investigate the effect of domain confinement on the Wenner probe resistivity measurement in the presence of rebar mesh. One scenario incorporated a concrete with depth of 120 mm and the other one a concrete with infinite depth. Rebar spacing was also varied from 100 mm to 200 mm, and only configurations #1, #4, #5, #6, #9 were investigated. Configuration # 4 was selected because of its relatively high accuracy compared to other configurations followed by #5 and #6, which are similar to #4 with slightly lower accuracy. To broaden the applicability of the results, configurations #1 and #9 were also included in the study. Surprisingly, no significant difference was observed when concrete depth was changed from infinity to 120 mm. This was true for all electrode spacings, rebar spacings and cover thicknesses investigated that include around 90 different cases. In Figure 5-5 a plot of the values obtained from predictions on both domains are compared against each other. It is obvious that measurements from all configurations are placed around a 45° line indicating a strong agreement between the results of these two cases. The average of ratio obtained by dividing the results of a 120 mm deep concrete to those from the infinite concrete depth is 1.00 with standard deviation of 1.08×10^{-5}.

Influence of concrete depth was further investigated in the absence of steel rebars. It was found that limiting concrete depth to 120 mm from infinity only causes 5.4% deviation in the predictions. Therefore, the initial impact from confining the depth of the domain to 120 mm was not significant. Major portion of electrical current imposed by the Wenner probe tend to transfer from the regions of concrete close to the surface, which is the reason behind having this insignificant variation. Another reason behind this

observation is that once current fluxes inside concrete reach the depth where rebars are present, the majority of the current flux tends to travel through rebar mesh due to its conductive nature rather than moving deeper into concrete. Thus, only small portion of current moves deeper into concrete with negligible effect on predicted electrical resistivity.

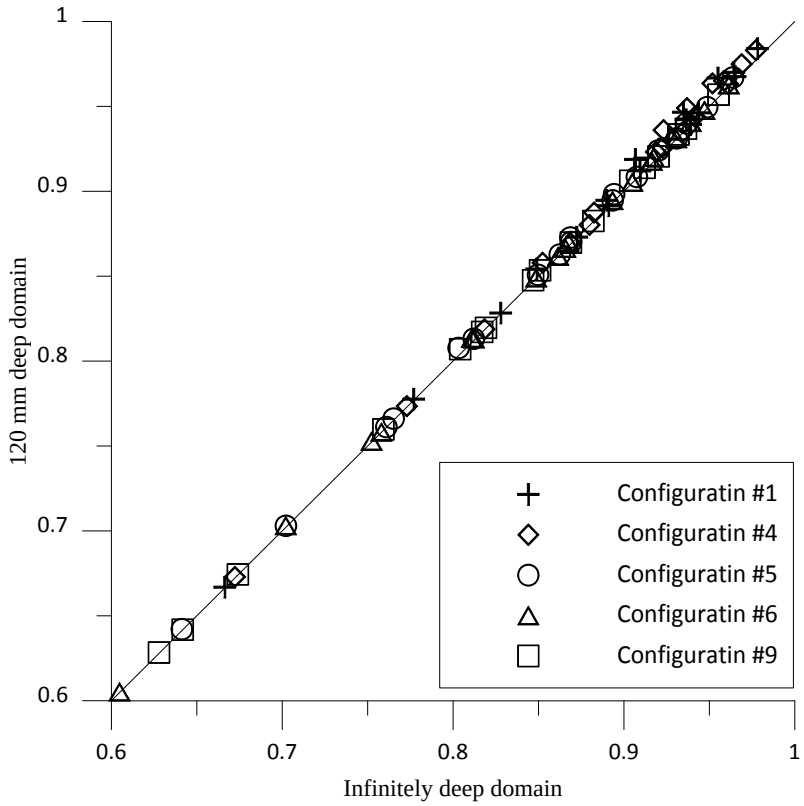

Figure 5-5: Comparing normalized results from an infinitely deep domain with the one that is 120 mm deep.

5.2.7 Summary of rebar mesh effect

Similar to previous studies carried out on taking measurement over a single bar (Weydert and Gehlen, 1999; Gowers and Millard,1999; Sengul and Gjorv, 2009), this study also showed that using smaller electrode spacing would decrease measurement

deviation from the actual resistivity of concrete when measurements are taken over rebar mesh. Likewise, presence of rebars parallel to the Wenner probe was found to have the most significant adverse effect on the performance of the probe. Location of perpendicular rebar was assumed to have no significant impact on resistivity measurement using Wenner probe; however, with rebar mesh, location of perpendicular rebars play a significant role such that measurements could vary as much as 20% with the change in location of perpendicular rebar. As reported by Millard (1991), variation of rebar diameter was found to have some influence on measurements; however, in this study this effect was found negligible.

In an existing structure none of the abovementioned parameters would be under the control of the examiner except the electrode spacing, the location of probe and its orientation. An important factor that can be easily managed on-site for the electrical resistivity measurement is the location and orientation of the Wenner probe. As much as 30% increase in accuracy of concrete resistivity measurement can be achieved just by selecting an appropriate orientation or location for the Wenner probe. Configuration #4 is the most suitable arrangement to minimize the rebar mesh interference on the electrical resistivity measurement.

Distance between the current imposing electrodes and rebars is believed to be the main governing factor in affecting resistivity measurement. In general, this distance can be accounted responsible for the variations observed by change in either cover thickness or rebar spacing. Theoretically, closer the rebars to current electrodes, the easier the current fluxes in concrete can reach them. Hence, more portion of the current tends to pass through the rebars instead of concrete.

Table 5-1 provides a summary of all the results obtained from simulating electrical resistivity measurement for concrete with rebar mesh. Results from all cases related to each configuration were averaged to provide a symbolic mark on how measurements would deviate from the actual resistivity of concrete. In this table, length of the arrows is an indication of magnitude of deviations and the direction shows weather the effect caused increase or decrease in measurement.

Table 5-1: Summary of the results for effect of rebar mesh on Wenner probe resistivity measurements.

	Electrode spacing (mm)		**Cover thickness (mm)**			**Rebar spacing (mm)**			
Configuration #	**38**	**50**	**25**	**40**	**60**	**50**	**100**	**150**	**200**
1	▼	▼	⬇	▼	-	⬇	▼	-	-
2	▼	⬇	⬇	▼	▼	⬇	⬇	▼	▼
3	▼	⬇	⬇	▼	▼	⬇	⬇	▼	▼
4	▼	▼	▼	▼	-	⬇	▼	-	-
5	▼	▼	⬇	▼	-	⬇	▼	▼	▼
6	▼	▼	⬇	▼	-	⬇	▼	▼	-
7	▼	⬇	⬇	▼	-	⬇	▼	▼	▼
8	▼	⬇	⬇	▼	▼	⬇	⬇	▼	▼
9	▼	⬇	⬇	▼	▼	⬇	⬇	▼	▼
⬇ < 0.75			0.75 ≥ ▼ < 0.9			0.9 ≤ - ≤ 1.0			

5.3 Concrete with Crack

It has been shown earlier that electrical resistivity measurement is influenced by the presence of crack in concrete (Lataste et al., 2003; Wiwattanachang and Giao, 2011). However, no systematic study has been carried out to show how cracking affects the Wenner probe measurements. This section is dedicated to the results obtained from investigating a variety of parameters such as crack location, orientation and depth that are considered influential on Wenner probe electrical resistivity measurements.

5.3.1 Effect of crack location

When Wenner probe is placed on the surface of cracked concrete, location of the crack with respect to the probe can be classified with four categories: in the middle of the two inner potential measurement electrodes (L1), between the potential and current electrode (L2), behind the probe (L3), or parallel to the probe (P). The results of these four configurations are shown in Figure 5-6. Looking at the same figure, it can be seen that depending on the crack type and its location, measured resistivity could be an overestimate, underestimate or relatively accurate representation of the actual value for concrete with no cracks.

Considering insulated cracks in Figure 5-6, from the three orthogonal cracks (i.e., L1, L2 and L3), those at location L1 and location L3 as well as the parallel crack (P), always cause higher resistivity measurements than the actual resistivity of concrete. For a crack at location L2, measurements show values less than the actual resistivity of concrete. Similar observations on the effect of the crack location on the electrical resistivity of concrete were also reported by Lataste et al. (2003). As explained in more

detail in Section 2.5, a square probe was used in their study to measure electrical resistivity, which had a different electrode configuration compared to the Wenner probe. Consequently, orientations and locations of the crack by Lataste et al. (2003) were different from those presented in this work.

Insulated cracks located behind the Wenner probe (L3) or parallel to the probe (P) at a certain distance show geometrical confinement effects as described by Millard (1991); hence, overestimation of resistivity is expected. Insulated crack in the middle of the probe (L1) would also behave as a barrier forcing current fluxes to move deeper into the concrete. Figure 5-7 provides an overview on the distribution of equipotential lines and current flux for a crack at location L1. The downward movement needs higher electrical potential distribution in the direction of the flux to provide the required energy. As a result, equipotential lines with larger values (either positive or negative) will be located closer to the potential measurement electrodes. Eventually this phenomenon leads to higher values reading for ΔV followed by higher value measurement in the electrical resistivity.

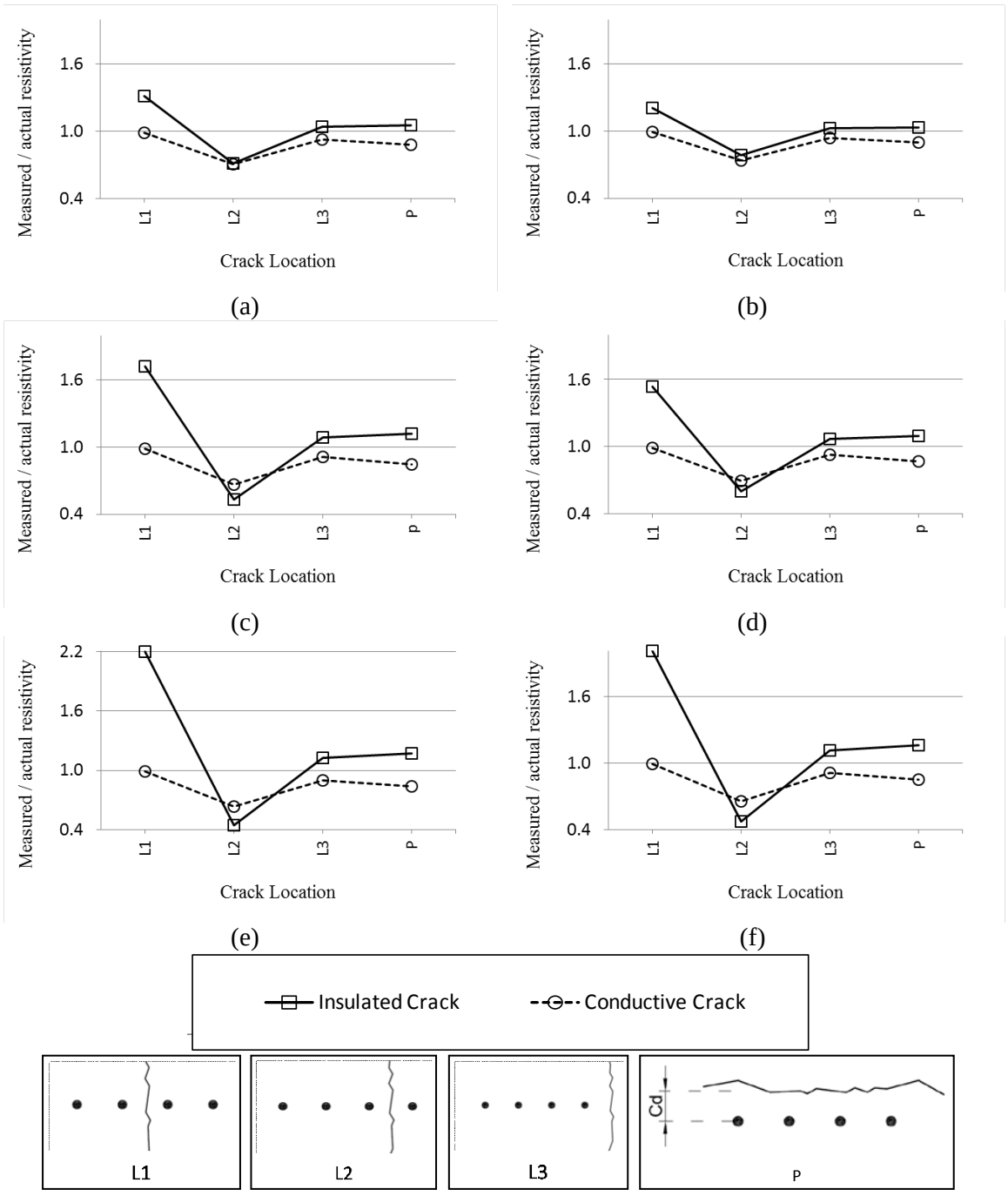

Figure 5-6: Influence of location of the crack on electrical resistivity measurement for different electrode spacings, crack types and heights: (a) a = 38 mm, C_h = 20 mm; (b) a = 50 mm, C_h = 20 mm; (c) a = 38 mm, C_h = 40 mm; (d) a = 50 mm, C_h = 40 mm; (e) a = 38 mm, C_h = 80 mm; (f) a = 50 mm, C_h = 80 mm

Lataste et al. (2003) results showed that the presence of an insulated crack parallel to the current electrodes in the middle of the square probe led to reduction in measured electrical resistivity. For the Wenner probe, a perpendicular crack at location L2 demonstrates similar behaviour whereas parallel crack causes overestimation of the concrete resistivity. Further investigation of this phenomenon revealed that there was a common feature between the two probe systems (i.e., square and the Wenner probes) that led to the same behaviour. In both probes, when current electrodes are isolated from potential measurement electrodes via an insulated crack the underestimation of the actual resistivity of concrete occurred. For the Wenner probe case, this is analogous to the crack location L2 whereas in the square probe case, a parallel crack in the middle of the probe (Figure 2-9(b)) causes this isolation. In Figure 5-8, electrical potential distribution and current fluxes are shown for crack at location L2. A simple explanation for such behaviour could be the confinement of high electrical potential areas by the crack that unbalances the system so that negative electrical potential areas would be shifted toward the crack and as a result values measured for ΔV decreases leading to a reduction in the measured resistivity.

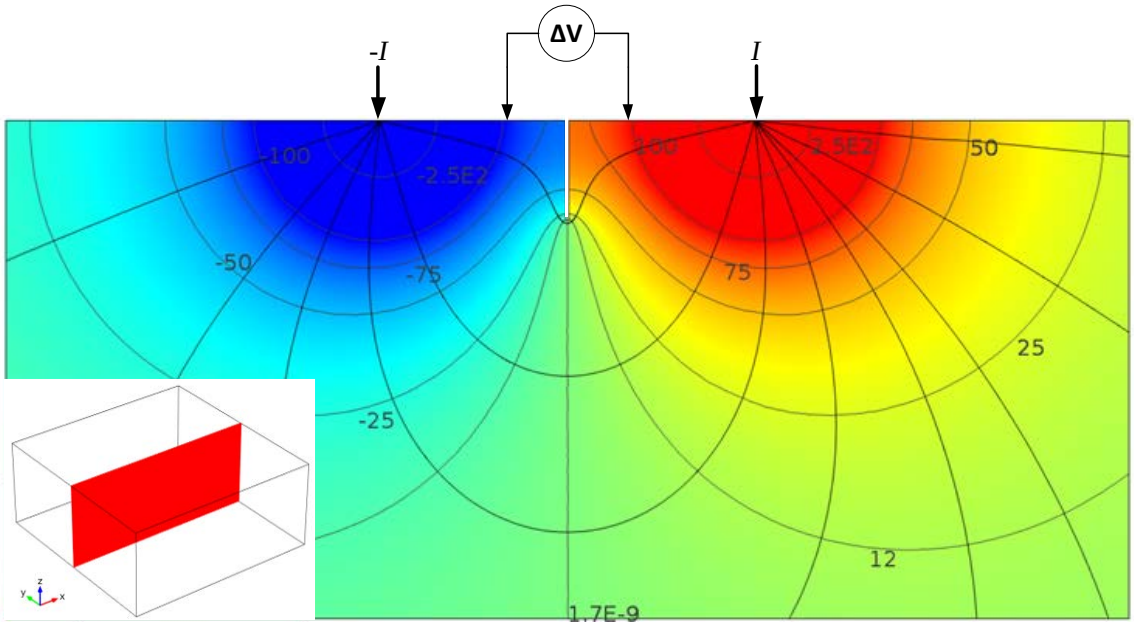

Figure 5-7: Equipotential lines distribution and respective current flux paths in the presence of an insulated crack in the middle of the potential probes (i.e., location L1) for a = 50 mm, C_h = 40 mm.

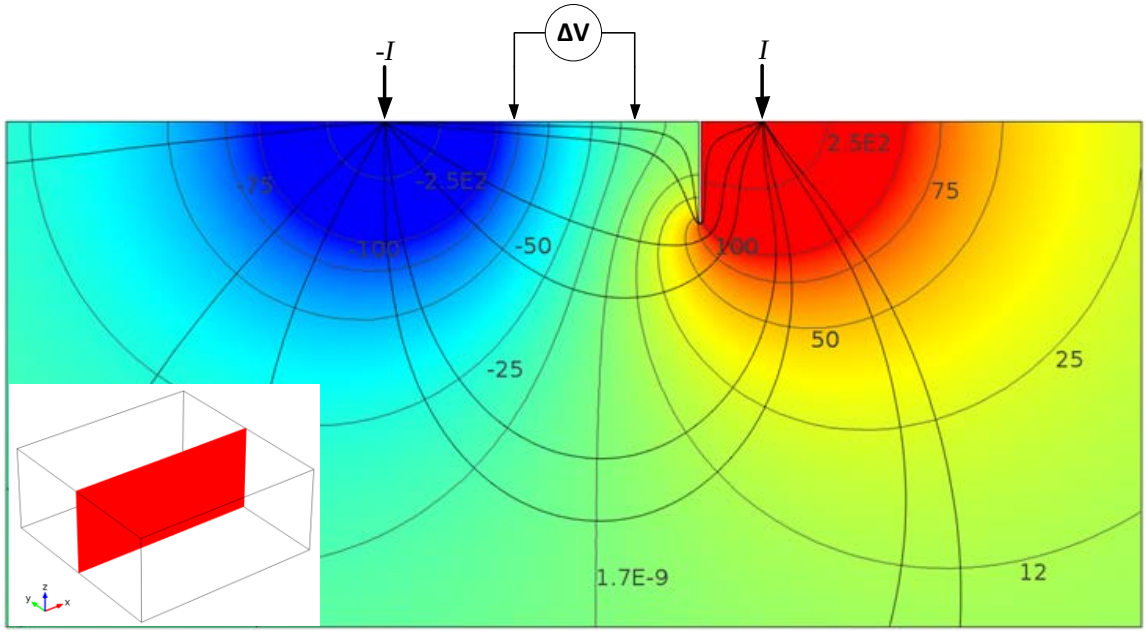

Figure 5-8: Equipotential lines distribution and respective current flux paths in the presence of an insulated crack between the potential and current electrode (i.e., location L2) for a = 50 mm, C_h = 40 mm.

On the other hand, resistivity measurements in the presence of an orthogonal conductive crack at location L2, L3 and parallel to the probe, P, provide lower values compared to the actual resistivity of concrete (Figure 5-6). For crack at the location L1 no significant change was observed. Lataste et al. (2003) concluded that conductive crack perpendicular to the current electrodes of the probe did not have an effect on the measurements. For the Wenner probe, however, different performance can be experienced depending on the location of the crack. The probe behaves similar to what they predicted only when crack was at the middle of the inner electrodes (i.e., location L1). Due to the symmetry of the system, a crack in the middle will be located exactly on an equipotential line with the value of zero. This value can also be simply calculated from Equation 3-13. Hence, a conductive crack on this equipotential line does not cause any disturbance on current fluxes and equipotential lines. Likewise, even rebars with significantly bigger volume compared to a crack located at the middle of the probe inside the concrete does not influence resistivity measurements considerably (Weydert and Gehlen, 1999; Sengul and Gjorv, 2009).

In contrast, the two other perpendicular crack scenarios (i.e., location L2 and L3) do cause reduction in the measured resistivity. For crack at location L2, the overall behaviour observed is similar to what has been discussed for an insulated crack at this location with slight differences. Beside some confinement of current flux distribution, equipotential lines are expanded along the crack as well. An illustration of equipotential lines and current fluxes for such condition is provided in Figure 5-9 . Due to the conductive nature of the crack some amount of current passed through the crack, and routes taken by current fluxes are not as deviated as those for an insulated crack. Hence,

reduction in electrical potential is not as high as the one observed for the insulated crack cases.

For a crack behind the probe (i.e., location L3), lateral displacement of current flux along the crack plays a significant role in disturbing equipotential lines. As seen in the plan view of the domain in Figure 5-10, equipotential lines are expanded in the direction of the crack. They are also receded towards the crack from the centre of the probe causing a reduction in the electrical potential around the positive potential measurement electrode, which results in a reduction in the resistivity measurement. Recession of equipotential lines beside the confinement effect can also be observed for the crack at location L2. For a conductive crack parallel to the probe (i.e., location P), reduction in the measured resistivity was expected since a more conductive passage is provided for the electrical current to flow that is in the same direction of current fluxes inside concrete. As explained in Section 5.1 about the directional nature of current flow inside the concrete, the effect of parallel crack is similar to that of rebar along the probe; both reduce the measured resistivity due to providing a conductive parallel passage for electrical current.

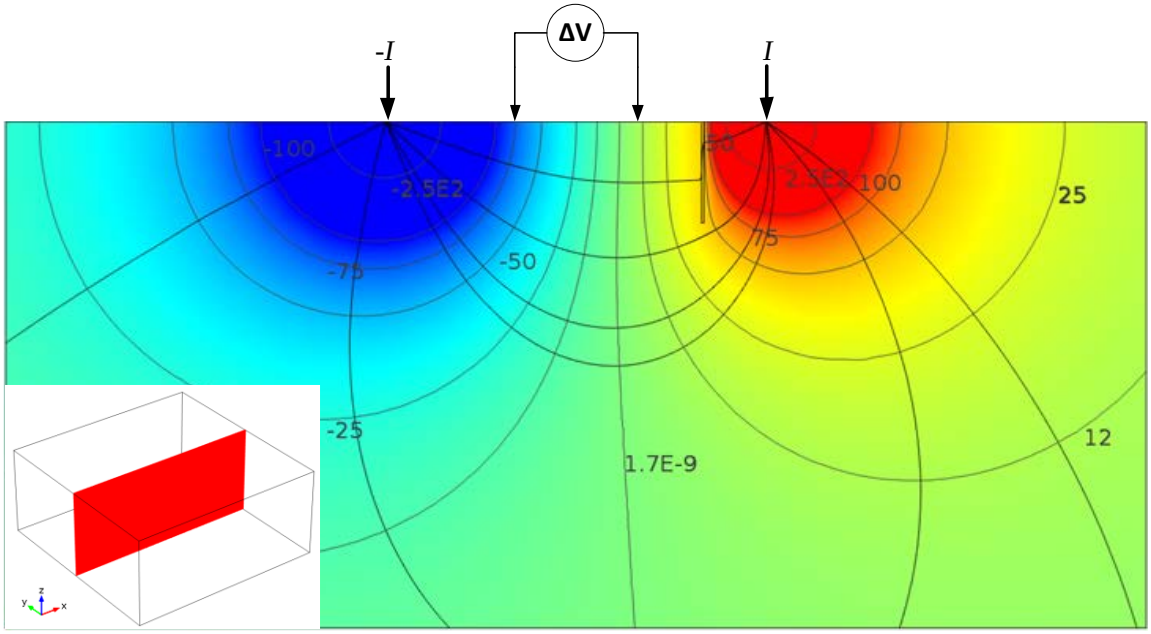

Figure 5-9: Equipotential lines distribution and respective current flux paths in the presence of a conductive crack between the potential and current electrode (i.e., location L2) for a = 50 mm, C_h = 40 mm.

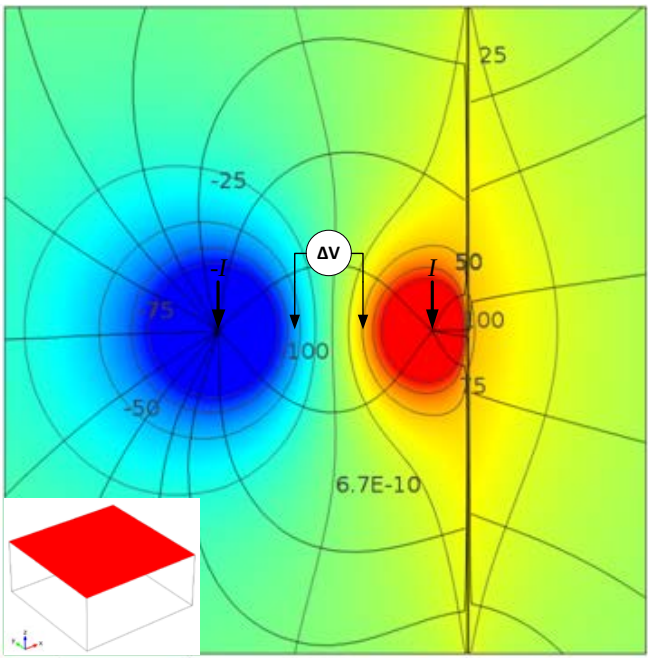

Figure 5-10: Plan view of equipotential lines distribution and respective current flux paths in the presence of a conductive crack behind the probe (i.e., location L3) for a = 50 mm, C_h = 40 mm.

5.3.2 Effect of crack height

The overall behaviour of the Wenner probe in the presence of a crack at certain locations was discussed in the previous section. A simple explanation on the mechanism causing such performance was also provided. It was shown that cracks could cause confinement or provide an alternative passage for the current to flow. In this section the effect of the crack height is investigated using the developed model. Figure 5-11 illustrates deviations observed in the measured electrical resistivity compared to the actual resistivity of concrete as height of the crack changes.

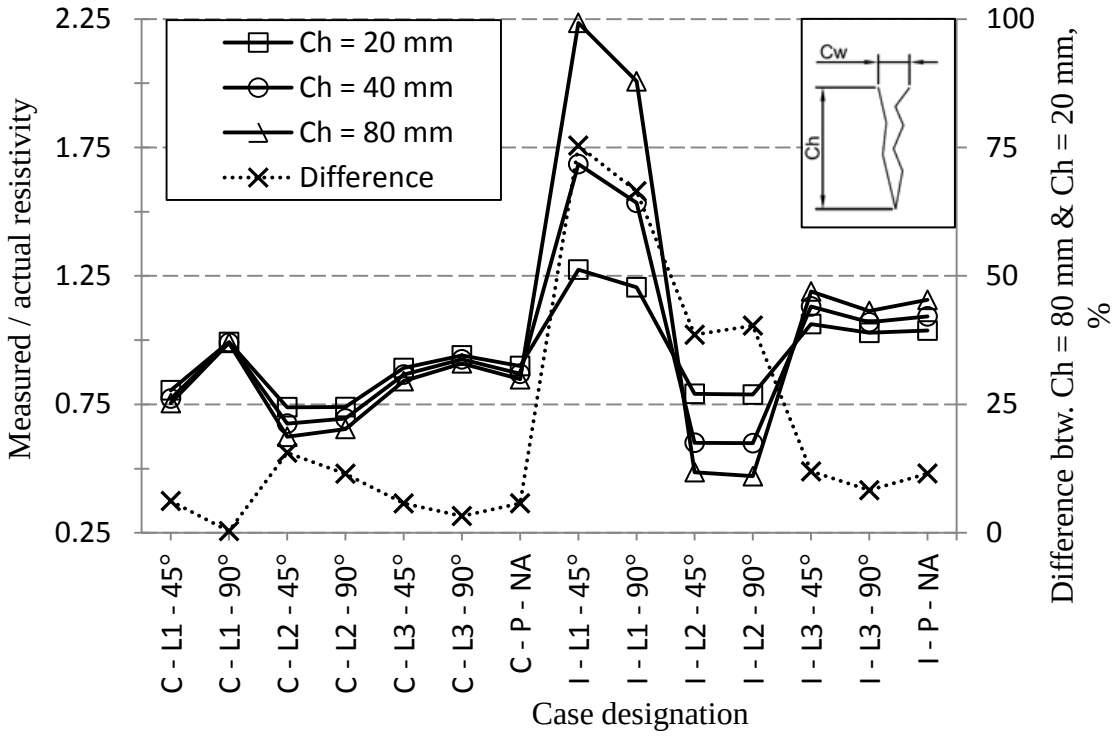

Figure 5-11: Crack height variation and its influence on measured values with respect to the actual resistivity of concrete for different crack types, locations and angles for a = 50 mm.

The first seven cases that have designations starting with letter *"C"* represent conductive cracks at different locations with different crack angles while the other seven starting with the letter *"I"* represent insulated cracks. Significant variations shown in this figure belong to the cases with an insulated crack located in the middle of the probe (i.e., location L1). Measured values are 25% higher than the actual resistivity of concrete for a crack with the height of only 20 mm. This scenario will get worse as the crack height increases to 80 mm in which values twice the actual resistivity of concrete are attained. Following crack at the location L1, insulated crack at the location L2 had the second most severe impact on the Wenner probe resistivity measurement. For crack height of only 20 mm, more than 20% reduction from the actual resistivity of concrete was attained. This reduction increased beyond 50% as the crack height reached 80 mm. These results are in agreement with data provided from numerical investigation carried out by Lataste et al. (2003) for the square probe. Deviations in measurements in excess of twice the initial resistivity of the domain modelled was reported for insulated crack with the height of 80 mm located perpendicular to the direction of the imposed current, as shown earlier in Figure 2-9(b).

For conductive cracks, the amplitude of deviations in measurements is not comparable to the insulated crack scenarios. Reduction of 25% from the actual resistivity of concrete was obtained for conductive crack at the location L2 for the crack height of 20 mm, which became close to 35% as the crack height was extended to 80 mm. Surprisingly, impact from increasing crack height at the location L2 was not as significant as those obtained from the presence of an insulated crack at the location L2. In contrast, Lataste et al. (2003) study showed significant reduction in the presence of a

conductive crack parallel to the direction of the imposed current by the square probe. Two reasons could be identified for such dissimilarity: First, the conductive crack in the study carried out by Lataste et al. (2003) was located closer to the current electrodes in the square probe; i.e., almost half the distance used in this study that amplified the effects of a crack on the resistivity measurement. Second, due to difference in the arrangement of the electrodes in the square probe, parallel conductive crack can create a high conductive path for the current as well as separating potential and current electrodes which will further confine current fluxes inside the concrete (Figure 2-9(b)). Both these phenomena cause reduction in the measured resistivity as explained earlier leading to a more severe response by the square probe compared to Wenner probe.

The *"Difference"* line in Figure 5-11 depicts the difference between obtained values for the crack height of 80 mm and that of 20 mm. This is useful to illustrate the sensitivity of the Wenner probe measurements to the variation in the crack height. Overall, the Wenner probe measurements are more sensitive to crack height variation for the insulated crack than that of the conductive crack. Even with an insulated crack, when crack is at location L1 and L2, measurements are more sensitive to changes in crack height compared to the two other crack locations, L3 and P.

On the other hand, only a conductive crack at location L2 had a relatively strong impact on the measured resistivity. One reason that conductive crack height variations had lesser effect on measurement deviations is the nature of current flux distribution in concrete. Deeper regions in concrete are exposed to smaller portion of current fluxes (Telford et al., 1990). Consequently, most influence is from the upper region of the crack close to the surface of concrete regardless of the height. The only exception is for cracks

at location L2 where some confinement of current flux distribution also occurs that depended on crack height.

5.3.3 Effect of crack angle

Another parameter studied and found to be influential on the resistivity measurements is the crack orientation with respect to the direction of the Wenner probe. Measurement deviation from the actual resistivity of concrete for cracks at two distinct angles (i.e., 90° and 45°) is shown in Figure 5-12.

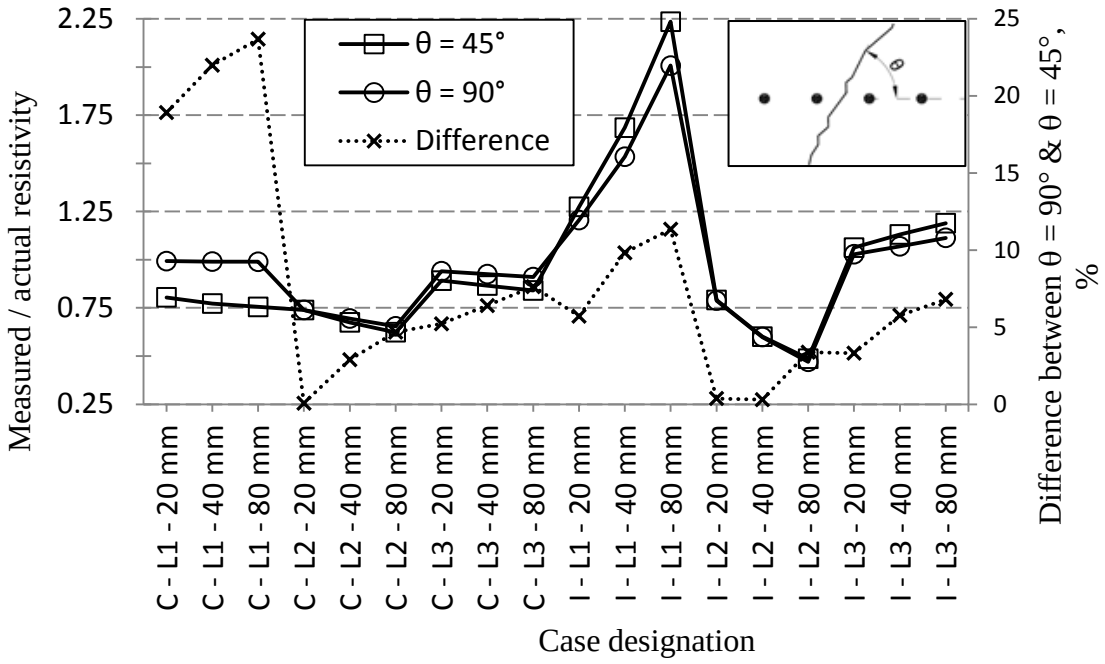

Figure 5-12: Crack angle variation and its influence on measured resistivity with respect to the actual resistivity of concrete for different crack types, locations and heights for a = 50 mm.

In most cases there is a variation in the measured resistivity as the angle of crack changes. This is discernible by considering the *"Difference"* line which depicts changes in the measured resistivity as crack rotates from 90° to 45° (i.e., from perpendicular to diagonal).

For conductive crack, more than 20% reduction in measured resistivity occurs when a crack located in the middle of the probe (i.e., location L1) rotated. A perpendicular crack at this location originally does not have any influence since it lies on an equipotential line with the value of zero whereas in diagonal orientation, it provides a path with lower resistivity for the current to pass though. This remarkably affects the measurements. On the other hand, rotation of an insulated crack has a comparable effect only when crack height reaches to 80 mm. Influence of orientation for a crack located at location L2, regardless of being conductive or insulated, is insignificant. Difference between measured resistivity for the two crack angles at this location was less than 5%.

Further investigation of the numerical data reveal that there is a direct relationship between the height of the crack and the amount of variation observed due to the change in the crack angle as shown in Figure 5-13. In this figure the amount of absolute variation in the measured resistivity with respect to the actual resistivity of concrete as the crack orientation changes from perpendicular to diagonal is illustrated. Values for crack height of 20 mm are assumed as the basis to obtain measurement deviation when crack height changes from 20 mm to 80 mm. Despite the existing correlation between crack height and crack orientation, overall impact is not significant; i.e., only 5% change on average.

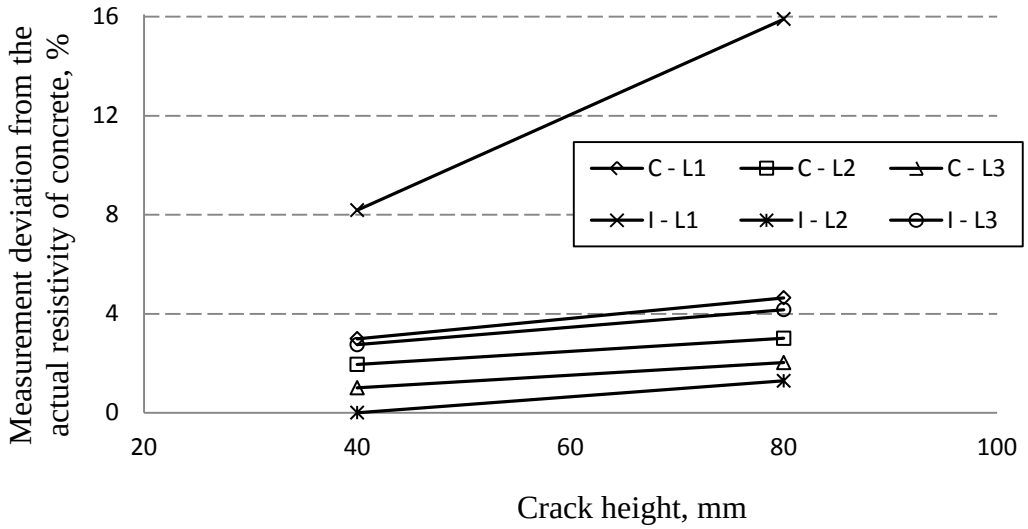

Figure 5-13: Relationship between crack height and crack angle from 90° to 45° for a = 50 mm.

5.3.4 Effect of electrode spacing

Figure 5-14 and Figure 5-15 depict resistivity measurement variation due to changes in electrode spacing of the probe for an insulated and conductive crack, respectively. Considering the difference between measurements obtained from 50 mm and 38 mm electrode spacings, one can see that data taken at the vicinity of an insulated crack are more sensitive to the change in electrode spacing. This is such that for a crack in the middle of the probe, i.e., location L1, more than 10% change is observed by just varying the electrode spacing. For the Wenner probe, 60% of the imposed current is carried by a volume of concrete located only one electrode spacing below the surface of concrete (Telford et al., 1990). Hence, the measured value for the concrete resistivity is mainly related to a hemisphere with the radius of one electrode spacing right beneath the centre of the probe. Consequently, a crack with a certain height has a higher impact if the electrode spacing is smaller.

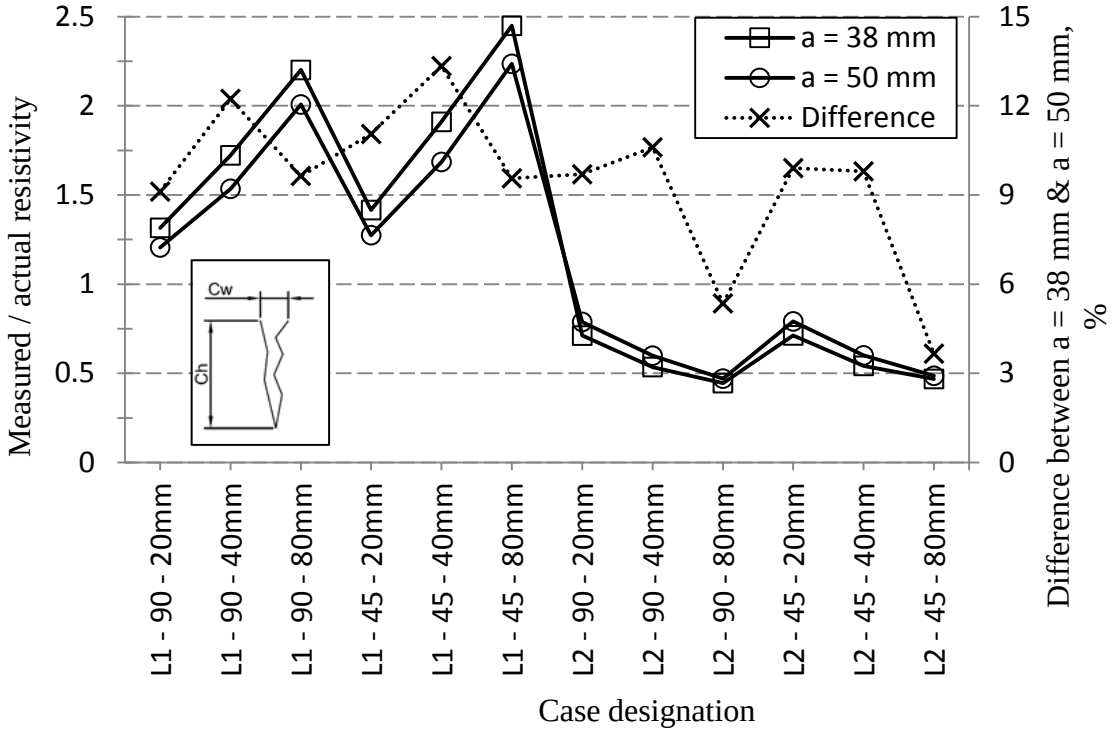

Figure 5-14: Measured resistivity with respect to the actual concrete resistivity in the presence of an insulated crack with different crack heights, orientations and locations for two electrode spacing of 38 mm and 50 mm.

On the contrary, as shown in Fig. 5-15, measurements in the presence of a conductive crack are less sensitive to the variation in electrode spacing. Similar explanation to the one given in section 5.3.2 regarding the influence of conductive crack height can be provided for the observed behaviour. Majority of the imposed current will be passing through shallower depths of the concrete. When the crack is conductive and relatively deep, most of its impact is at the areas close to the surface and thus changes in the crack height would not significantly affect this phenomenon. With the values considered for the crack height in this study, changing electrode spacing from 50 mm to 38 mm does not significantly affect the measurements (see Figure 5-15).

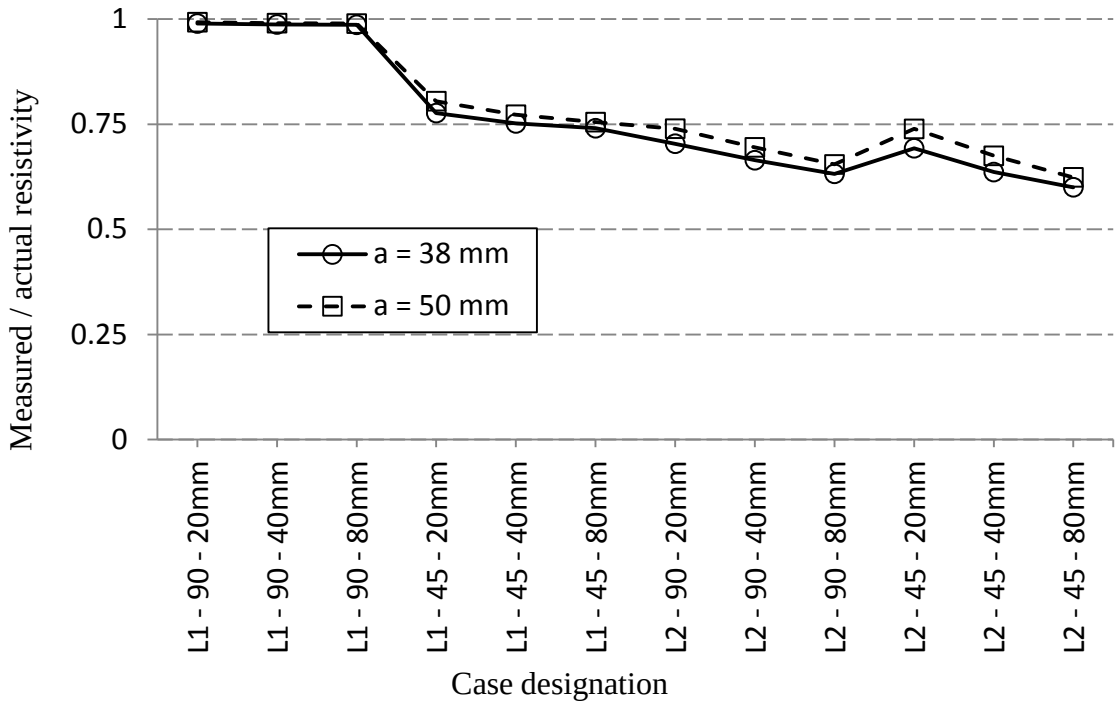

Figure 5-15: Measured resistivity with respect to the actual concrete resistivity in the presence of conductive crack with different crack heights, orientations and locations for two electrode spacing of 38 mm and 50 mm.

In section 5.2.2 the effect of varying electrode spacing on the resistivity measurements of concrete with embedded rebar mesh was discussed. It was concluded that measurement deviation from the actual resistivity of concrete increases as the electrode spacing increases. When taking measurement on concrete with crack, an opposite behaviour was observed. Increasing electrode spacing, either did not have significant impact on measurements or it decreased the measured resistivity compared to the actual resistivity of concrete depending on the type of crack present.

5.3.5 Effect of crack length

Limited number of cases was modelled to investigate the influence of varying crack length in more details. Figure 5-16 shows results from a scenario in which a crack with the height of 40 mm is located on concrete, and measurements were taken using a Wenner probe with the electrode spacing of 50 mm. In these cases the length of the crack was varied from 150 mm to 450 mm.

First point to mention in this figure is related to deviations in the measured resistivity observed for each crack length. It is apparent that values taken for crack length of 300 mm are very close to those of 450 mm. This clearly shows that further increase in crack length does not influence the measurement. It is widely believed that the sensitivity of Wenner probe to defects and irregularities is proportional to its electrode spacing as discussed in this study and those by Millard (1991), Sengul and Gjorv (2009), Gowers and Millard (1999) and Moreno et al. (2009). Therefore, it is not surprising to see small variations when crack length increases from 300 mm (i.e., six times the electrode spacing) to 450 mm (nine times the electrode spacing).

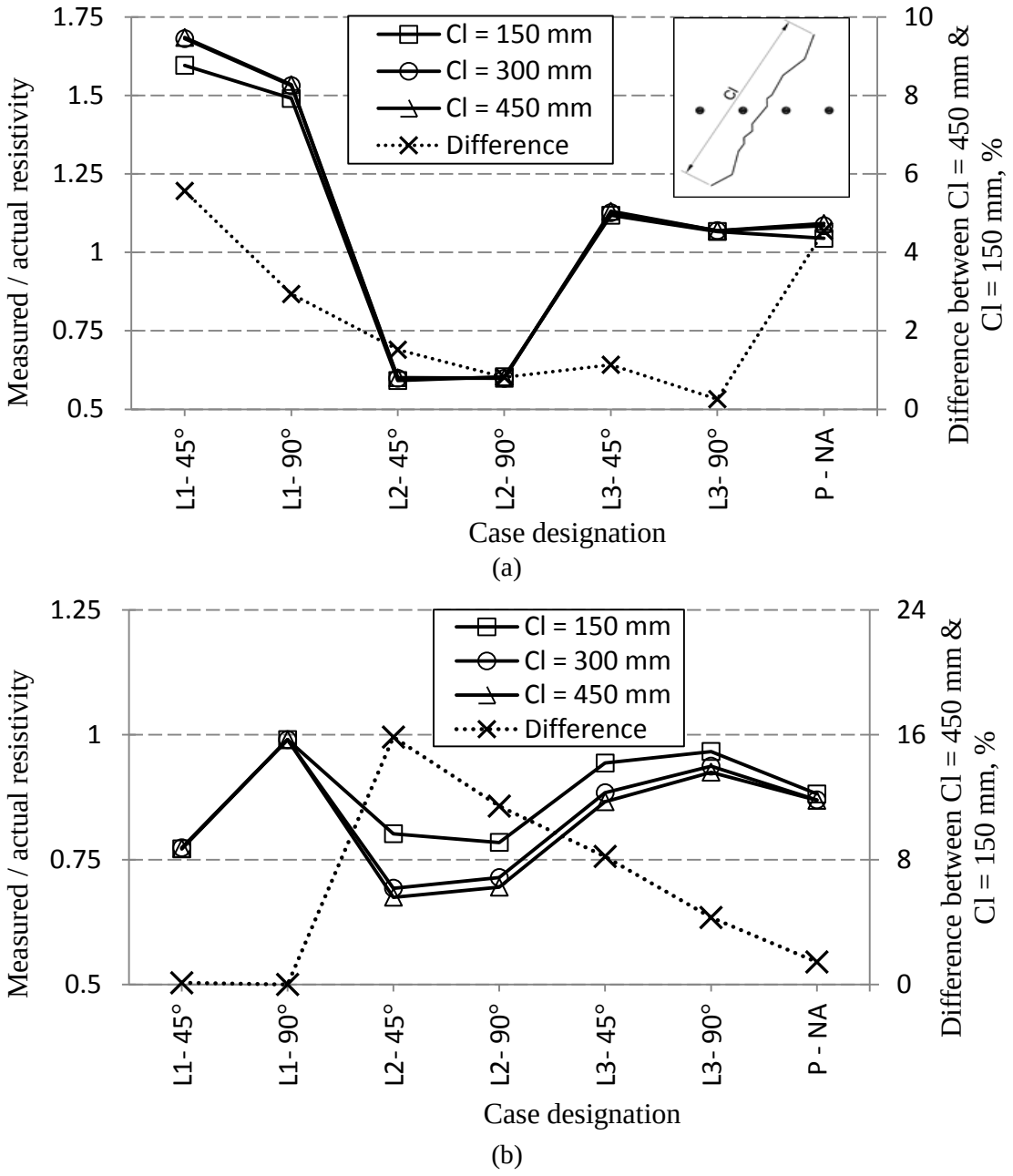

Figure 5-16: Influence of variation in the length of a crack located at different positions and orientations with respect to the Wenner probe for C_h = 40 mm, C_w = 1 mm, a = 50 mm: (a) insulated crack; (b) conductive crack.

The second point to highlight is the insensitivity of some configurations to changes in the crack length in the abovementioned range. This behaviour is more obvious in the dash-line plot showing the difference between measurement deviations obtained from

crack length change of 150 mm to 450 mm (Figure 5-16(b)). For instance, altering crack length does not remarkably affect measurements in the presence of insulated crack at the location L2 and L3. Likewise for conductive crack at location L1, measured resistivity for the investigated various crack lengths is almost constant. The highest variation is observed for insulated crack at location L1 which shows 10% increase in the measured resistivity. For conductive crack, the location L2 has the highest deviation (16%) by crack length increase.

Further investigation revealed that those configurations seemed to be insensitive to crack length variations were actually highly sensitive to the presence of crack. The reason why they appeared to be insensitive is the range of crack length values chosen in the first attempt. Figure 5-17 illustrates resistivity measurement deviation as a function of the crack length for those five high sensitive cases. It is clearly visible that all those curves experience a plateau as the crack length reaches 100 mm (i.e., two times the electrode spacing) where afterwards no significant changes happen. The only exception is perpendicular conductive crack at the middle of the probe, i.e., L1 case. As discussed in Section 5.3.1 this crack is located on an equipotential line with the value of zero having no impact on resistivity measurements. More important point to highlight is that for crack length as small as 50 mm, measured resistivity deviated from the actual resistivity of concrete by more than 15% when the crack height was 20 mm and it became close to 25% as crack height increased to 40 mm. This indicates care should be taken when dealing with defects especially insulated cracks at location L2.

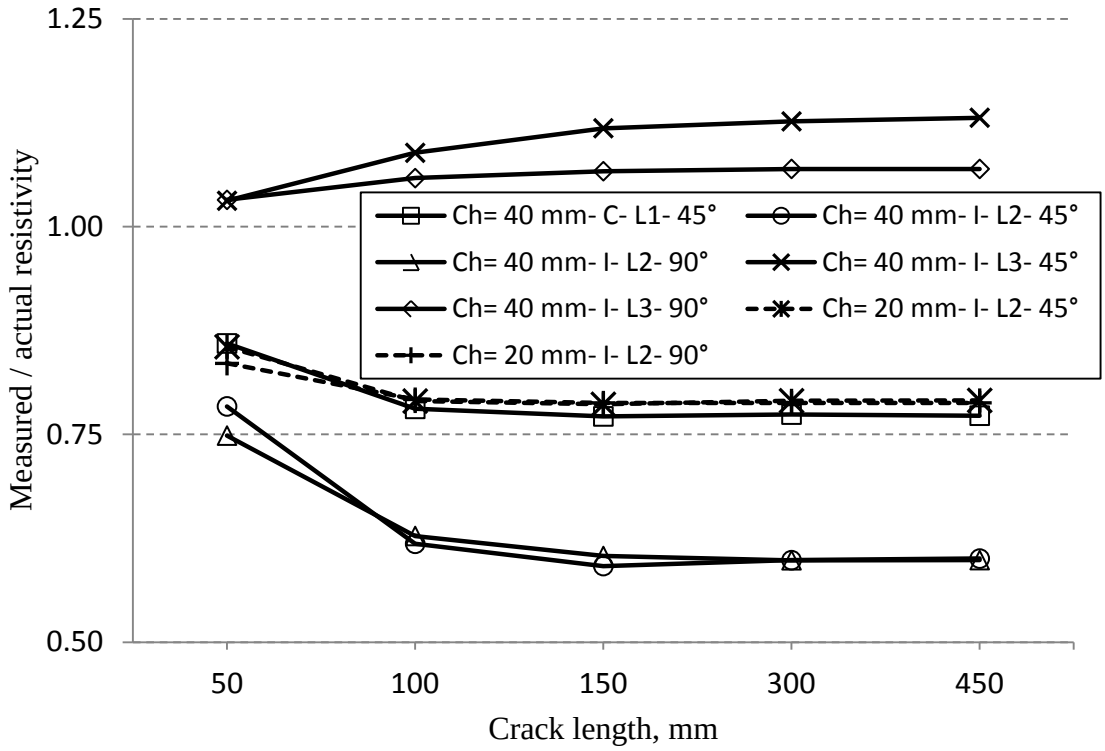

Figure 5-17: Influence of crack length variation on measurements plotted for smaller crack lengths for C_w = 1 mm, a = 50 mm.

5.3.6 Effect of crack width

Sensitivity of measurements to crack width variation is shown in Figure 5-18. Only values for a limited number of cases with various combinations of crack height, crack orientation and electrode spacing were studied since including all the possible combinations were not feasible. It is expected to see similar behaviour as crack width varies for all other scenarios which were not modelled. As illustrated in Figure 5-18, only those measurements at the vicinity of a conductive crack are under the influence of variation in crack width. The negligible effect from the variation in the crack width of an insulated crack was also concluded by Lataste et al. (2003). For conductive crack, results

show large deviations when crack was parallel to the probe or located at location L2 (i.e., between potential and current electrodes). For these locations, decreasing crack width caused electrical resistivity to increase by almost 7%. The mechanism behind impact of conductive crack at those locations on electrical resistivity measurement was explained in Section 5.3.1. In brief, as the width of the crack decreases, the resistivity of the passage provided by crack for current would increase; hence, less current would pass through the conductive crack, which in return lessens its impact.

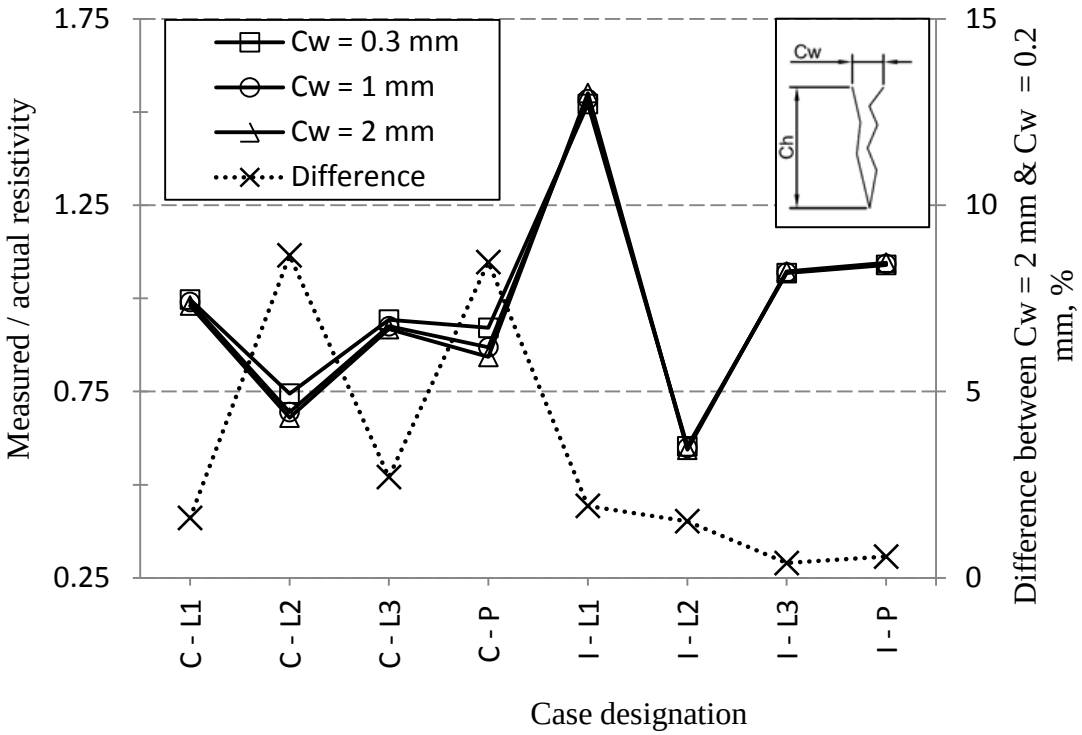

Figure 5-18: Variation in resistivity measurement for different crack widths for C_h = 40 mm, a = 50 mm, θ = 90°.

5.3.7 Effect of concrete resistivity

The last influential parameter affecting the electrical resistivity measurements on concrete with conductive crack present is the ratio between the resistivity of concrete and

contents filling the crack. Resistivity of the crack is affected by the water content inside the crack and the type of ions and minerals mixed with the water filling the crack. Resistivity of crack content varies based on the type of ions present and their concentration (Ghods, 2010). Ghods (2010) reported typical pore solutions available inside concrete have electrical resistivity ranging from 0.04 Ω-m to 2 Ω-m. Concrete on the other hand, has electrical resistivity typically ranging from 50 Ω-m to those in excess of 200 Ω-m (Broomfield, 1997; McCarter et al., 2005). To have a better understanding of how variation in the resistivity of either crack or concrete might affect measurements using Wenner probe, a wide range of concrete-to-crack resistivity ratios were modelled. Similar to Section 5.3.6, only one specific combination of crack width, orientation and height along with single electrode spacing was used to carry out this investigation.

Assuming measurements taken on a concrete surface without any defect as a reference, normalized values for resistivity measurement in the presence of crack are shown in Figure 5-19. Comparing data provided in this figure with the analysis done earlier in Section 3.4.2, one could see the similarity in the behaviour of the Wenner probe between these two sections. In Section 3.4.2 varying the ratio of concrete to rebar resistivity was investigated, and it was observed that ratios above 10^3 had no significant effect. Likewise, in Figure 5-19, variation in the measured resistivity becomes insignificant as concrete-to-crack resistivity ratio exceeds 10^3. It can be concluded that for the crack at location L2, measurements would deviate from the original resistivity of concrete by almost 30% as the crack becomes 1000 times more conductive than concrete. However, further reduction in resistivity of the crack does not cause significant changes

in the measurements. Similar behavior is observed for cracks in parallel to the probe or located at half the electrode spacing behind it.

On the other hand, when concrete-to-crack resistivity ratio decreases, influence of crack starts to diminish. It can be seen in the figure that for concrete only ten times resistive than the crack, measurement deviations of less than 5% is experienced.

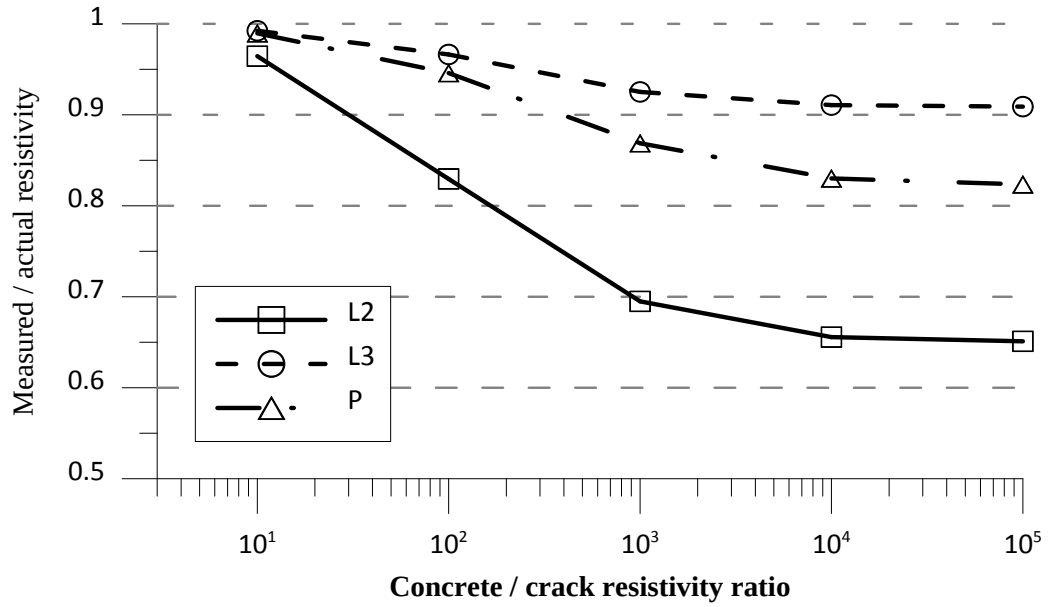

Figure 5-19: Resistivity measurement variation due to changes in concrete to crack resistivity ratios for C_w = 1 mm, C_h = 40 mm, a = 50 mm, θ = 90°.

5.3.8 Summary of influence of a single crack on resistivity measurement

Several factors were found to be influential on the electrical resistivity measurement on concrete at the vicinity of a crack. These parameters were investigated one by one to characterize their influence as well as the cause and mechanism by which they affect the Wenner probe measurements. Location of the crack was found to be one important parameter that can alter measurements. Regardless of the type of crack, it was found that if there is a crack between the current and potential electrodes of the Wenner

probe (i.e., L2), measurements taken would always provide an underestimated value for the resistivity of concrete. Cracks that provide conductive passage for electrical current would also cause measurement data to be less than or equal to the actual resistivity of concrete regardless of their location.

Measurements taken over insulated cracks are more sensitive to the height of the crack than those obtained from a crack filled with moisture and ions acting as a conductive crack. This effect is high when crack is at location L2, and it is highest when insulated crack is at the middle of the probe (i.e., L1). Similarly, the orientation of the crack with respect to the probe was found to have most significant impact on measurements when crack is located in the middle of the probe (i.e, L1). However, for those cracks at location L2, the change of crack angle does not have any substantial effect on the measurements.

Changing electrode spacing of the Wenner probe was found to be influential only if one deals with an insulated crack. Unlike concrete with rebar mesh cases, increasing electrode spacing would decrease measurement deviations from the actual resistivity of concrete.

Cracks with a length as small as one electrode spacing could have significant impact on resistivity measurement using Wenner probe, especially if they are located between two adjacent current and potential electrodes (i.e., L2).

For insulated cracks, the width of crack opening does not affect electrical resistivity measurements; however, if it is filled with conductive solutions, it would affect data obtained such that the bigger the opening, the higher measurement deviations. Finally,

only crack that is 100 times more conductive than the concrete was found to affect electrical resistivity measurements noticeably.

Table 5-2 provides a summary of results obtained from all the simulated cases regarding effect of crack on the Wenner probe resistivity measurements. In this table, for each type of crack and its location, a symbol presents the average value of measured to actual resistivity of concrete expected for each parameter indicated on the column. In brief, downward arrows indicate expected underestimation in the electrical resistivity measurements while upward arrows indicate expected overestimation in the results, while length of an arrow suggests the magnitude of this deviation. Dashes are considered to represent scenarios for which deviations were not significant.

Table 5-2: Summary of the results for effect of crack on Wenner probe resistivity measurements.

Crack type	Crack location	Electrode spacing (mm)		Crack height (mm)			Crack angle (°)			Crack width* (mm)			Crack length* (mm)				
		38	50	20	40	80	90	45	0	0.3	1	2	50	100	150	300	450
Conductive	L1	▼	▼	▼	▼	▼	-	▼		-	-	-	▼	▼	▼	▼	▼
	L2	⬇	⬇	⬇	⬇	⬇	⬇	⬇		▼	⬇	⬇			▼	⬇	⬇
	L3	▼	▼	-	▼	▼	-	▼		-	-	-			-	-	▼
	P	▼	▼	▼	▼	▼			▼	-	▼	▼			▼	▼	▼
Insulated	L1	▲	▲	▲	▲	▲	▲	▲		▲	▲	▲			▲	▲	▲
	L2	⬇	⬇	▼	⬇	⬇	⬇	⬇		⬇	⬇	⬇	▼	⬇	⬇	⬇	⬇
	L3	▲	-	-	▲	▲	-	▲		▲	▲	▲	-	-	-	-	▲
	P	▲	-	-	▲	▲			▲	▲	▲	▲			-	-	-

⬇ < 0.75	0.75 ≤ ▼ < 0.9	0.9 ≤ - < 1.1	1.1 ≤ ▲ < 1.25	1.25 ≤ ⬆

(*): data from limited number of cases.

5.4 Combined Effect of Rebar Mesh and Concrete Crack

In the two previous sections of this chapter (Section 5.2 and Section 5.3) the effect of embedded rebar mesh and the presence of a crack were studied separately. In reality, resistivity measurements on the surface of the concrete will be under the influence of both rebar mesh and crack. Therefore, it was important to see how the Wenner probe technique would perform when those influential conditions are present together. Taking measurements over rebar mesh is unavoidable as rebars are a major component of the reinforced concrete. The main goal of this section is to understand whether the presence of crack would further influence the measurements and to what extend those influences reach.

Results from Section 5.2.1 showed taking measurements in configuration #4 over embedded rebar would provide the closest values to the actual resistivity of concrete. Configuration #9, on the other hand, was the one suggested by Polder et al., (2000). So only these two configurations were considered for this study.

5.4.1 Insulated crack and rebar mesh

The resistivity measurements in the presence of an insulated crack for configuration #4 are shown in Figure 5-20. The solid line represents data from a condition in which no rebar is present and only the crack is affecting the measurements. The first point to highlight in this figure is the fact that measurements for both rebar and crack (i.e., dashed lines) are all less than the no-rebar case. This indicates all measurements are affected by the rebar mesh and as discussed in more details in Section 5.2, they are all reduced compared with no-rebar case. Moreover, influence of rebar increases as the mesh

becomes denser (i.e., smaller spacing). For 100 mm spacing rebar mesh, the minimum values of the resistivity was measured compared to those where rebar spacing were either 150 mm or 200 mm.

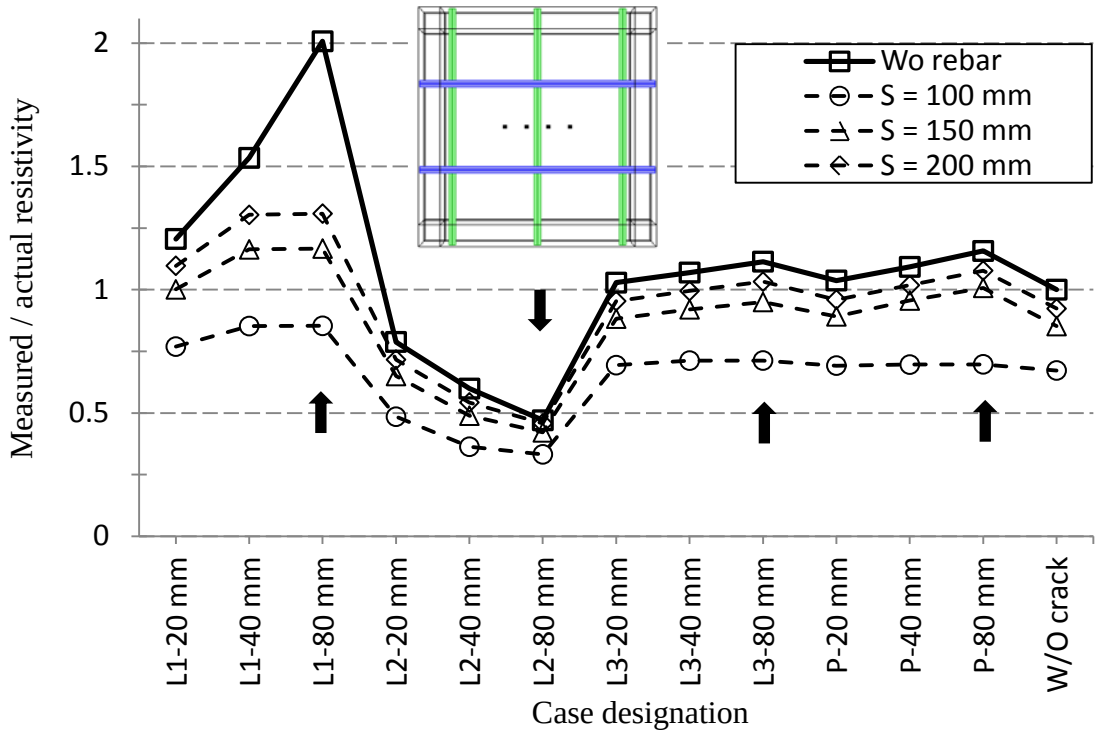

Figure 5-20: Resistivity measurement data taken over rebar mesh with different rebar spacings for configuration #4 and in the presence of an insulated crack perpendicular to the probe for T = 25 mm.

Another point to highlight in Figure 5-20 is the overall trend observed in the measurements. The trend is very similar to the one only affected by the crack alone as shown with the solid line in this figure. From this, it can be assumed that each parameter (i.e., presence of crack or rebar mesh) has an independent effect on Wenner probe regardless of the other except for the following cases.

When crack height became considerably larger than the cover thickness, a noticeable change in the trend is observed. In Figure 5-20, a clipping effect is visible at

the point where crack depth increases to 80 mm for cover thickness of 25 mm. These locations are marked using a solid arrow in the chart. For example, following the trend in the solid line (i.e., crack-alone effect), it is expected that resistivity measurement for the case for which the crack is at location L1 with the height of 80 mm exceeds the value obtained when crack height was 40 mm. Surprisingly, no significant change between the measurements for the two crack heights is observed. Likewise, this phenomenon is visible for crack at location L2.

Measurements using configuration #9 also shows similar behaviour as crack height increases significantly. Figure 5-21 illustrates measured data for configuration #9 where all other conditions are the same as Figure 5-20.

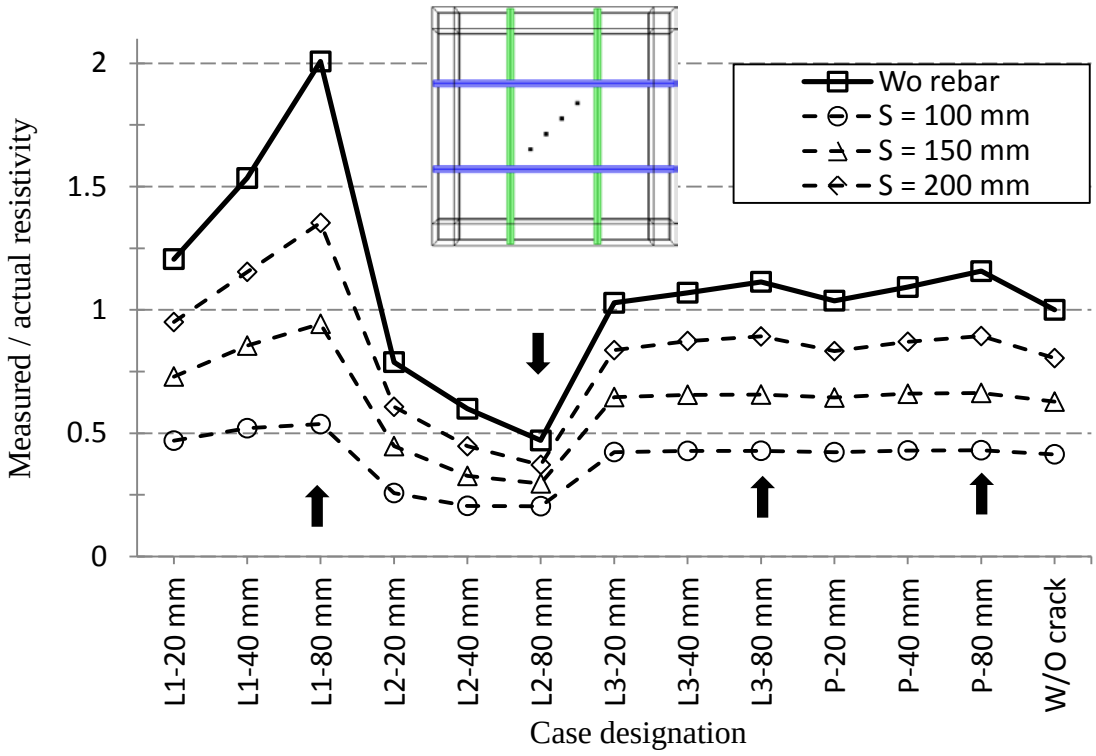

Figure 5-21: Resistivity measurement data taken over rebar mesh with different rebar spacings at configuration #9 in the presence of an insulated crack perpendicular to the probe for T = 25 mm.

Comparing Figure 5-20 with Figure 5-21, it is evident that for crack in location L1, the clipping effect for configuration #9 is not as significant as #4. For example, when there is only a crack, measured resistivity increased by 30% when crack height increased from 40 mm to 80 mm. This was 4% for rebar spacing of 100 mm, 10% for spacing of 150 mm, and 17% for rebar spacing of 200 mm when rebar mesh of configuration #9 was used. For configuration #4, on the other hand, increase in electrical resistivity due to increase in crack height from 40 mm to 80 mm was negligible for all three rebar spacings of 100 mm, 150 mm and 200 mm (Figure 5-20). In configuration #4, presence of two parallel rebars to the probe provide a more favourable passage for the current to flow when crack height increases blocking the usual fluxes in concrete. On the contrary, direction of the rebars in configuration #9 are not exactly aligned with the direction of current flow inside concrete thus even when crack height increases still some amount of current fluxes will pass through concrete. This could be the reason behind the different extent at which increase in crack height over passing rebars affects electrical resistivity measurement in the two abovementioned configurations.

Referring to Figure 5-20 and Figure 5-21, it can be concluded that measuring electrical resistivity when there is an insulated crack at location L1 or L2 would significantly vary depending on the crack height or measurement configuration making any predictions almost impossible. However, if configuration #4 is used and crack is either behind the probe or parallel to it (i.e., at location L3 or P) reasonably accurate data could be obtained. For rebar spacing $S \geq 150$ mm, maximum deviation in the measured data from the actual resistivity of concrete will be less than 15%. This maximum deviation is valid for all cover thickness and crack angles used in this study. Figure 5-22

illustrates measurement data for configuration #4 comparing results under the influence of both insulated crack and rebar mesh. Closeness of the data points to the 45° line for scenarios for which crack is either at location L3 or location P is an indication that crack has limited influence on the measurements. For crack in other locations, however, measurements using the Wenner probe would be significantly altered by the crack.

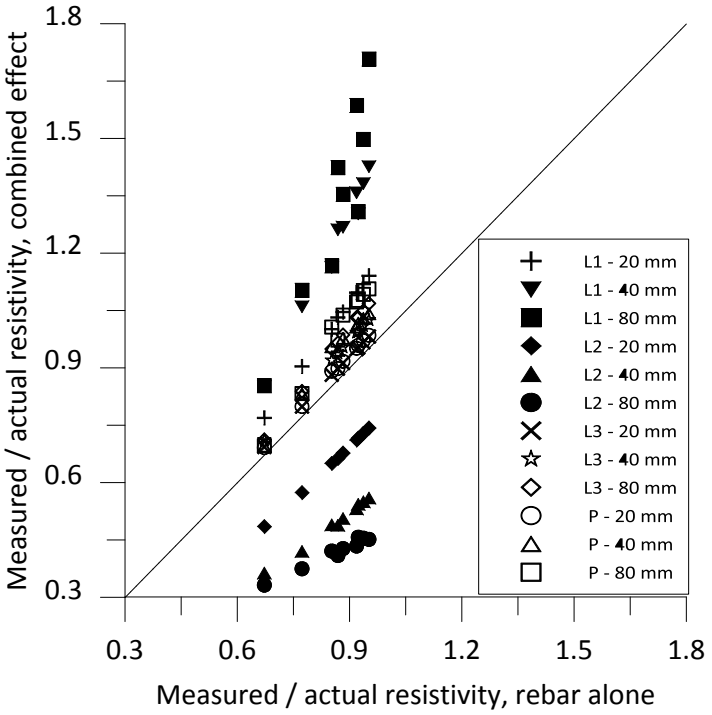

Figure 5-22: Influence of an insulated crack and its location on measured resistivity over rebar mesh at configuration #4.

5.4.2 Conductive crack and rebar mesh

Following the discussion on the combined effect of insulated crack and rebar mesh, impact form the presence of a conductive crack was also investigated. Figure 5-23 depicts data obtained from configuration #4 over a rebar mesh. Similar to the previous section, the overall trend of the measured data closely follows the one seen for crack-alone

scenario (i.e., solid line). During the discussion regarding the impact of a conductive crack on Wenner probe in Section 5.3.1, it was concluded that always values smaller than the actual resistivity of concrete will be attained. In Figure 5-23, it is also evident that measured values are further reduced as a consequence of rebar mesh presence; thus, all measurements would be less than the actual resistivity of concrete.

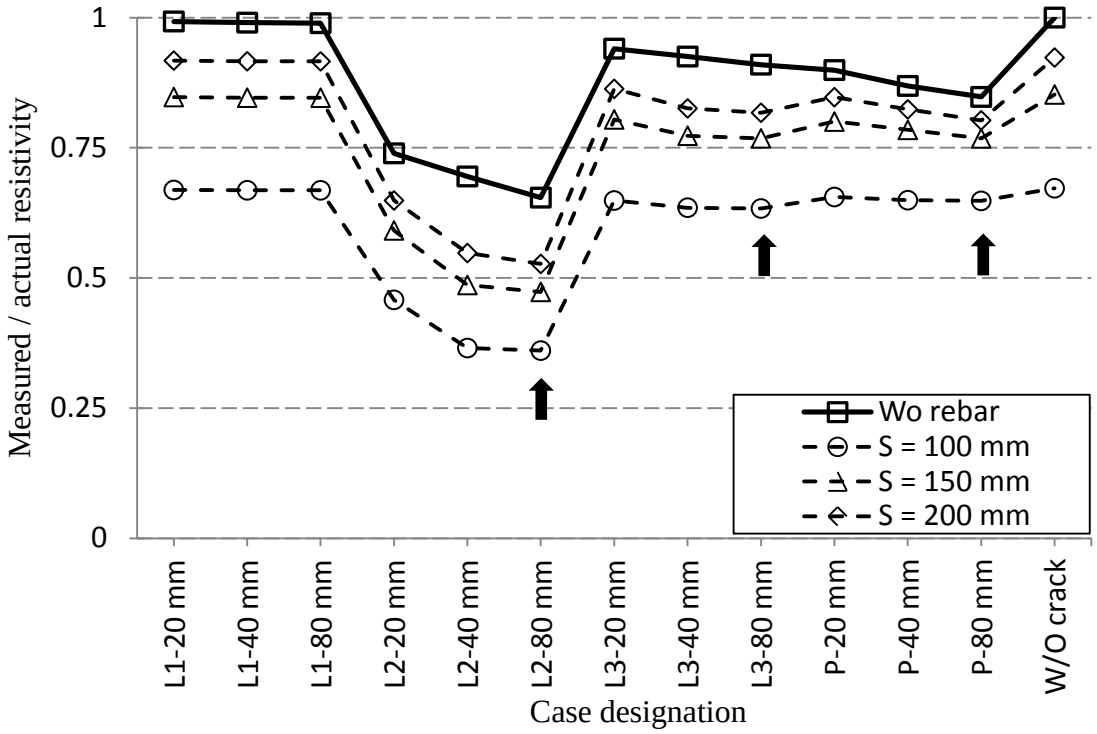

Figure 5-23: Resistivity measurement data taken over rebar mesh with different bar spacing at configuration #4 and in the presence of a conductive crack perpendicular to the probe for T = 25 mm.

Moreover, the clipping effect observed for an insulated crack is also noticeable for conductive cracks. The major difference is that when crack is at location L1, no contribution is observed by the depth of the crack. The horizontal line at the beginning of each plot is the indicator of this behaviour. However, if the orientation of crack changes

from perpendicular to diagonal, influence from the crack and clipping effect becomes visible.

In Figure 5-24, data from measurement at configuration #9 is plotted with conductive crack placed at different locations for various crack heights. Similar to configuration #4, same features are present in this chart. The similarity of clipping effect for deep cracks, similarity of data trends and underestimation of concrete resistivity are some of those already mentioned features related to the combined effect of rebar mesh and crack on the measurements.

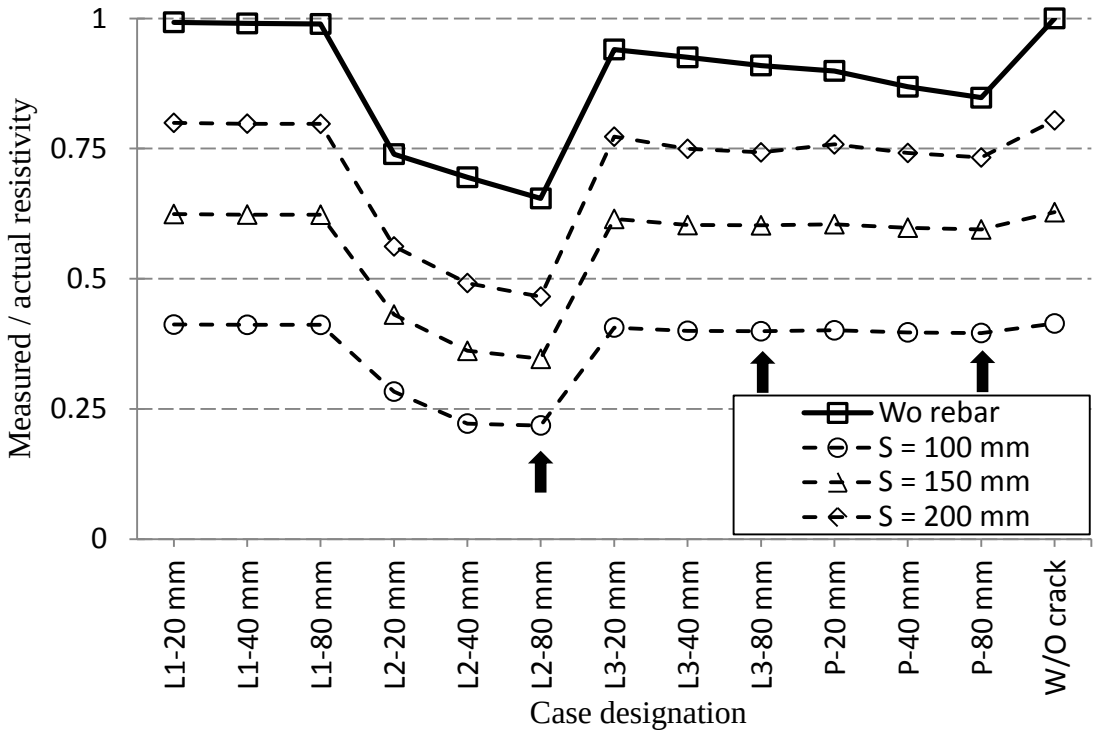

Figure 5-24: Resistivity measurement data obtained over rebar mesh with different rebar spacings at configuration #9 in the presence of a conductive crack perpendicular to the probe for T = 25 mm.

Results from simulations of both rebar mesh-Wenner probe configuration suggest that when conductive crack is present, the presence of rebar would further affect measurements. This behaviour could be justified as follows: In Section 3.4.2, impact of different resistivity ratios between rebar and concrete on electrical resistivity measurement using the Wenner probe was investigated. It was concluded that ratios greater than 10^3 had negligible effect on resistivity measurements. Similarly, impact from resistivity ratio of concrete to conductive crack investigated and discussed in Section 5.3.7 resulted in the same conclusion. In this study, ratio between resistivity of concrete to rebar was in the order of 10^6 and the resistivity of concrete to conductive crack was in the order of 10^3. Following this argument, it is evident that even conductive crack is three orders of magnitude more resistive than rebar. Therefore, rebar has its governing effect while conductive crack still affected measurements. Similar observation was reported by Moreno et al. (2009) when presence of multi-layered concrete cover was investigated. It was reported that rebar affected all measurements regardless of thickness or resistivity of surface layer causing a further reduction in measured electrical resistivity. In that study, ratio considered for the resistivity of concrete to the resistivity of surface layer was in the order of 10^2, and both resistivities were significantly large compared to the resistivity of rebar.

Unlike section 5.4.1, where for the presence of an insulated crack and taking measurements in configuration #4 with respect to the rebar mesh, conditions for reasonable measurements were found, no such condition can be identified when a conductive crack is present. Figure 5-25 depicts comparable results to Figure 5-22 but for measurements at the vicinity of a conductive crack. Having all the data points below the

45° line is a clear indication of measurements that are smaller than those in the presence of only rebar mesh; the extent of the variation depends on location, orientation or height of the crack. Deviation as much as 30% can be observed from actual resistivity of concrete when conductive crack is even located behind the probe (i.e, L3 case). However, it was found that in configuration #4, for conductive crack at location L3 or P, resistivity values are on average 20% less than the actual resistivity of concrete if rebar spacing S ≥ 150 mm. Measured resistivity at this condition varies by 10% depending on the cover thickness, crack orientation and height.

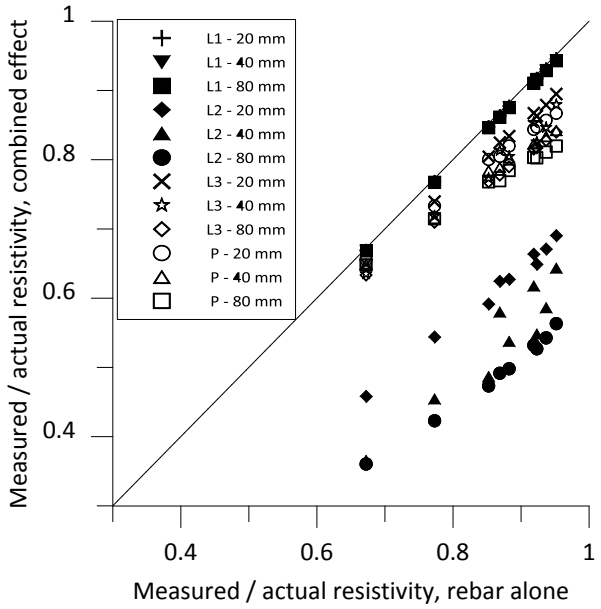

Figure 5-25: Influence of a conductive crack and its location on measured resistivity over rebar mesh at configuration #4.

5.4.3 Summary of combined rebar mesh and concrete crack effect

Following remarks can be provided as the summary of this section where combined effect of rebar mesh and crack in concrete was investigated.

It was found that rebar would still significantly affect resistivity measurements at the vicinity of a conductive crack. Simulation results indicate that taking resistivity measurement when a crack is present either in the middle of the probe (i.e., location L1) or between the two adjacent current and potential electrodes (i.e., location L2), would be significantly altered by the crack. In this case no reasonable data could be obtained and all the measurements are highly dependent upon crack type, height or orientation.

Similar to what was concluded in Section 5.2, taking resistivity measurement in configuration #4 over rebar mesh provides results that are closer to the actual resistivity of concrete. Measurements are within 15% of the actual resistivity of concrete if an insulated crack exists parallel or behind the probe (i.e., P or L3). On the other hand, if a conductive crack is present at location L3 or P, on average measured resistivity is 20% less than the actual resistivity of concrete.

Similar to two previous sections, Table 5-3 provides a summary of all the simulated cases. Symbols were used to indicate the extent of deviations from the actual resistivity of concrete in the measurements expected to be observed. While direction of the arrow suggests the direction of deviations (i.e., downwards means reduction) its magnitude is an indication of the magnitude of deviations. Dashes are considered to represent scenarios were deviations were not significant.

Table 5-3: Summary of the results for combined effect of crack and rebar mesh on Wenner probe resistivity measurements.

Crack type	Crack location	Electrode spacing (mm)		Crack height (mm)			Crack angle (°)			Cover thickness (mm)			Rebar spacing (mm)		
		38	50	20	40	80	90	45	0	25	40	60	100	150	200
Conductive	L1	▼	▼	▼	▼	▼	▼	⬇		▼	▼	▼	⬇	▼	▼
	L2	⬇	⬇	⬇	⬇	⬇	⬇	⬇		⬇	⬇	⬇	⬇	⬇	⬇
	L3	▼	▼	▼	▼	▼	▼	▼		▼	▼	▼	⬇	▼	▼
	P	▼	▼	▼	▼	▼			▼	▼	▼	▼	▼	▼	▼
Insulated	L1	N.A													
	L2														
	L3														
	P														

⬇ < 0.75	0.75 ≤ ▼ < 0.9	0.9 ≤ - ≤ 1

6. Conclusion and Future works

Electrical resistivity of concrete plays a major role in controlling the corrosion rate of embedded reinforcement in concrete. In addition, many recent studies have shown that resistivity and micro-structural changes as well as ion (e.g. chloride) ingress in concrete are highly correlated. This has led to a growing interest in using electrical resistivity as a performance indicator for condition assessment of structures. Wenner probe is the most commonly used technique for measuring the surface electrical resistivity of concrete due to its simplicity; however, a wide range of parameters can adversely affect the performance of this technique in practice by introducing some level of inaccuracy in the measurements. A number of researchers tried to identify these error-inducing parameters and quantify their effect. Probe characteristics, dimensions of the concrete area under investigation, presence of rebar at the proximity of the probe and environmental conditions during measurements are some of these parameters. The literature showed that the presence of crack and its influence on the accuracy of measurements, and the impact of rebar mesh and its density on the results are two areas that were not systematically investigated. The main goal of this study was to systematically explore these two areas and quantify their individual as well as combined effect on the electrical resistivity measurements using the Wenner probe technique.

The investigation was carried out by numerical analysis of a developed finite element model solving the Laplacian's equation of electrical potential distribution, which replicates the real life conditions applicable to the Wenner probe resistivity measurement technique. A commercial finite element modelling software package called COMSOL

Multiphysics™ was used for this purpose. The parameters investigated in the first part of this study included the location and orientation of the crack with respect to the probe and the type (i.e., conductive or insulated), height, width, and length of the crack. In the second part, the impact of orientation and location of the Wenner probe with respect to the embedded rebar mesh, density of reinforcement, concrete cover thickness and the depth of concrete members on the accuracy of resistivity measurements were investigated. In the last part of this study, the combined effect from cracks and embedded reinforcement on the performance of the Wenner probe was investigated. The main conclusions of this study are presented in the following section.

6.1 Conclusions

Numerical simulations showed that electrical resistivity measurements using Wenner probe were highly affected by the presence of rebar mesh so that the calculated values were all an underestimate of the actual resistivity of concrete. Concrete cover thickness and spacing between reinforcement bars were both influential in a way that reduction in each of them caused an increase in measurement errors. When rebar spacing was 50 mm or cover thickness is 25 mm, on average, measurement values were 30% less than the actual resistivity of concrete. It also became evident that location and orientation of the probe with respect to the embedded reinforcement significantly alters resistivity measurements using Wenner probe. It was found that resistivity measurements midway between the two parallel rebars provide more accurate results compared to the current RILEM suggestion (RILEM TC 154-EMC, 2000) in which measurements diagonal to the direction of rebars is recommended to reduce their negative effect. With rebars interconnected in a reinforcement mesh, perpendicular rebars were found to adversely

affect the accuracy of measurements unlike previous observations that reported insignificant impact of a single perpendicular rebar.

In the presence of a crack, results showed that resistivity measurement were altered significantly. Depending on the type of the crack (i.e., conductive or insulated) and its location with respect to the probe, measurements can either be an underestimate or an overestimate of the actual resistivity of concrete. For an insulated crack in the middle of the probe, on average, measurements were 60% higher than the actual resistivity of concrete whereas the same crack between the current and potential electrodes led to the values 40% less than the actual resistivity of concrete. In the presence of a conductive crack, all measurements were less than the actual resistivity of concrete; however, Wenner probe was more sensitive to cracks between the current and potential electrodes such that, on average, measurements were 30% less than the actual resistivity of concrete. Increase in crack height and length amplifies the impact of crack on the performance of Wenner probe, especially, in the case of an insulated crack. Orientation of the crack also affected the accuracy of the measurements such that decrease in the angle between crack and probe increased measurement error. Moreover, the decrease in crack width reduced the error in measurements for a conductive crack and Wenner probe was found to be more sensitive to variations in orientation in this situation compared to an insulated crack. For insulated cracks, no effect was observed on measurements as crack width changed. Therefore, the inference is that electrical resistivity measurements over any crack should be avoided.

When both crack and rebar mesh were present together in concrete, the simulations showed that in most cases crack and rebar affected measurements independent from each

other with rebar mesh further reducing the measured values. However, there were some exceptions: when cover thickness was 25 mm, as the crack height increased over 40 mm passing the depth of rebars, impact from the crack was governed by the presence of the rebar mesh. Presence of crack between Wenner probe electrodes disturbed measurements in such that no certain conclusions could be made about the performance of the probe. On the other hand, when crack is parallel to the probe or behind the probe, and measurements are taken midway between the parallel rebars, the performance of the Wenner probes was found to be satisfactory. In the aforementioned condition, measurements in the presence of an insulated crack were around the actual resistivity of concrete with 15% variance depending on the height or location of the crack. For conductive crack present in similar situation, measurements were on average 20% less than the actual resistivity of concrete with 10% variance. It was also found that compared to the resistivity measurements diagonal to the orientation of rebars as suggested by the RILEM standard (RILEM TC 154-EMC, 2000), taking resistivity measurements midway between the two parallel rebars provides more accurate results even in the presence of crack.

6.2 Recommendations for future work

Following is a list of some research topics related to the course of this study that requires further investigation:

- Numerical evaluations made in this study for the performance of Wenner probe need to be validated experimentally by measuring the electrical resistivity of concrete that contains similar feature of interest including crack, rebar mesh, etc.

- For the location of the crack behind the probe or parallel to the probe, only one distance was investigated in this work. This can be further extended to obtain better insight on the determination of a specific distance where Wenner probe measurement is not affected by cracks. The outcome can be used as a guideline for field applications.
- The practicality of the model can be increased by considering different crack patterns such as multiple cracks in order to evaluate their impact on the Wenner probe measurements.
- It was found that when rebar mesh is present, resistivity measurements midway between the top parallel rebars provide more accurate results compared to taking measurements diagonally. In this study, when crack and rebar mesh were both present, only one parallel measurement configuration was simulated. The other two possible parallel measurement scenarios as demonstrated in Section 5.2 can be further explored to broaden the outcome of this study.
- Corrosion of rebar in concrete causes cracking and delamination of concrete cover which lead to a separation between rebar and concrete. This effect can limit the access of electrical current fluxes to rebars during the measurement, which may have some effects on the performance of Wenner probe in the corroding areas of reinforced concrete structures. Further investigation of this phenomenon can shed some light into these cases.

References

AASHTO TP 095-11-UL (2011). *Standard method of test for surface resistivity indication of Concrete's ability to resist chloride ion penetration*. Wahington, DC: American Association of State Highway and Transportation Officials.

ACI 318 (2011). *Building code requirements for structural concrete and commentary*. Farmington Hills, Michigan: American Concrete Institute.

Andrade, C., Sarría, J., & Alonso, C. (1999). Relative humidity in the interior of concrete exposed to natural and artificial weathering. *Cement and Concrete Research, 29*(8), 1249-1259.

Andrade, C., & Alonso, C. (2001). On-site measurements of corrosion rate of reinforcements. *Construction and Building Materials, 15*(2-3), 141-145.

Aperador Chaparro, W., Vera López, E., & Mejía De Gutiérrez, R. (2012). Corrosion behavior of steel bar embedded in alkali-activated slag concrete subjected to carbonation and chloride attack. *Dyna, 79*(171), 80-87.

ASTM Standard C3 (2012a). *"Standard Test Method for Compressive Strength of Cylindrical Concrete Specimens"*. ASTM International, West Conshohocken, PA, DOI: 10.1520/C0039_C0039M-12A, www.astm.org.

ASTM Standard C876 (2009). *"Standard Test Method for Corrosion Potentials of Uncoated Reinforcing Steel in Concrete"*. ASTM International, West Conshohocken, PA, DOI: 10.1520/C0876-09, www.astm.org.

ASTM Standard C1202 (2012). *"Standard Test Method for Electrical Indication of Concrete's Ability to Resist Chloride Ion Penetration"*. ASTM International, West Conshohocken, PA, DOI: 10.1520/C1202-12, www.astm.org.

ASTM Standard C1556 (2011a). *"Standard Test Method for Determining the Apparent Chloride Diffusion Coefficient of Cementitious Mixtures by Bulk Diffusion"*. ASTM International, West Conshohocken, PA, DOI: 10.1520/C1556-11A, www.astm.org.

Berthouex, P. Mac, & Linfield C. Brown (2002). *Statistics for Environmental Engineers*. Boca Raton, FL: Lewis.

Brameshuber, W., Raupach, M., Schröder, P., & Dauberschmidt, C. (2003). *Proceedings of international symposium of Non-Destructive Testing in Civil Engineering 2003: Non-destructive determination of the water content in the concrete cover using the multi-ring electrode*. Berlin, Germany: DGZfP E.V.

Butler, S., & Sinha, G. (2012). Forward modeling of applied geophysics methods using comsol and comparison with analytical and laboratory analog models. *Computers & Geosciences, 42*, 168-176.

Chi, J. M., Huang, R., & Yang, C. (2002). Effects of carbonation on mechanical properties and durability of concrete using accelerated testing method. *Journal of Marine Science and Technology, 10*(1), 14-20.

Chrisp, T., Starrs, G., McCarter, W., Rouchotas, E., & Blewett, J. (2001). Temperature-conductivity relationships for concrete: An activation energy approach. *Journal of Materials Science Letters, 20*(12), 1085-1087.

CAN/CSA A23.2 (2009). *Concrete materials and methods of concrete construction/Test methods and standard practices for concrete*. Toronto, ON: Canadian Standards Association.

CAN/CSA A23.3 (Eds.). (2004). *Design of concrete structures* (2010th ed.). Toronto, ON: Canadian Standards Association.

COMSOL AB. (2012). *AC–DC Module User's Guide*. COMSOL Multiphysics V4.3a.

Dean, S., Illowsky, B. (2013). *Descriptive Statistics: Measuring the Center of the Data. Connexions*. http://cnx.org/content/m17102/1.13/.

EDDY CURRENT TECHNOLOGY (2002). *Electrical conductivity of materials.* (No. R8418 Rev 2). Retrieved from http://www.eddy-current.com/ect-conductivity-report.pdf

EN 10080 (2005). Steel for the reinforcement of concrete - weldable reinforcing steel - general. *Official Journal of the European Union, 89/106/EEC.*

Enevoldsen, J., Hansson, C., & Hope, B. (1994). The influence of internal relative humidity on the rate of corrosion of steel embedded in concrete and mortar. *Cement and Concrete Research, 24*(7), 1373-1382.

Ewins, A. J. (1990). Resistivity measurements in concrete. *British Journal of Non-Destructive Testing, 32*(3), 120-126.

Feliu, S., Andrade, C., Gonzalez, J., & Alonso, C. (1996). A new method forin-situ measurement of electrical resistivity of reinforced concrete. *Materials and Structures, 29*(6), 362-365.

FM 5-578 (2004). *Florida Method of Test for Concrete Resistivity as an Electrical Indicator of its Permeability.* FL, USA: Department of Transportation Florida.

Ghods, P. (2010). *Multi-scale investigation of the formation and breakdown of passive films on carbon steel rebar in concrete* (Ph.D. Dissertation), Carleton University, ON, CA.

Goueygou, M., Abraham, O., & Lataste, J. (2008). A comparative study of two non-destructive testing methods to assess near-surface mechanical damage in concrete structures. *NDT & E International, 41*(6), 448-456.

Gowers, K., & Millard, S. (1999). Measurement of concrete resistivity for assessment of corrosion severity of steel using wenner technique. *ACI Materials Journal, 96*(5), 536-541.

Gu, P., & Beaudoin, J. J. (1998). Obtaining Effective Half-Cell Potential Measurements in Reinforced Concrete Structures. *Institute for Research in Construction*: *Construction Technology Update*, 18(4): Institute for Research in Construction, ON,CA.

Gucunski, N., Imani, A., Romero, F., Nazarian, S., Yuan, D., Wiggenhauser, & H., Kutrubes, D. (2013). *Nondestructive testing to identify concrete bridge deck deterioration.* (No. S2-R06A-RR-1). Washington: Transportation Research Board.

Gunay, H. B. (2011). *Electrochemical and microscopic investigation of the passivation and depassivation processes of iron and steel in simulated concrete pore solutions* (M.A.Sc. Thesis). Carleton University, ON, CA.

Hamilton, H.R., Boyd, A., Vivas, E., & Bergin, M., (2007). *Permeability of Concrete – Comparison Of Conductivity And Diffusion Methods* (No: 00026899) Department of Civil and Coastal Eng. Gainesville, FL: University of Florida.

Lane, D.S., Detwiler, R.J., & Hooton, R. D. (2010). Testing Transport Properties in Concrete, *Concrete International, 31*(11), 33-38.

Lataste, J., Sirieix, C., Breysse, D., & Frappa, M. (2003). Electrical resistivity measurement applied to cracking assessment on reinforced concrete structures in civil engineering. *NDT & E International, 36*(6), 383-394.

Martinez, I., Andrade, C., Rebolledo, N., Bouteiller, V., Marie-Victoire, E., & Olivier, G. (2008). Corrosion Characterization of Reinforced Concrete Slabs with Different Devices. *Corrosion., 64*(2), 107-123.

McCarter, W., & Garvin, S. (1989). Dependence of electrical impedance of cement-based materials on their moisture condition. *Journal of Physics D: Applied Physics, 22*(11), 1773-1776.

Mehta, P. K., & Monteiro, P. J.(Eds.) (2006). *Concrete: microstructure, properties, and materials* (3rd ed.): McGraw-Hill Professional.

Millard, S. (1991). Reinforced concrete resistivity measurement techniques. *ICE Proceedings, 91*(1) 71-88.

Millard, S., Harrison, J., & Gowers, K. (1991). Practical measurement of concrete resistivity. *British Journal of Non-Destructive Testing, 33*(2), 59-63.

Moreno, F. P., Liu, Y., & Paredes, M. (2009). *Proceeding of Corrosion 2009 Conference & Expo: Understanding the Effect of Rebar Presence and/or Multilayered Concrete*

Resistivity on the Apparent Surface Resistivity Measured via the Four Point Wenner Method. Atlanta, Georgia, USA: NACE International.

Morris, W., Moreno, E., & Sagüés, A. (1996). Practical evaluation of resistivity of concrete in test cylinders using a wenner array probe. *Cement and Concrete Research, 26*(12), 1779-1787.

Morris, W., Vico, A., & Vázquez, M. (2004). Chloride induced corrosion of reinforcing steel evaluated by concrete resistivity measurements, *Electrochimica Acta*, *49*(25), 4447–4453.

Østvik, J., Larsen, C., Vennesland, Ø., Sellevold, E., Andrade, M., Marchand, J., & Paradis, F. (2006). *Proceeding of 2nd International RILEM Symposium on Advances in Concrete through Science and Engineering*: *Electrical resistivity of concrete-part I: Frequency dependence at various moisture contents and temperatures.* Quebec City, Canada: RILEM Publication.

Pease, B. J. (2010). Influence of concrete cracking on ingress and reinforcement corrosion. (Ph.D. dissertation) Purdue University School of Civil Engineering USA.

Portland Cement Association (Eds) (2011). *Design and Control of Concrete Mixes* (15th ed.). Engineering Bulletin 001. IL, USA: PCA.

Polder, R., Andrade, C., Elsener, B., Vennesland, Ø., Gulikers, J., Weidert, R., & Raupach, M. (2000). Test methods for on site measurement of resistivity of concrete. *Materials and Structures, 33*(10), 603-611.

Poyet, S. (2009). Experimental investigation of the effect of temperature on the first desorption isotherm of concrete. *Cement and Concrete Research, 39*(11), 1052-1059.

RILEM TC 154-EMC (2000). Electrochemical techniques for measuring metallic corrosion: Test methods for on site measurement of resistivity of concrete. *Materials and Structures 33*(234). 603-611.

Saleem, M., Shameem, M., Hussain, S., & Maslehuddin, M. (1996). Effect of moisture, chloride and sulphate contamination on the electrical resistivity of portland cement concrete. *Construction and Building Materials, 10*(3), 209-214.

Sengul, O., & Gjorv, O. E. (2008). Electrical resistivity measurements for quality control during concrete construction. *ACI Materials Journal, 105*(6), 541-547.

Sengul, O., & Gjorv, O. E. (2009). Effect of embedded steel on electrical resistivity measurements on concrete structures. *ACI Materials Journal, 106*(1), 11-18.

Shahroodi, A. (2010). *Development of Test Methods for Assessment of Concrete Durability for Use in Performance-Based Specifications* (M.A.Sc. Thesis) University of Toronto, ON, CA.

Telford, W. M., Geldart, L. P., & Sheriff, R. E. (Eds) (1990). *Applied geophysics* (2nd ed.). New York, NY: Cambridge UP.

Wei, X., & Li, Z. (2006). Early hydration process of portland cement paste by electrical measurement. Journal of Materials in Civil Engineering, 18(1), 99-105.

Weydert, R., & Gehlen, C. (1999). 39 electrolytic resistivity of cover concrete: Relevance, measurement and interpretation. *Durability of Building Materials and*

Components 8: Service Life and Durability of Materials and Components, *1*, 409-419.

Wiwattanachang, N., & Giao, P. (2011). Monitoring crack development in fiber concrete beam by using electrical resistivity imaging. *Journal of Applied Geophysics*, *75*(2), 294-304.

Xiao, L., & Li, Z. (2008). Early-age hydration of fresh concrete monitored by non-contact electrical resistivity measurement. *Cement and Concrete Research*, *38*(3), 312-319.

Zimney, E. J., Dommett, G. H., Ruoff, R. S., & Dikin, D. A. (2007). Correction factors for 4-probe electrical measurements with finite size electrodes and material anisotropy: A finite element study. *Measurement Science and Technology*, *18*(7), 2067-2073.